The photochemical isomerisation and acid/base rectivity of pyrazolotriazole azomethine dyes.

White, Michael V

THE PHOTOCHEMICAL ISOMERISATION AND ACID/BASE REACTIVITY OF PYRAZOLOTRIAZOLE AZOMETHINE DYES.

Thesis submitted for the degree of Master of Philosophy by

Michael V. White

University of Wales: Swansea

December 2003

DECLARATION

This work has not previously been accepted in substance for any degree and is not concurrently submitted in candidature for any degree.

Signed ..... (candidate)
Date ..... 16th July 2004 .....

STATEMENT 1

This thesis is the result of my own investigations, except where otherwise stated.
Other sources are acknowledged with explicit references. A bibliography is appended.

Signed ..... (candidate)
Date ..... 16th July 2004 .....

STATEMENT 2

I hereby give my consent for my thesis, if accepted, to be available for photocopying and for inter-library loan, and for the title and summary to be made available to outside organizations.

Signed ..... (candidate)
Date ..... 16th July 2004 .....

ACKNOWLEDGMENTS

I would like to thank Dr. P. Douglas for his unfaltering patience and understanding during this work. His guidance and encouragement have been invaluable to this research. Heart felt thanks go also to Dr. M. Garley for his help with the computer programs and data acquisition, also to Mr. R. Berry for useful discussions.

I am also extremely grateful to my wife, Erica, for her encouragement and support in this research and the forbearance of our son Alexander.

ABSTRACT

This thesis deals with two aspects of the chemistry of pyrazolotriazole azomethine dyes (PT dyes):
a). the kinetics and yield of photoinduced isomerisation and
b). the kinetics of dye hydrolysis in acidic and basic media.

Microsecond flash photolysis has been used to investigate the effects of solvent, excitation wavelength and oxygen on the yields of photoinduced isomerisation for a range of pyrazolotriazole azomethine dyes substituted at the 6-position. The rates of thermal relaxation show no obvious dependence on solvent solvatochromic parameters examined; this suggests that solvent factors such as dielectric properties and basicity are not uniquely significant in determining the relaxation times of the dye isomers.

The isomer yields for the two dyes examined with substituents which contained the carbonyl group, i.e. $6CO_2Et$-PT and 2COPh-PT show an unexpected dependency on excitation wavelength and on the presence or absence of oxygen. It is tentatively suggested that this is a consequence of the availability of substituent localised carbonyl excited states for these dyes. It is suggested that these states are populated by uv excitation to give a localised carbonyl triplet state which can undergo energy transfer into the pyrazolotriazole azomethine triplet state leading to relatively efficient isomerisation via the triplet manifold.

There was no change observed in isomer yield when using ethyl-iodide in a nitrogen saturated solution with either $6CO_2Et$-PT or 6COPh-PT dyes indicating no effective external heavy atom effect from this solvent.

In acid media, the pyrazolotriazole azomethine dyes undergo hydrolysis with first order kinetics. Arrhenius constants and pre-exponential constants were measured for a number of different dyes. Base hydrolyses of the 6CO2Et-PT and 6COPh-PT dyes showed second order kinetics.

Preliminary investigations of acid catalysed decomposition using millisecond stopped flow suggest a complex reaction scheme involving, possibly, three successive reactions.

CONTENTS

LIST OF TABLES

List of Tables

LIST OF FIGURES

List of Figures

List of Figures

List of Figures

LIST OF ABBREVIATIONS

6H-PT	6H substituted pyrazolotriazole azomethine dye
6CO_2Et-PT	6CO_2Et substituted pyrazolotriazole azomethine dye
PT dyes	pyrazolotriazole azomethine dyes
k	rate constant
σ	Hammett constant
ε	dielectric constant
η	density (g/ml)
nm	nanometre
nmr	nuclear magnetic resonance spectroscopy
NOE	nuclear overhauser effect
I_O	current response light on/off
vt	signal response
ms	millisecond
mg	milligram
DMSO	dimethyl sulphoxide
v/v	volume/volume
m/v	mass/volume
uv-vis	ultraviolet-visible spectra

1. INTRODUCTION TO COLOUR PHOTOGRAPHY

1.1 Vision

The electromagnetic radiation that we have evolved to see is just a small 'window' in the total electromagnetic spectrum, and is confined to the narrow band extending from 400nm to 700nm. The human eye, with the colour-sensitive specialised cells, called 'cones', can detect light in three distinct regions, blue, red and green. The sensitivities of cones are not the same at all wavelengths. However the mixing of the eye's response to these so-called primary colours results in the sensation of the vast number of colours we can 'see'.

1.2 History of colour photography

The production of a wide range of colours by the mixing of these three primary colours led Antonius de Dominis in 1611 to posit that white light was a mixture of these three colours[1]. Isaac Newton in 1666 demonstrated that light was actually a mixture of seven discernable, discrete colours when he carried out his famous experiment, by passing sunlight through a prism[2]. Newton perceiving that the colours were a product of our 'sensation' of sight described the phenomenon as 'ghost-like', spectral, and he coined the word spectrum to describe the phenomenon[3]. The news of this discovery led many artists and scientists to examine more closely the concepts of light and colour. The Dutch scientist Christiaan Huygens in 1678 suggested a wave model to explain the behaviour of light. The wavelength defined the colour of the light. Newton himself had adopted a corpuscular model of light. These two models of the behaviour of light were to lead the way to the revolutions in

physics at the end of the nineteenth and early twentieth centuries, and are now regarded as complementary.

Jacob Christoph Le Blon attempted the production of colour engravings based on Newton's discovery in 1722[1]. He was able to produce polychrome effects with red, blue and yellow dyes using an additive process of colour superimposition.

Carl Wilhelm Scheele took the first steps toward photography in 1777 when he adapted Newton's prism experiment to expose silver halide to different colours of light and discovered that different quantities of silver were reduced and deposited depending upon the colour of the light used[1]. The physicist Thomas Young in 1802 was the first to propose the mechanism whereby the eye perceives colour i.e. that it was sensitive to the three primary colours[1]. This led James Clark Maxwell, in 1861, to produce the first colour photograph using a superimposition of three colours[3,4]. Maxwell arranged three projectors and coloured filters which he attenuated using negatives previously obtained through blue, green and red filters. By combining these separate blue, green and red images he obtained the first colour photographic image.

Louis Ducos du Hauron in 1862 proposed an additive theory of colour photography and followed this with an outline of the subtractive theory of colour photography in 1869[5,6]. In the subtractive process, colours are achieved by the filtering out of primary colours from white light. The three subtractive primary colours du Hauron described as cyan (light greenish-blue), magenta (light bluish-red), and yellow. These are the complements of the primary colours blue, green and red; the cyan colour absorbs red light, magenta absorbs green light, and yellow absorbs blue light.

Du Hauron's theory was to prove impractical until 1873 when Herman Vogel discovered a means of sensitizing halide film using dyes[1]. He was able to sensitize the previously blue sensitive silver bromide emulsions to register green. Rudolph Fischer in 1912 used these sensitized emulsions and the subtractive process to propose a dye-coupled process of colour photography[6,7]. This was utilised by Eastman Kodak in 1935 after overcoming a number of technical difficulties and called the Kodachrome process[8]. Modification of this technique by Agfa led to the coupling chemicals being incorporated into the film emulsion i.e. the Agfacolour process. By 1940 Kodak produced a similar process, Ektachrome[9,10,11].

1.3 The additive and subtractive colour process [3,4,5,7,8,12]

The use of additive mixes of the primary colours can give a colour photograph with good reproductive properties. However, a problem arises because this technique relies on the transmission of single primary colours. One layer of a single primary coloured photographic dye filters out two thirds of the white light wavelengths; for example a red dye layer would remove all green and blue wavelengths. The combination of these primary colour filters in a superimposed system, if of sufficient optical density, could result in zero light transmission or a considerable lack of sensitivity in many lighting conditions. As a consequence of this, additive photographic processes rely upon a side-by-side arrangement of primary filters in the film or a sequential process where the blue green and red filtered images are superimposed in quick succession. Both these techniques are difficult to engineer and are consequently costly.

From a manufacturing and economic point of view the best method of film production is via a subtractive dye superimposed system where the emulsions contain dyes that only absorb one third of the visible light and transmit the other two thirds. This allows a stepwise coating of the film in three passes or so, which avoids unnecessary mechanical complexity and cost.

1.4 Producing a photographic image

1.4.1 Imaging colour[9,12]

As already mentioned, the most frequently employed method of producing a colour photographic image is to use the subtractive process. Light is first reflected from the coloured scene or object and via a lens focused onto the film. The film consists of a number of layers of so-called 'emulsions'. These consist of silver halide suspensions in gelatin; it is this solid suspension that records the photograph. Each layer also contains a sensitising dye that causes that emulsion layer to react to the presence of light of a particular wavelength. Consequently only light in a particular wavelength band will be absorbed by the silver halide. In the subtractive process other wavelengths will be transmitted to layers below. Typically the blue light recording medium is on the top of the layers and is the first to be exposed. Silver halide is naturally sensitive to blue and ultraviolet wavelengths, so a yellow layer is usually positioned beneath it to prevent blue and ultraviolet 'contamination' of the magenta and cyan emulsion layers underneath. Often these layers are repeated underneath at a different level of sensitivity to optimise film sensitivity under different light intensity; these are referred to as the 'fast and slow' layers of the film, further layers may also be introduced to separate the different light sensitive emulsion layers adequately.

1.4.2 The latent image

In 1938 Gurney-Mott proposed a mechanism that gave a model of how the silver halide produced an image on exposure to light[11]. In this electron transfer model it has been proposed that initially a photon of light is absorbed by a molecule of sensitiser dye (D) absorbed on a silver halide crystal. Following photon absorption an electron transfer step occurs to give oxidised dye (D^+) and an electron is transferred to the silver halide crystal. The electron then reduces a silver ion to a silver atom and at the same time the sensitiser dye and a halide radical are formed[12,22]:

$$D + h\nu \text{ --------> } D^+ + e^-$$

$$AgBr + e^- + D^+ \text{--------> } Ag^0 + Br^\cdot + D$$

The absorption of more photons increases the concentration of silver atoms on the silver halide crystal's surface, which, when the emulsion is developed, will serve as "conductors" for electrons from the developer to the silver halide crystal. The silver atoms are termed a 'latent image' site[12]. These sites will cause the silver halide crystal to be reduced by the developer, typically a *p*-phenylenediamine derivative[7], to silver metal on the 'negative'.

1.5 Couplers and colour

When the silver halide is reduced by the developer the oxidised developer molecule can be used to couple to a suitable dye or 'coupler'[7]. This reaction between oxidised developer and colour coupler to give a colour dye forms the colour record in the emulsion layer. The series of reactions which take place following formation of the latent image and which lead to formation of a colour record are shown in figure 1.1. In these

Figure 1.1. Sequence of reactions that take place in the formation of a colour record.

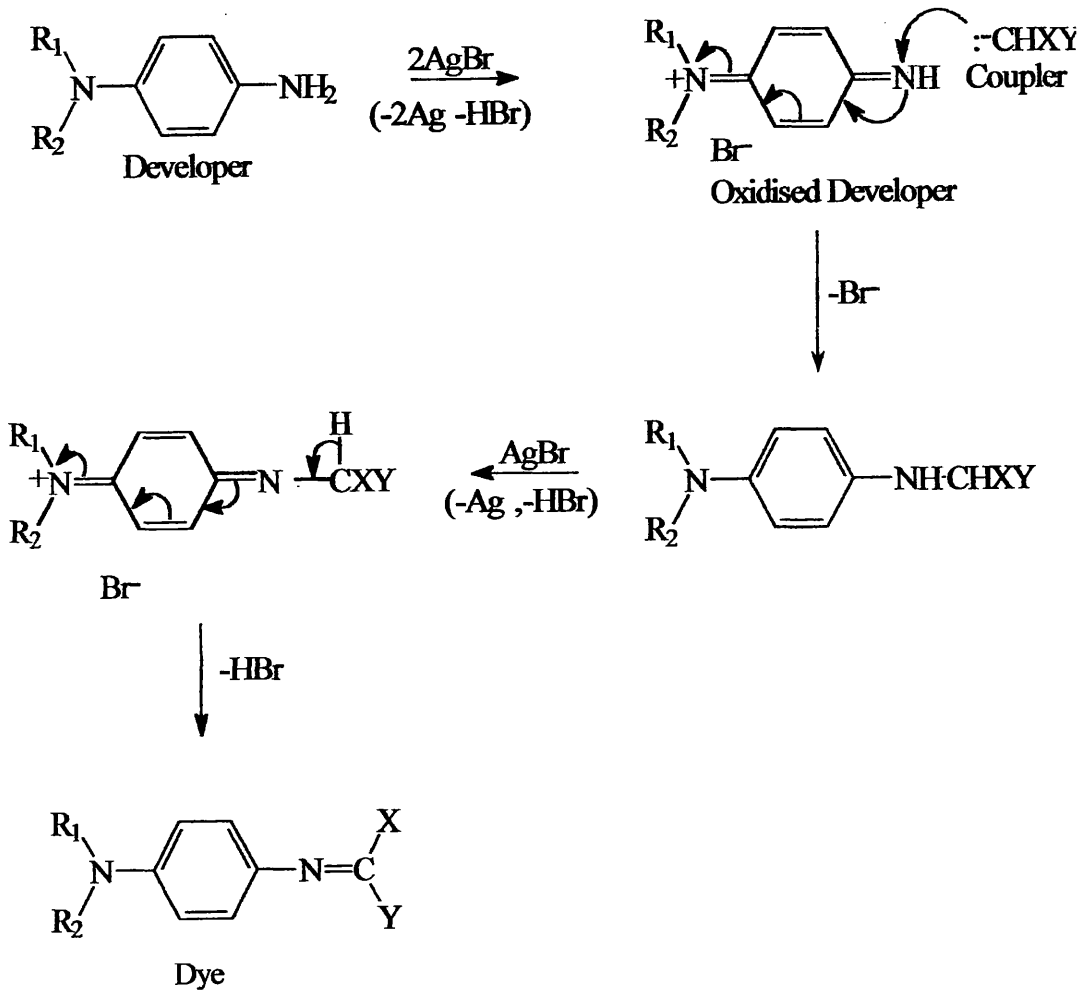

series of reactions the formation of reduced silver is the rate determining step[13].

1.5.1 Sequence of steps in the formation of the colour image[9]

1) Reduction of silver halide to form a latent image site.
2) Reduction of site by colour developing agent.
3) Formation of highly reactive semiquinone radical in film emulsion.
4) Further oxidation of semiquinone to quinonediimine ion.
5) Coupling of the quinonediimine ion with the coupling agent to produce a coloured dye in the emulsion of the film.

The coupling compounds may be present in the film emulsion or introduced at the developing stage in the processing solution. The structure of the coupler determines the colour of the dye formed.

The difficulties and complexities of making a stable colour image have led to considerable efforts in synthesizing dyes that are chemically and photochemically robust. Compounds that exhibit this contain C=C, N=N and C=N double bonds, and examples include azo-dyes and azamethine dyes.

1.5.2 Types of couplers

Three different types of couplers are used to generate the yellow, magenta and cyan dyes of subtractive colour photography.

Yellow-forming couplers: α–pivaloylacetanilide and α–benzoylacetanilide couplers are the most common types used. See figure 1.2. They give dyes which absorb in the 400-500nm region; the dye's spectral and chemical characteristics can be modified by incorporating suitable groups at R_1. The 'ballast'

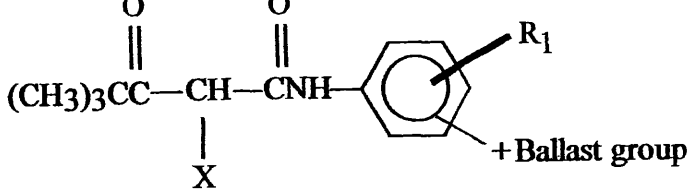

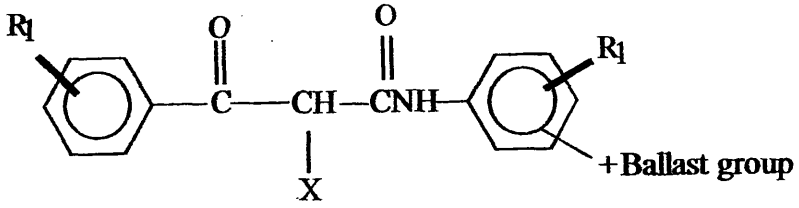

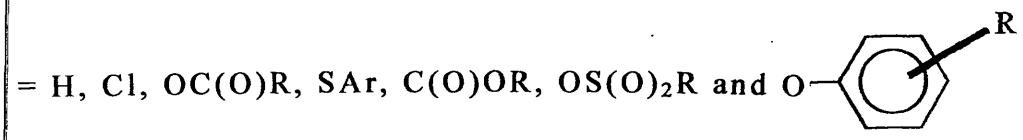

Figure 1.2. Yellow-forming couplers [26]. The ballast group is added to prevent migration of the coupled dye into adjacent layers of film emulsion.

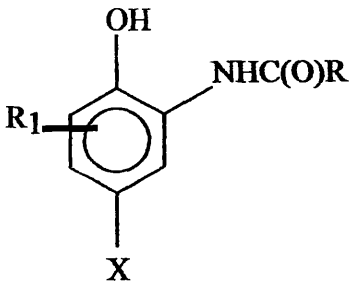

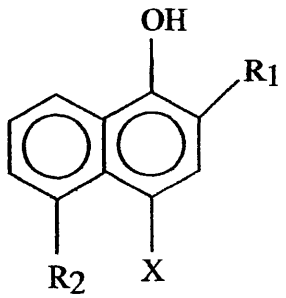

R_1 = Cl, R
X = H, Cl, OAr, OR, SAr
R = organic group

R_1 = $C(O)NH(CH_2)_nAr$
R_2 = H, NHC(O)R
X = H, Cl, OAr, OR, SAr

Figure 1.3.Cyan Couplers [14]

group is incorporated to ensure the dye remains in the emulsion layer and does not diffuse away from the point of "image wise" formation.

Cyan-forming couplers: These consist almost exclusively of either substituted phenols[16, 17, 18] or napthols[16, 19] (see figure 1.3). They form dyes on coupling that absorb red light in the 600-700nm range.

Magenta-forming couplers: These couplers are designed to produce dyes that absorb light in the range 500-600nm i.e. in the green region of the visible spectrum. A variety of suitable compounds have been used including 5-pyrazolinone[20], indazolone[21], pyrazolobenzimidazole[22] and pyrazolotriazole[23-25] couplers. Of these the 5-pyrazolinone couplers have been most commonly employed in the magenta record of colour photography[9]. The pyrazolotriazole couplers represent a more recent innovation and offer improvements over the pyrazolinone couplers in both thermal stability[12] and spectral 'purity'.

The ideal situation is for the dye couplers to absorb only in the wavelength range required. For magenta dyes, between 500 to 600 nm, cyan, 600 to 700 nm and for the yellow record 400 to 500 nm. Unfortunately deficiencies in the dye's absorption spectra are apparent; in particular cyan and magenta dyes often show unwanted secondary absorption bands at lower wavelengths than the desired primary bands. Yellow dyes are less susceptible to unwanted absorption than the cyan or magenta couplers, but the secondary absorption bands in the cyan and magenta record can present problems with colour degradation for blue and green reproduction together with brightness problems for yellow and red components, especially on printing from negatives[9]. These problems are compensated for by techniques such as masking[26]

and even the use of fluorescent couplers to compensate for loss of coloured coupler sensitivity[27].

1.6 Problems encountered in colour images

1.6.1 Image stability

The photochemical processes involved in seeing a colour photographic image must begin with the illumination of the subject and absorption of light by the photographic dye system. This results in the formation of excited state dye molecules, with electrons in high energy states. The energy involved is of the order necessary to cause chemical bond cleavage and certainly sufficient to produce isomeric rearrangement within a molecule. To prevent image degradation this energy has to be dissipated or released without damage to the photographic system. This can be achieved in one of three ways:

- re-emission as a photon;
- removal via a permanent chemical reaction with a stabiliser via a reaction which does not result in dye destruction;
- dissipation as heat.

There are problems associated with the first two of these routes from the point of view of the production of a photographic record. Re-emission of a photon requires a suitable fluorescent dye, and re-emission can distort the colour record of the film. Permanent chemical reactions are not always efficient and will result in consumption of any stabilisers added to the emulsion. Consequently in most cases the favoured route to a stable dye-coupler system is via thermal dissipation of the excited state energy.

The photochemical degradation of a dye can be separated into two distinct mechanisms[27]: those in which the dye absorbs the

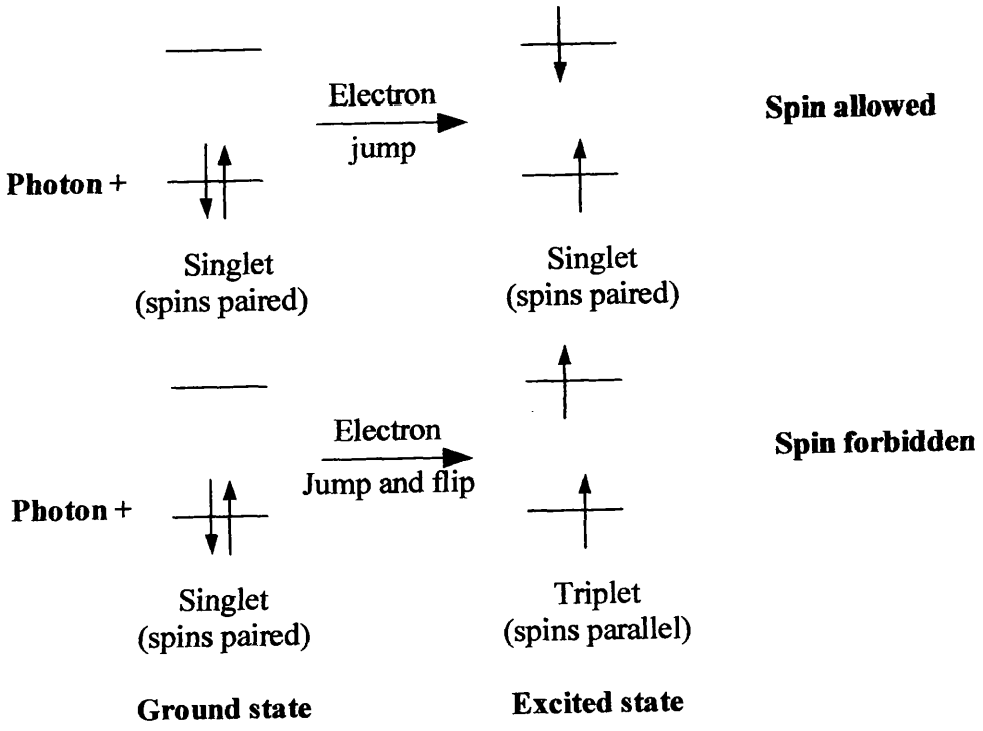

Figure 1.4. Orbital energy level diagram of ground state photon absorption.

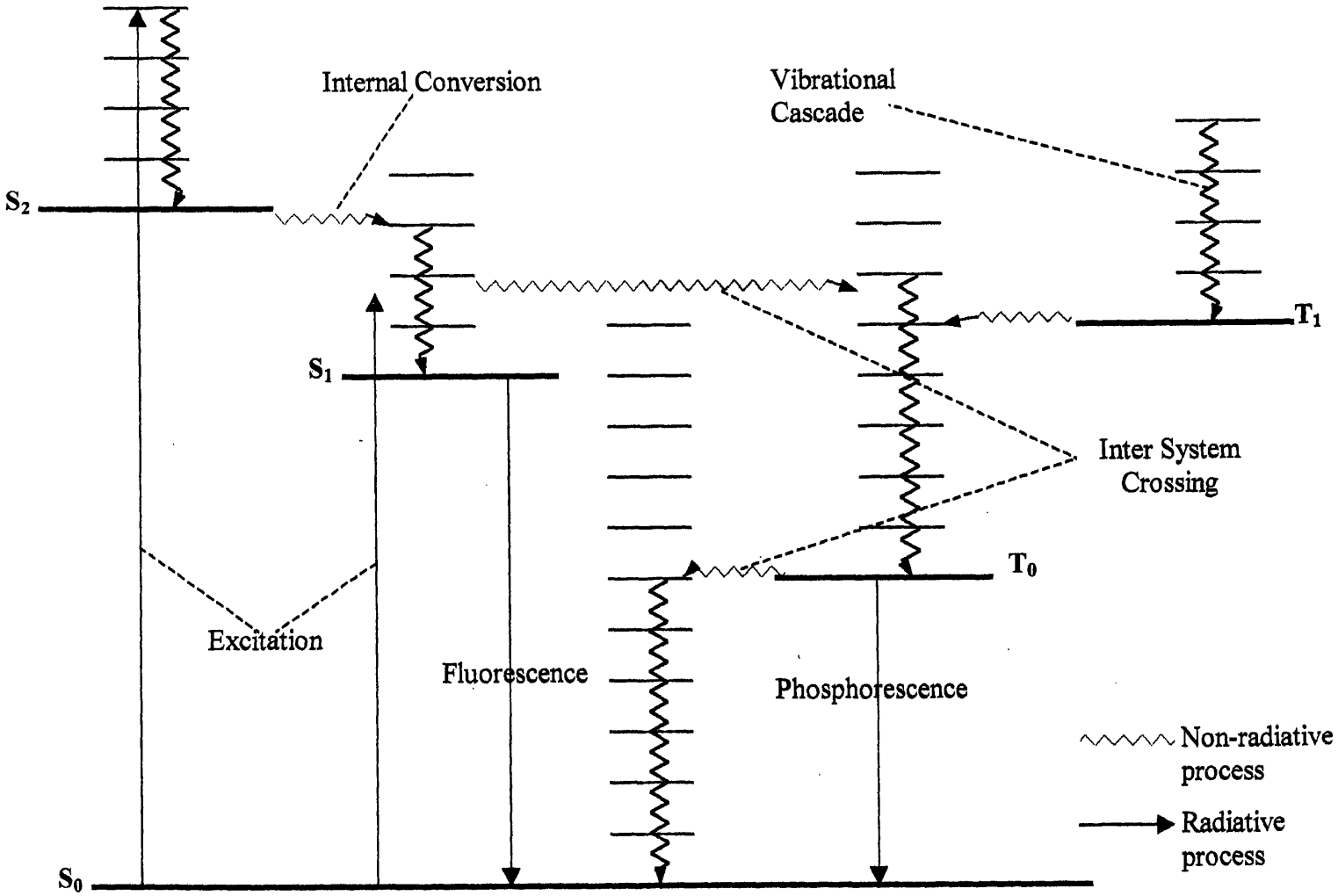

Figure 1.5. Jablonski diagram showing the intermolecular deactivation process of an excited state.

radiation itself; and those in which absorption of a photon occurs via the sensitiser, which then induces dye fading. These can be thought of as primary and secondary processes respectively. A significant discrepancy between the dye absorption and the spectrum of the light causing the degradation, the "action spectrum", suggests the secondary process i.e. the presence of a sensitiser[28].

1.7 Photochemical reactions

Photochemical reactions can be thought of as occurring in three separate steps.

1) The absorption of a photon or the absorptive act; this results in an electronically excited molecule, an electronic isomer.
2) The primary photochemical process.
3) The secondary or dark processes involving the intermediates produced from the primary process.

With the absorption of a photon in the first step a number of electronic isomers are possible. These are shown in figure 1.4. The molecule, if organic, will usually be excited from a ground state singlet to a higher energy singlet state i.e. S_1 or higher S_n. The excited molecule can then undergo photophysical processes to return to the ground state. These are described as radiative or radiationless processes. The radiative processes involve production of a photon during the interconversion to the ground state whilst the radiationless processes involve generation of heat. These processes can be illustrated on an state energy diagram or Jablonski diagram as in figure 1.5.[14]

Clearly, since the most commonly used method of energy dissipation in photographic dyes involves heat dissipation following excitation, the radiationless processes are the most pertinent to understanding their photochemistry.

1.7.1 Image fading

Improving the stability and useful lifetime of dyes and couplers has exercised colour film and paper manufacturers a great deal. All colour print film materials will fade with time, however the rates of fade of different dye components within the film product will not be the same [30].

The stability of colour photographers' materials can be studied under light and dark conditions: i.e. with respect to light fading and dark-fading. Light fading is caused by photochemical/physical reactions induced by visible and near ultraviolet light, whilst dark fading is affected by other environmental conditions such as pH, humidity and temperature. Sources of acidity which cause dye fading are the presence of acidic oxides, particularly sulphur dioxide and nitrogen oxides (NO_X). The presence of ozone in the atmosphere has also been studied as a cause of dye fading[31]. Whilst it has been found that yellow dyes exhibit the most pH sensitivity, all dyes are susceptible to degradation at both high and low pHs[30].

1.8 Magenta dyes

Pyrazolone azomethine dyes have been the main magenta image dyes in colour film production for some years and have been extensively studied[14, 27]. Smith studied the nature of the electronic transitions of these dyes, examining the characteristic x and y bands in a number of solvents together with molecular orbital calculations of these transitions[28, 30]. He concluded that the azomethine dyes existed as either syn- or anti-isomers about the C=N (azomethine bond), see figure 1.6, and that for any dye with R_1= H then the lowest energy state would be the syn isomer. Pyrazolone azomethine dyes do, however, present undesirable features as dyes for use as a photographic record, most notably, secondary absorption characteristics in the blue region (the x band) and relatively poor light stability. The magenta dyes

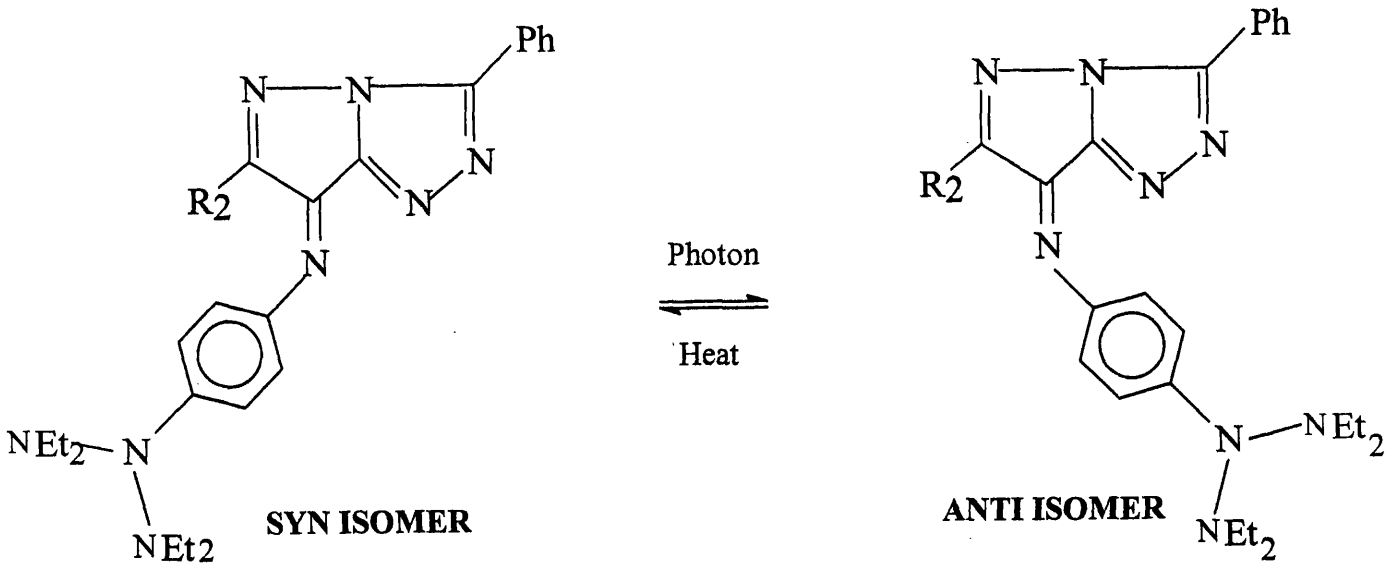

Figure 1.6. Syn – Anti configuration of pyrazolotriazole azomethine dyes.

derived from 5-pyrazalone couplers have been studied with respect to light and dark fading activity[30]. It was found that the dark fading was a result of a dimerising of the dye with unreacted coupler across a C=C bond, whilst the light fading reaction resulted in an azo group being formed. Both routes produce a yellowing of the print[32]. A new family of dyes, the pyrazolotriazole azomethine dyes (PT dyes) were designed to remedy these shortcomings. Developed by Bailey in 1977[31], the photochemistry and acid/base reactivity of these compounds forms the subject matter of this thesis.

Figure 1.7. Structures of pyrazolotriazole azomethine dyes. In this study most emphasis was placed on the $R_2 = CO_2Et$ form. That is the $6CO_2Et$-PT dye.

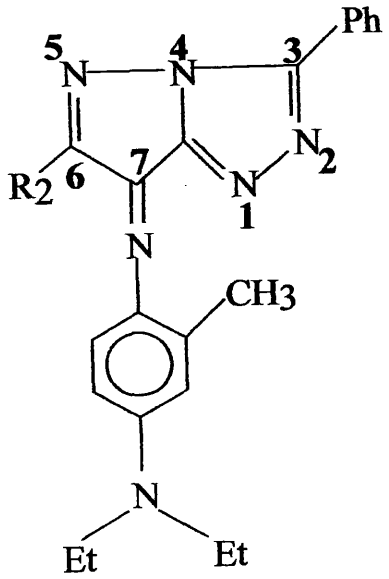

Identity of R_2 group
H
CO_2Et
CH_3
CF_3
SO_2Me
NHPh
COPh

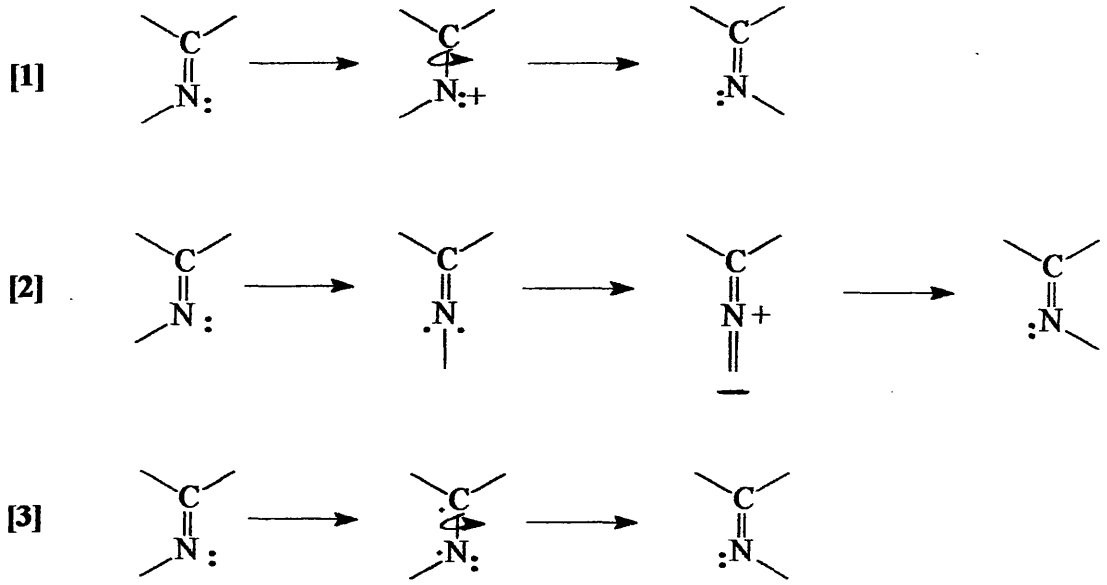

Figure 1.8. Mechanisms possible for syn-anti isomerisation in PT-dyes.
[1+3] Torsion or twist mechanisms.
[2] Linear inversion or lateral shift mechanism.

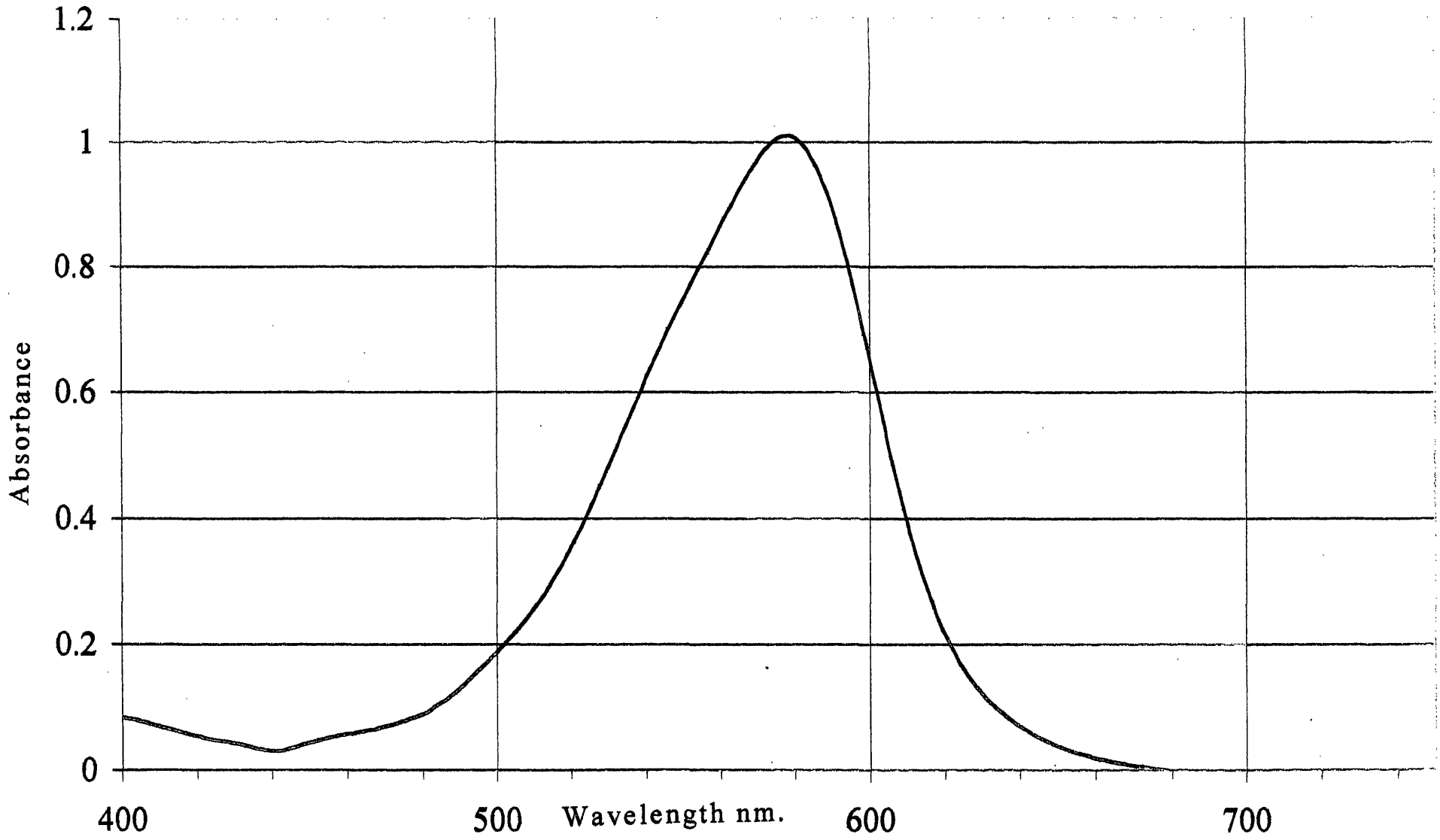

Figure 1.9 Absorption spectrum 6H-PT dye in chloroform (298K).
Dye concentration = 2×10^{-5} mol dm^{-3}

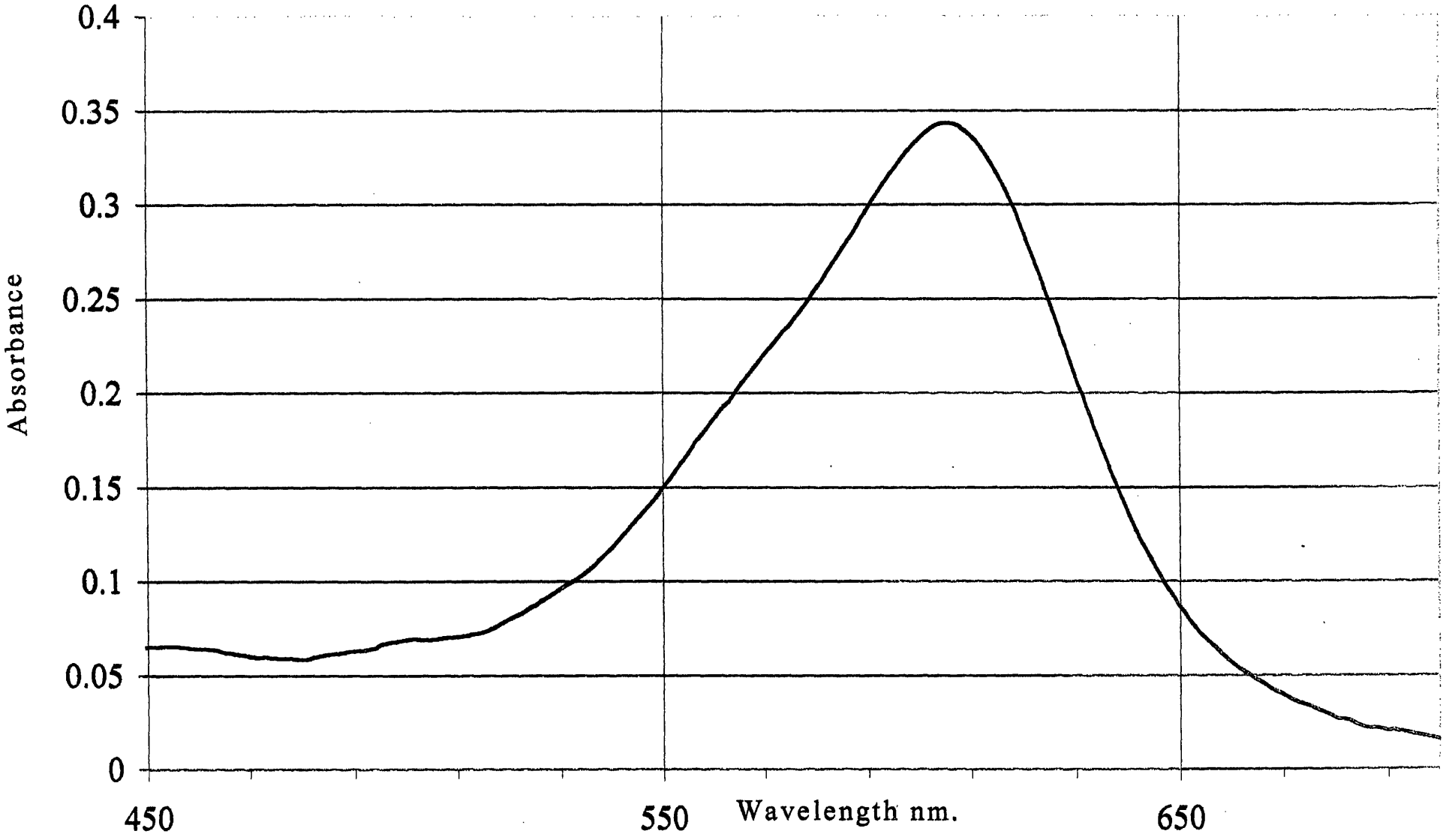

Figure 1.10 Absorption spectrum $6CO_2Et$-PT dye in chloroform (298K).
Dye concentration = 5.2×10^{-6} mol dm^{-3}

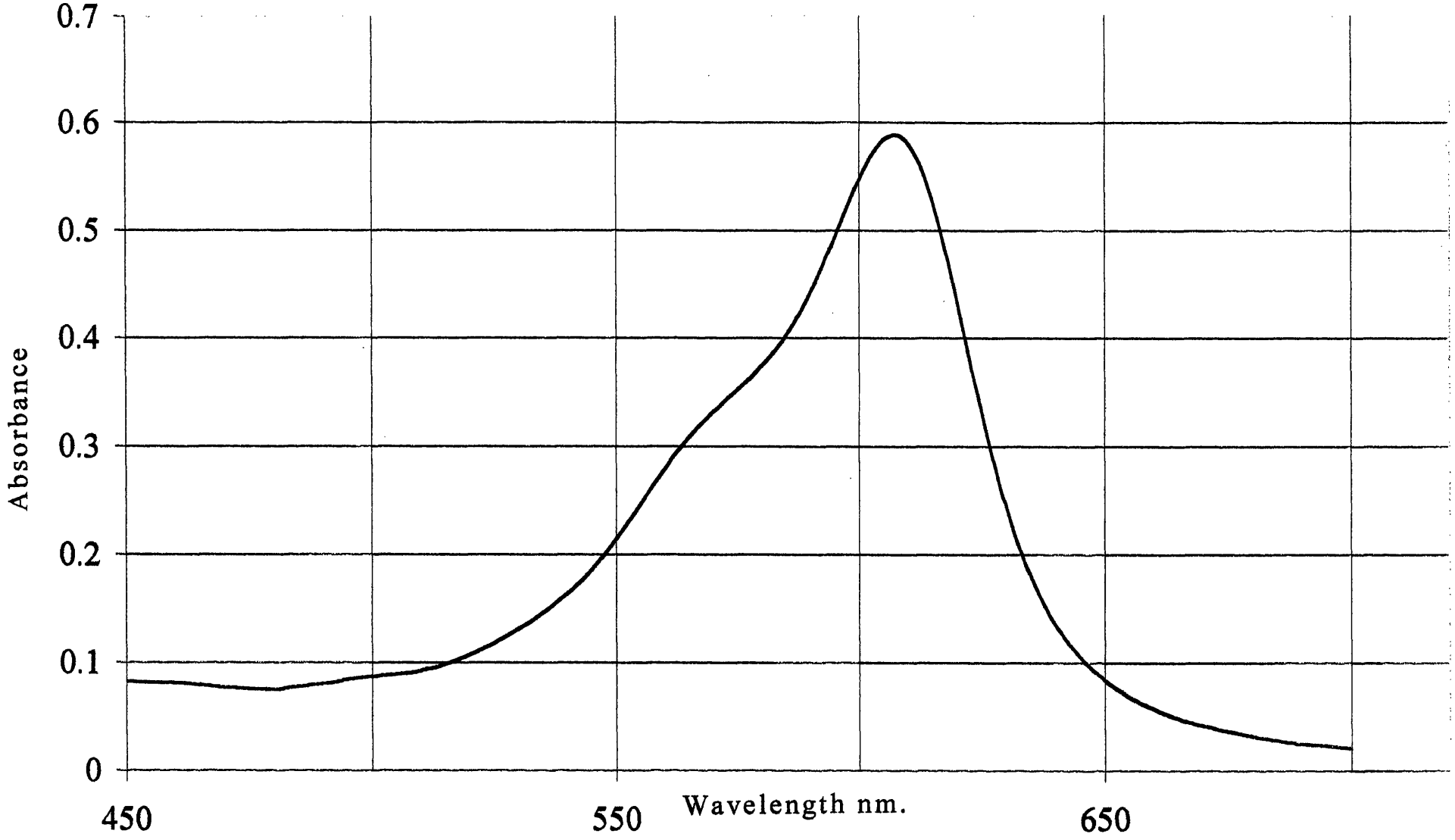

Figure 1.11 Absorption spectrum $6CF_3$–PT dye in chloroform (298K).
Dye concentration = 1.2×10^{-5} mol dm^{-3}

The general structure of the pyrazolotriazole azomethine dyes is given in figure 1.7. They are prepared via "oxidative coupling" or by condensation with a ketocoupler and a p-phenylenediamine. Typical PT dye spectra are shown in figures 1.9, 1.10, 1.11.

The singlet lifetimes of PT dyes are very short at room temperatures. Use of pico-second absorption and emission studies by Douglas et al[33] have shown three transient states in pyrazolotriazole azomethine dyes in fluid solution. It was possible to assign one transient to the fluorescent singlet state whilst the other two were assigned to a twisted excited singlet and a twisted ground-state conformation. It has also been shown that the PT dyes have a longer lived triplet state, a higher triplet energy and probably a higher triplet quantum yield than their pyrazolone analogues. Pyrazolone azomethine dyes photodegrade via both lowest energy singlet and triplet states; both fade routes could well be expected to be enhanced for the PT-azomethine dyes as described by Douglas[34].

1.8.1 Isomerisation

The azomethine dyes undergo direct and triplet-sensitized syn-anti isomerisation. This has been extensively studied and reported by Herkstroeter[32]. Flash photolysis generates a mixture of syn-anti isomers (see figure 1.6).

Evidence for the existence of syn- anti isomers of yellow, cyan, and magenta pyrazolone, azomethine dyes was obtained by Herkstroeter[15] when he observed metastable transients produced on flash photolysis of dyes in solvents at room temperature. He also observed an increase in isomer transient yield via energy transfer from triplet sensitizers with no effect from dissolved oxygen on the transients in the absence of the triplet sensitizer (this proves interesting in the light of work carried out on PT dyes in this study, see chapter 2). This work suggests that isomerisation occurs via the lowest excited singlet state when induced by the direct absorption of light[15].

The reactions that may occur immediately prior to isomerisation are of particular interest, since examples of dyes which cannot undergo isomerisation e.g. azine dyes[15], where the C=N bond is unable to rotate via the mechanism discussed, show enhanced fluorescence, high triplet yields, long-lived triplet states and poor light stability.

1.8.2 Isomerisation mechanisms

There are two postulated mechanisms for the syn-anti isomerisation about a C=N bond, see figure 1.8 [1]. The "torsion" mechanism involves a *rotation* about the C=N bond promoted by a reduction in double bond character i.e. $sp^2 > sp^3$ during the transition state, however the nitrogen atoms electrons remain sp^2 hybridised throughout as indicated by the C=N-C bond angle.

The "inversion" mechanism [2], sometimes called the 'lateral shift mechanism', results in an increase in bond angle from 120^0 to 180^0 due to a change in hybridisation from sp^2 to sp.

Work carried out on a series of dyes with varying substituents at the para position of the aromatic ring, and methyl groups at the 6- position [3,4], allowed Herkstroeter to arrive at Hammett plots for substituents on these azomethine dyes[32]. These plots were found to be V- shaped, with ρ changing from negative to positive at a σ value of about 0. This was interpreted as indicating that electron donating groups favour the torsion mechanism, whilst electron withdrawing groups favour the inversion mechanism.

1.9 This study

In recent years a good deal of attention has been paid to the dyes used in the formation of the magenta record of multilayer colour photography. The pyrazolone azomethine dyes used exhibit certain undesirable characteristics, some of which have been discussed in the previous sections, and this has led to an interest in the pyrazolotriazole azomethine dyes.

Pyrazolotriazole azomethine dyes are the subject of this thesis, and the structures of the dyes used in this work are shown in figure 1.7. Typical visible spectra are shown in figures 1.9, 1.10 and 1.11.

1.10 Conclusion

Since the late nineteenth century, there has been a steady evolution in the development of photographic chemistry. The goal has always been to develop a faithful, stable colour image. This has relied upon the development of couplers (figures 1.2, 1.3 and 1.7), that form yellow cyan or magenta colour dyes in the film layers. Stability of these dyes is affected by two sets of factors:

- light fading (photochemical processes);
- dark fading (pH effects, temperature etc).

Not all colour dyes are affected by these factors to the same degree [30].

Pyrazolotriazole azomethine dyes are used in the magenta record of colour film. This study examines these dyes in particular their photochemical stability and rate of fade in acidic and basic media where they should offer significant improvements on the stability of pyrazolone azomethine dyes.

2. PHOTOCHEMICAL REACTIONS

2.1 Introduction

Steady-state and microsecond flash photolysis techniques have been employed by a number of workers in studying the absorption and emission properties of pyrazolone and pyrazolotriazole azomethine dyes, see, for example Herkstroeter[15], Wilkinson et al [35], Wilkinson et al [36], Douglas et al [33], Douglas [34], Douglas and Townsend[37], Douglas and Clarke [38]. Flash excitation generates a non-equilibrium mixture of isomers, in both syn and anti configurations which relax over the micro/millisecond timescale, to give, at ambient temperatures, one isomer in preference to the other. NMR studies using the NOE[39] experimental technique by Douglas reveal that the 6H-PT dye exists in the syn configuration at room temperature[34].

In this chapter results from microsecond flash photolysis studies of the PT-dyes are presented. The main thrust of this work has been to examine the combined effects of oxygen and excitation wavelength on the transient isomer yield.

2.2 Transient difference spectra

The change in absorption at different wavelengths at a specified time after the flash (typically 5 ms) was determined and plotted against the wavelength. Figures 2.1 and 2.2 show such spectra for $6CO_2Et$-PT in a polar medium i.e. acetonitrile and in a non-polar medium, n-hexane. As can be seen the thermally unstable isomer shows an absorption which is shifted about 30-50nm to the red from that of the ground state isomer.

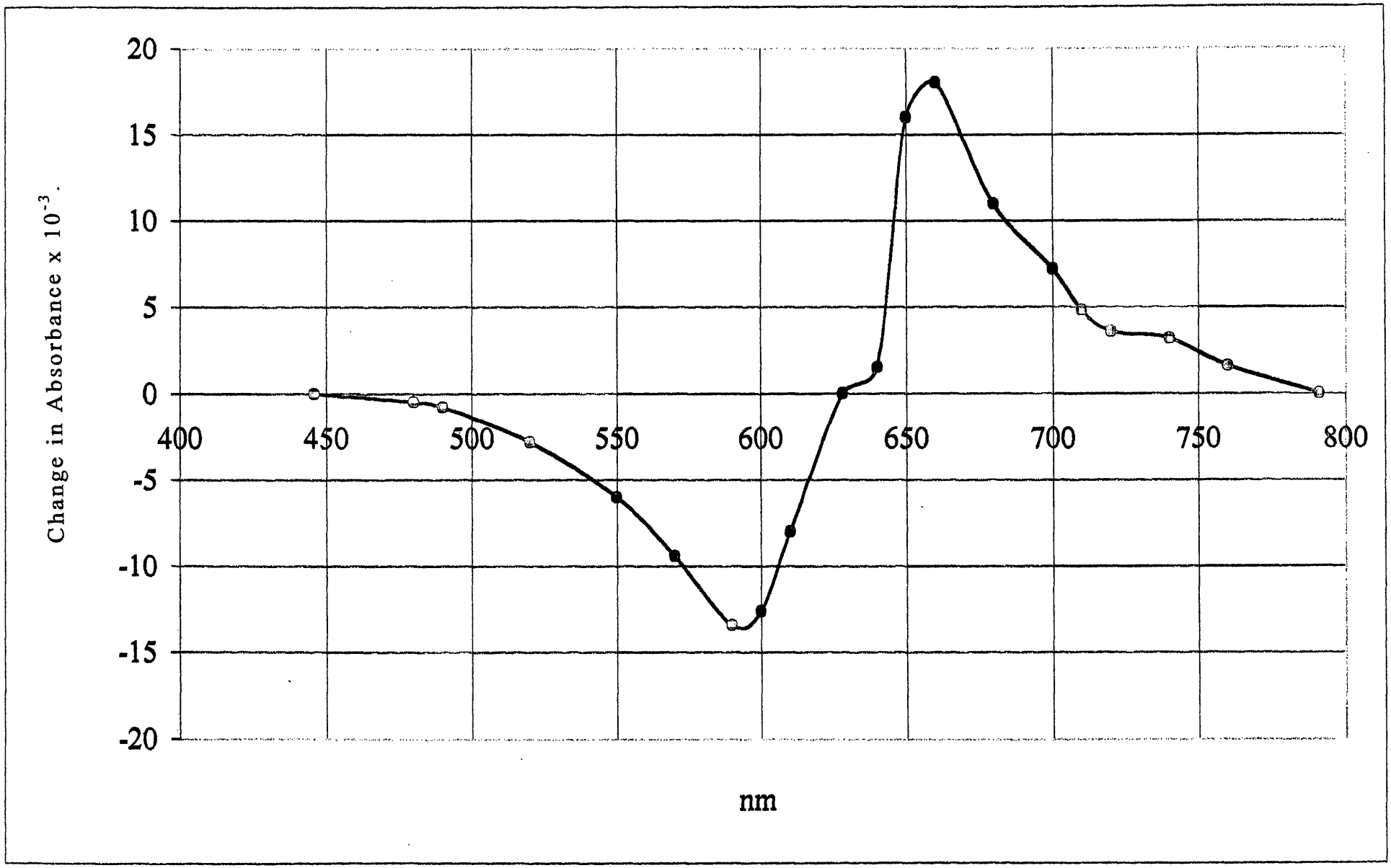

Figure 2.1. Transient difference spectrum $6CO_2Et$-PT dye in acetonitrile (298K)

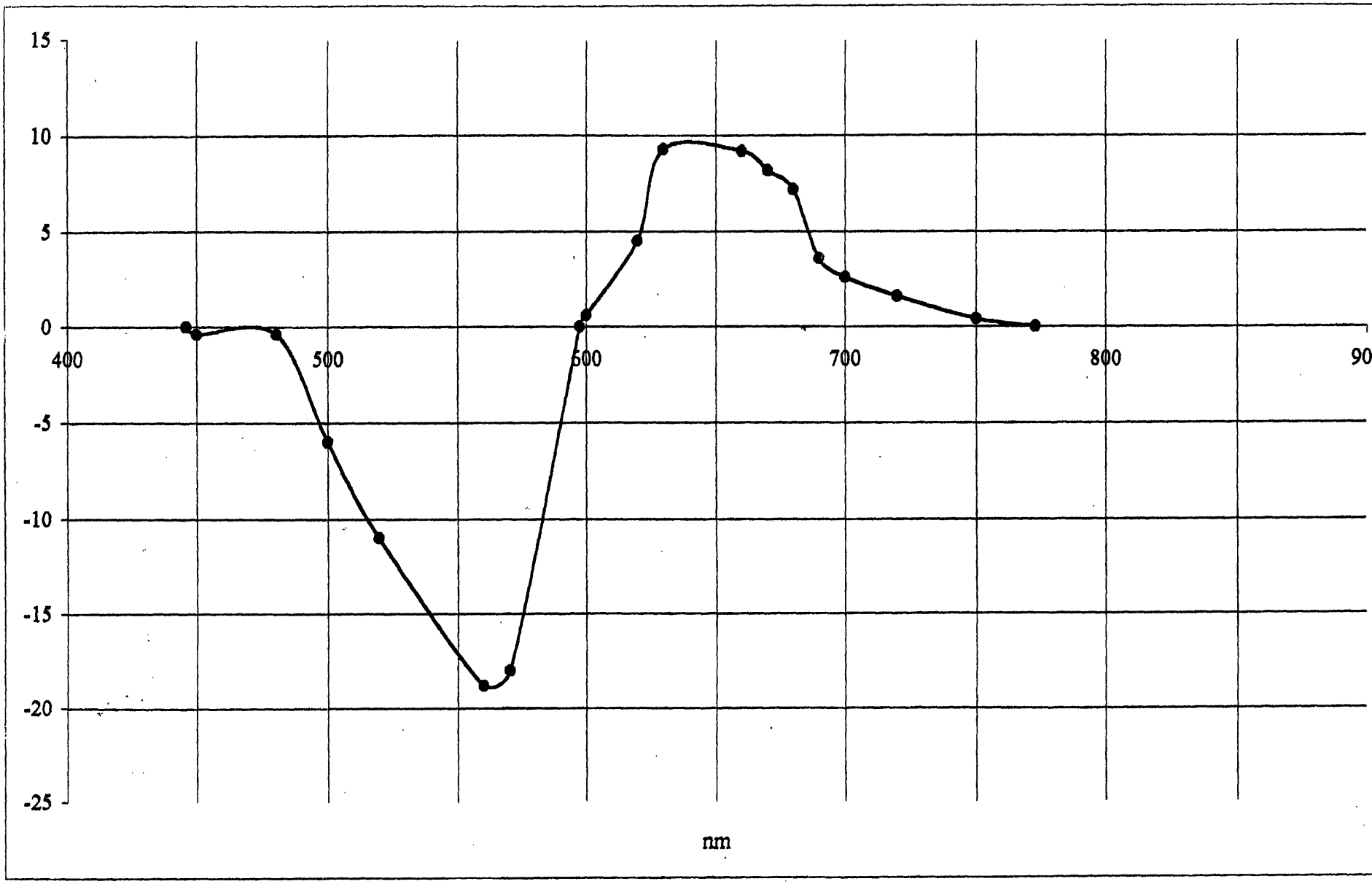

Figure 2.2. Transient difference spectrum $6CO_2Et$-PT dye in hexane (298K)

2.3 Solvent effects

The relaxation process by which the ground state isomer composition is restored is a first order process and solvent effects on the rate constant for the thermal back isomerisation of $6CO_2Et$-PT were investigated.

Figure 2.3 shows a typical isomerisation decay curve and the appropriate first order linear analysis. Table 2.1 collects rate constants for this process in three solvents: one non-polar, one polar but non-H bonding, and one polar and H-bonding.

Figure 2.3.a) Flash photolysis data $6CO_2Et$-PT dye in acetonitrile (298K). Absorbance against time (ms).

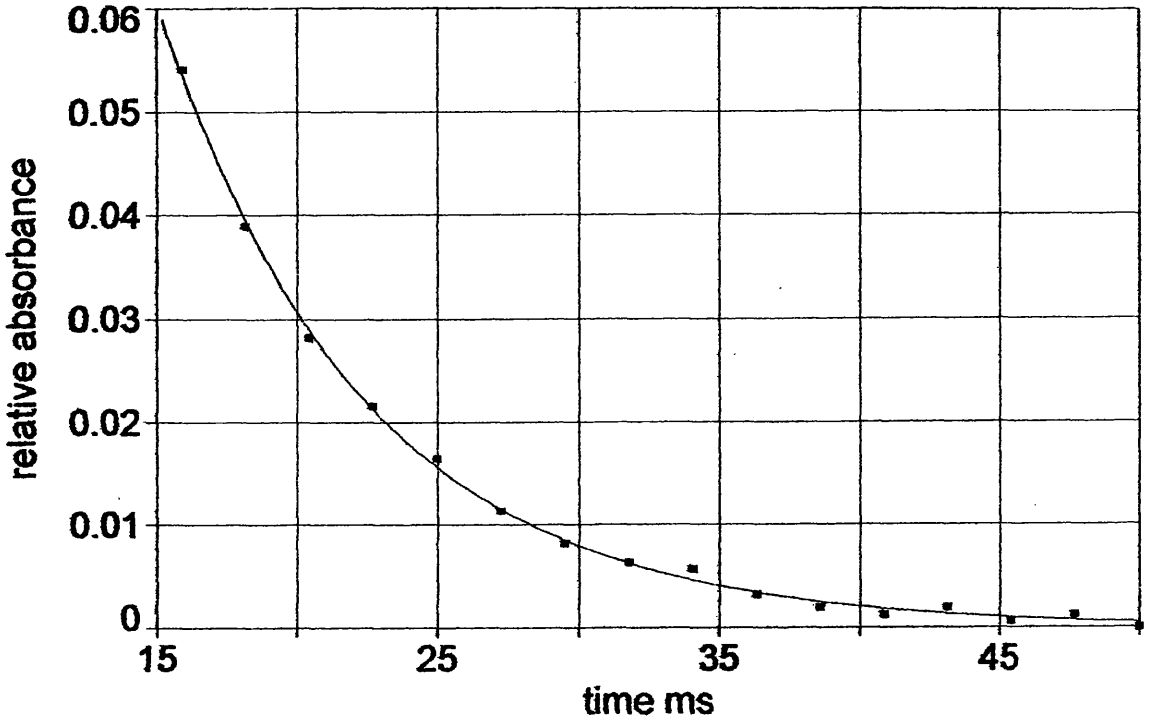

Figure 2.3.b) Flash photolysis data $6CO_2Et$-PT dye in acetonitrile (298K). log absorbance against time (ms).

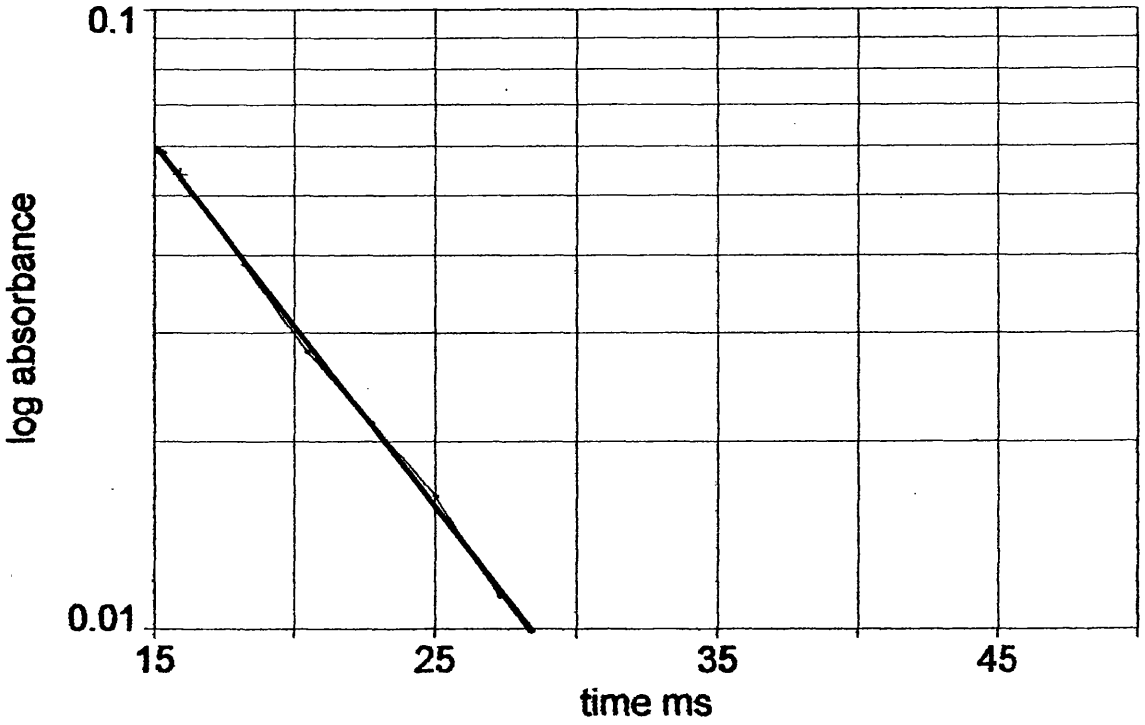

TABLE 2.1

Solvent effects on λ_{max} and thermal isomerisation rates for $6CO_2Et$-PT

Solvent	Dye	λ_{max}/nm	k/ s^{-1}
Acetonitrile	***$6CO_2Et$-PT***	605	140 (+/- 10)
n-Hexane	***$6CO_2Et$-PT***	608	770 (+/- 50)
Ethanol	***$6CO_2Et$-PT***	608	600 (+/- 40)

A comparison of solvent solvatochromic parameters with observed rates is given below. The π^* factor is an index of the solvent dipolarity/polarisability, the β factor a scale of hydrogen-bond acceptor basicity i.e. the ability of the solvent to donate an electron pair.

TABLE 2.2[40]

A comparison of rate data with solvatochromic parameters

SOLVENT	Rate constant	π^*	β	ε	η
Acetonitrile	140	0.75	0.31	35.94	1.44
n-Hexane	766	-0.08	0.00	1.89	0.766
Ethanol	605	0.54	0.77	24.3	0.789

The results show no obvious relationship between the solvent solvatochromic parameters given and the rates of relaxation; this suggests that solvent factors such as dielectric properties and basicity are not uniquely significant in determining the relaxation times of the dye isomers. This conclusion has also been drawn by Wilkinson et al[36].

2.4 The effect of oxygen concentration on isomer yield

Wilkinson et al[35, 36] reported no observable effect of oxygen on the isomerisation yields of any of the pyrazolotriazole azomethine dyes they studied. Herkstroeter working with azomethine dyes reports that molecular oxygen is a potential quencher of the dye triplet state[41]. Work by Kearns indicates that molecular oxygen could also quench the singlet states of the azomethine dyes studied[42]. The quenching reactions for the triplet states are mechanism one - energy transfer:

$$^3D^* + {}^3O_2 \longrightarrow {}^1D + {}^1O_2^* \qquad (1)$$

$$^3D^* + {}^3O_2 \longrightarrow {}^3(^3D\ {}^3O_2)^* \longrightarrow {}^1D + {}^3O_2 \qquad (2)$$

and for the singlet state[42] mechanism two - electron transfer:

$$^1D_1^* + {}^3O_2 \longrightarrow D^+ + O_2^- \qquad (3)$$

$$\longrightarrow {}^3D_1^* + {}^3O_2^* \qquad (4)$$

For molecular oxygen to quench either state the lifetime of the state must be sufficiently long for oxygen at the concentration found in air-equilibrated solvents (typically 10^{-3} mol dm^{-3} in most organic solvents)[40] to intercept the excited state. Taking a diffusion controlled rate of about 10^{10} mol dm^{-3} s^{-1} as the maximum possible quenching rate constant, then a minimum lifetime of 10^{-8}s is required[15]. Given the results from previous studies[37], it seems unlikely that either the singlet or the triplet states of the azomethine dyes will be sufficiently long lived to be efficiently quenched by oxygen. However, Douglas found a very small effect of oxygen on isomer yield when studying the PT dyes[29].

2.4.1 Results

Figure 2.4 shows isomer decay curves for $6CO_2Et$-PT in acetonitrile under a) nitrogen and b) air atmospheres. Kinetic analysis is shown in figures 2.5 and 2.6. The data show that the isomer yield is significantly quenched by oxygen while the rate of the thermal back reaction remains the same in an air atmosphere as in a nitrogen atmosphere. This was such an unexpected result that this experiment was repeated for a number of dyes in different solvents. Table 2.3 collects the results in terms of the ratio of isomer yield recorded under a nitrogen atmosphere and under air i.e. ($A[N_2]/A[O_2]$). Figures 2.7 and 2.8 and 2.9 show kinetic data for the 6COPh-PT dye which also showed significant oxygen quenching of isomer yield.

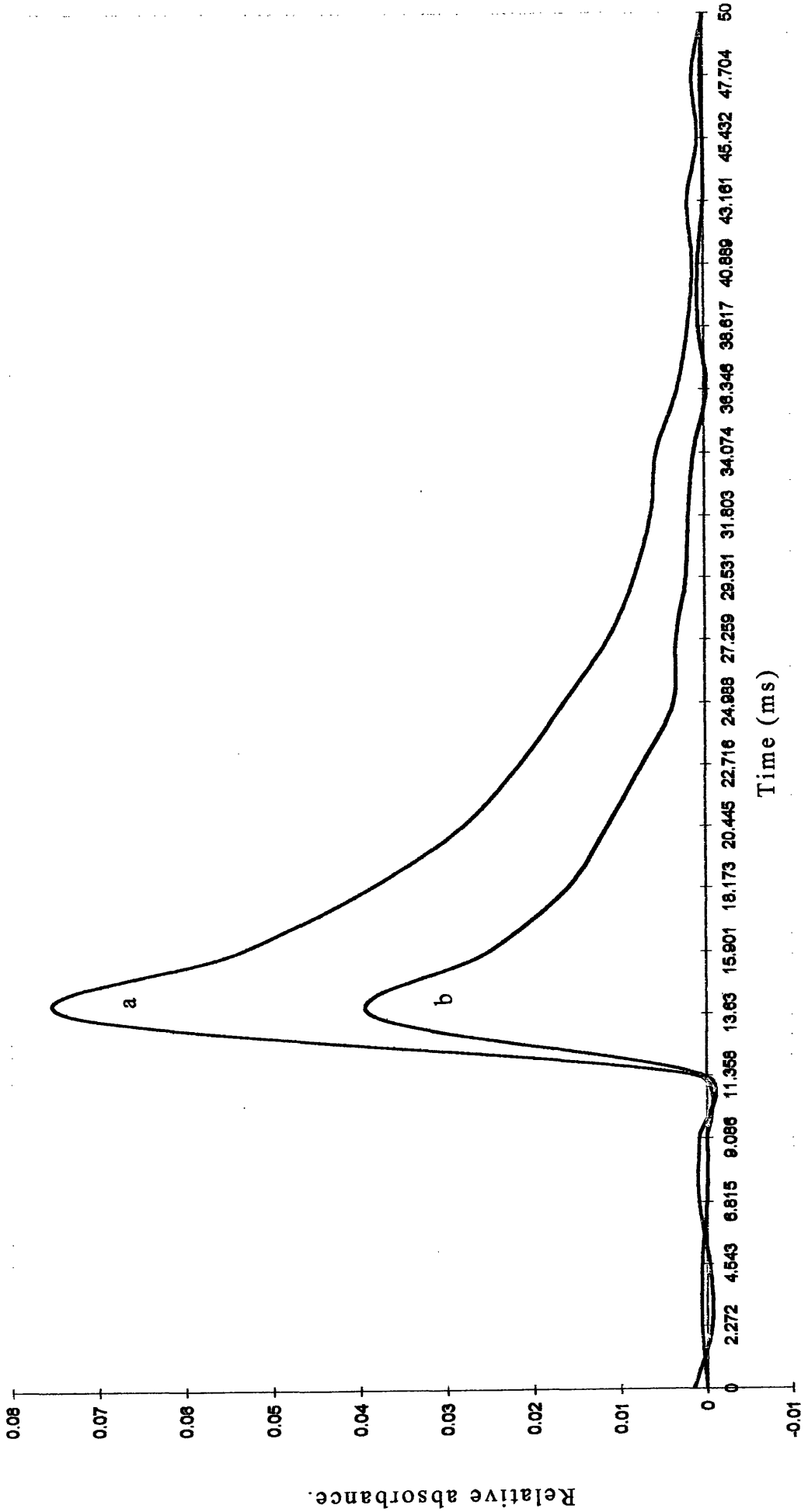

Figure 2.4. Flash photolysis data $6CO_2Et$-PT dye in acetonitrile (298K). a) Purged with nitrogen. b) air equilibrated. Dye concentration = 1.14×10^{-6} mol dm^{-3}

Figure 2.5.a) Flash photolysis data $6CO_2Et$-PT dye in acetonitrile (298K: air equilibrated). Relative absorbance against time (ms).

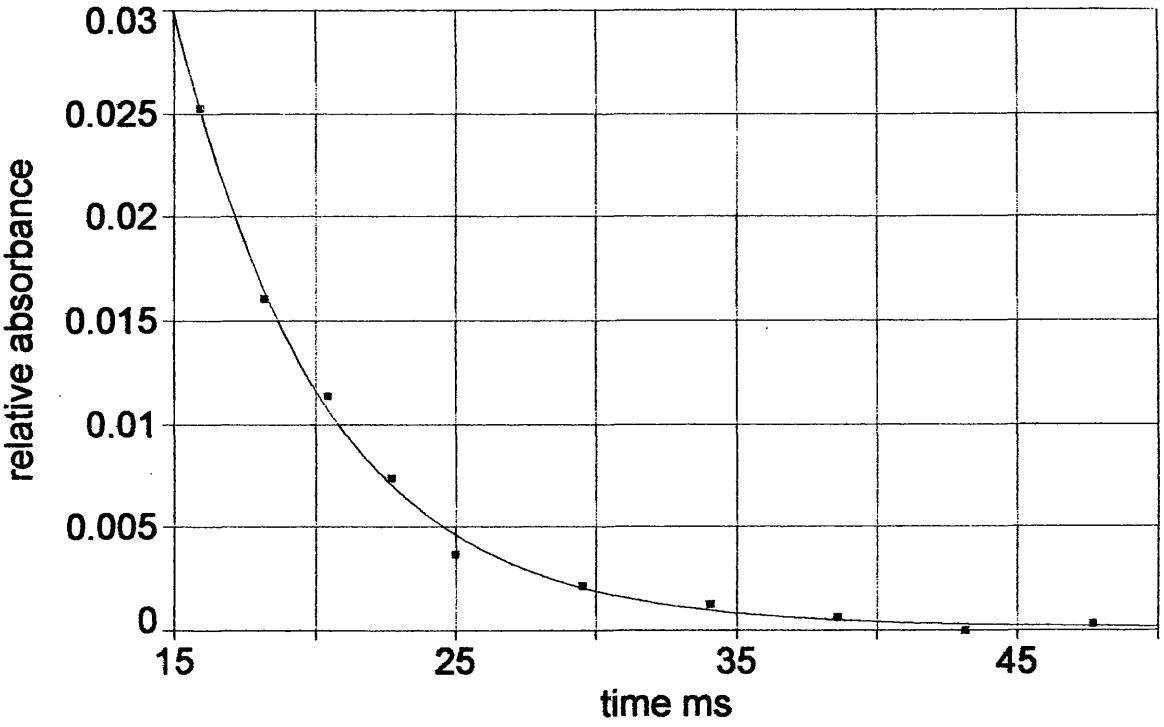

Figure 2.5.b) Flash photolysis analysis $6CO_2Et$-PT dye in acetonitrile (298K: air equilibrated). Log relative absorbance against time (ms).

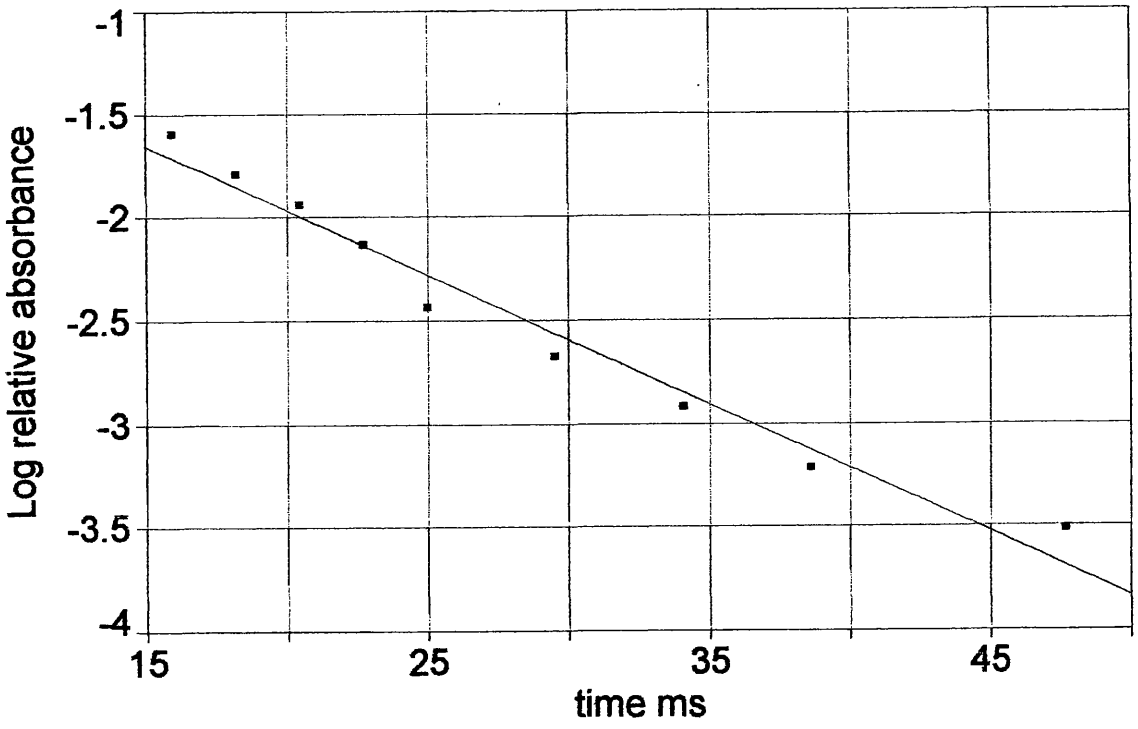

Figure 2.6.a) Flash photolysis data $6CO_2Et$-PT dye in acetonitrile (298K: purged with nitrogen). Relative absorbance against time (ms).

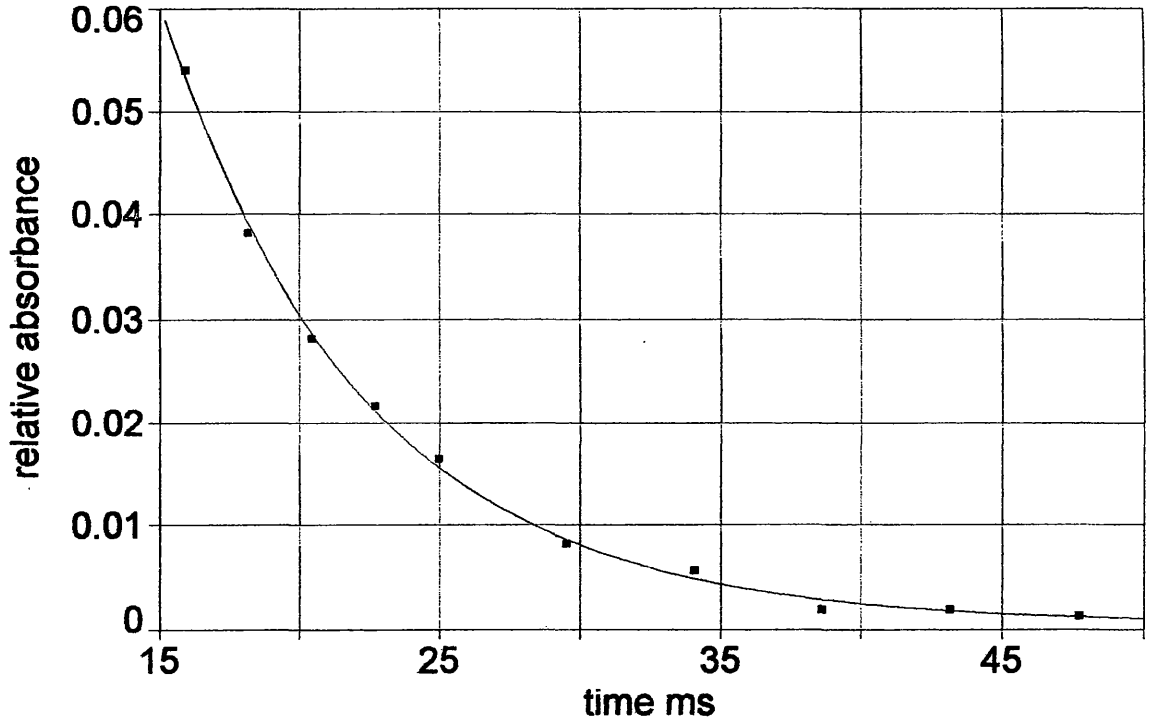

Figure 2.6.b) Flash photolysis analysis $6CO_2Et$-PT dye in acetonitrile (298K: purged with nitrogen). Log absorbance against time (ms).

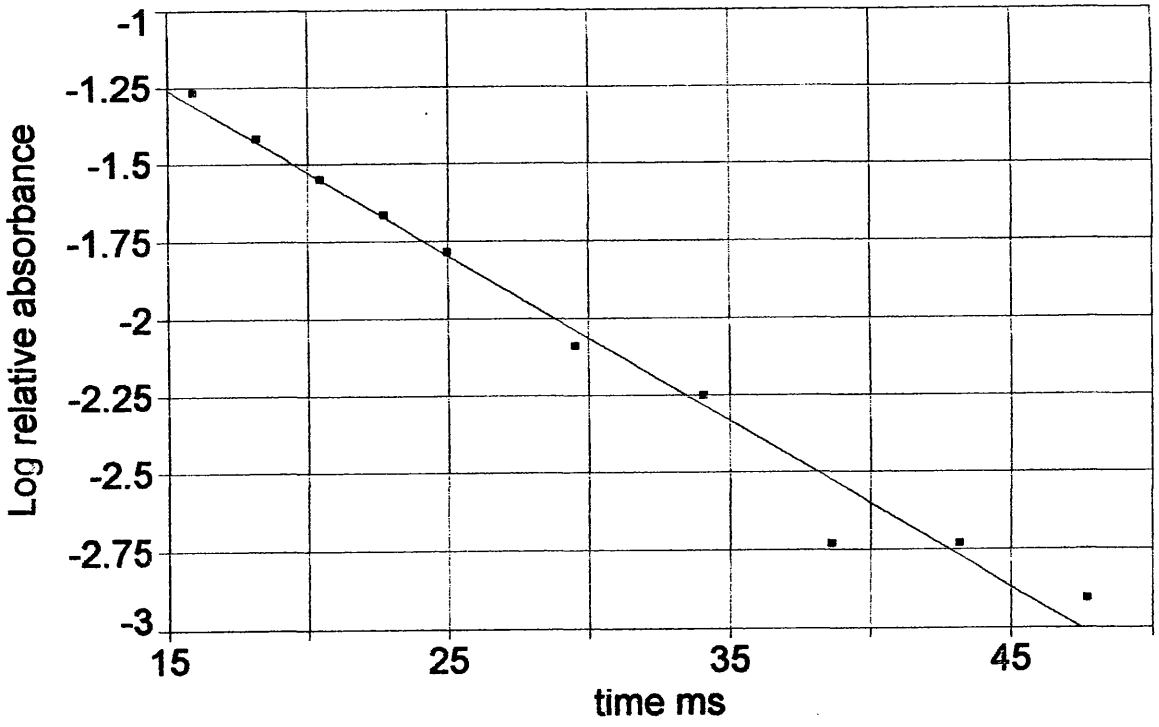

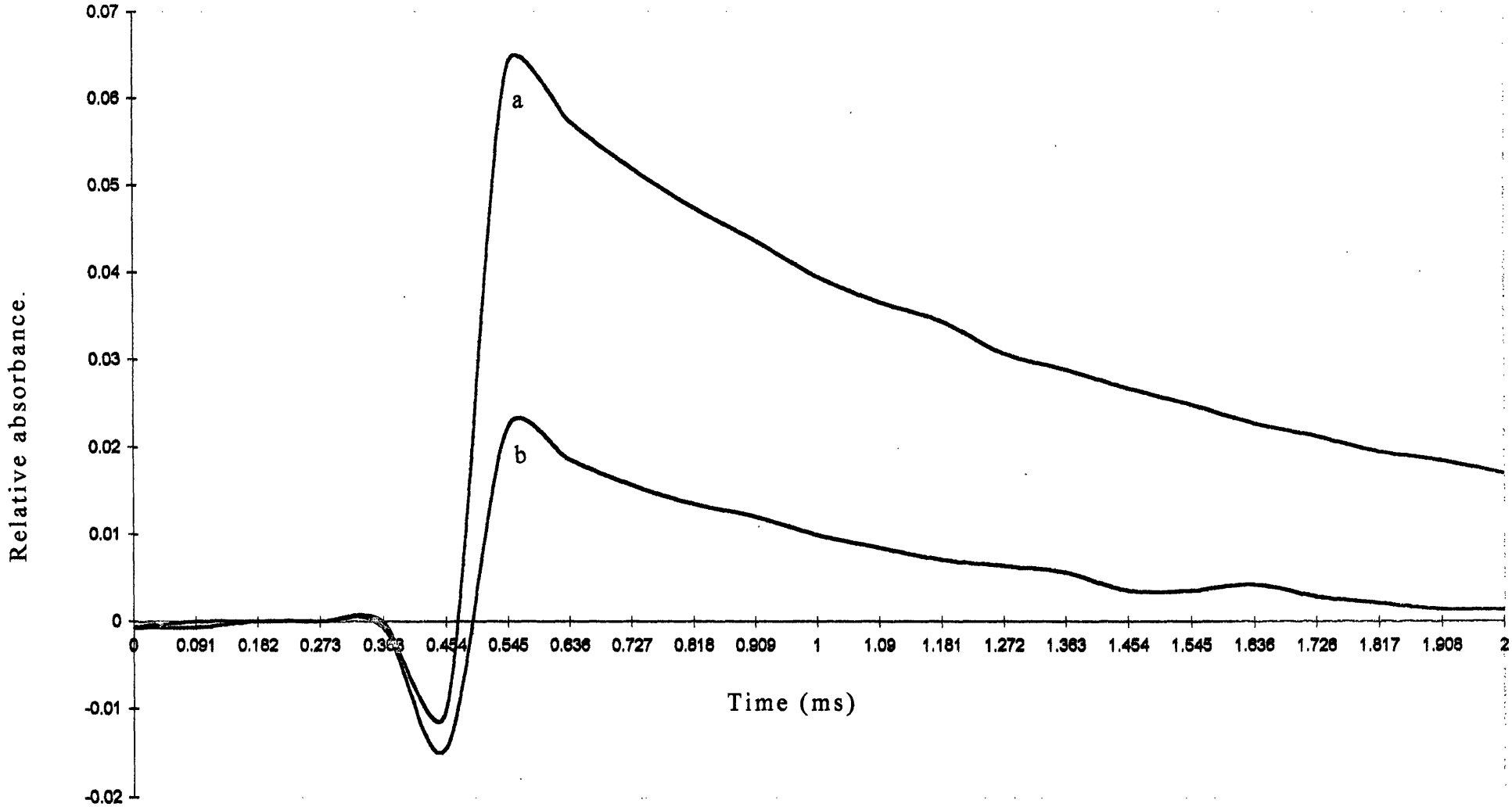

Figure 2.7. Flash photolysis data 6COPh-PT dye in acetonitrile (298K). a) Purged with nitrogen. b) air equilibrated.
Dye concentration = 1.1×10^{-7} mol dm^{-3}

Figure 2.8.a) Flash photolysis data 6COPh-PT dye in acetonitrile (298K: air equilibrated). Relative absorbance against time (ms).

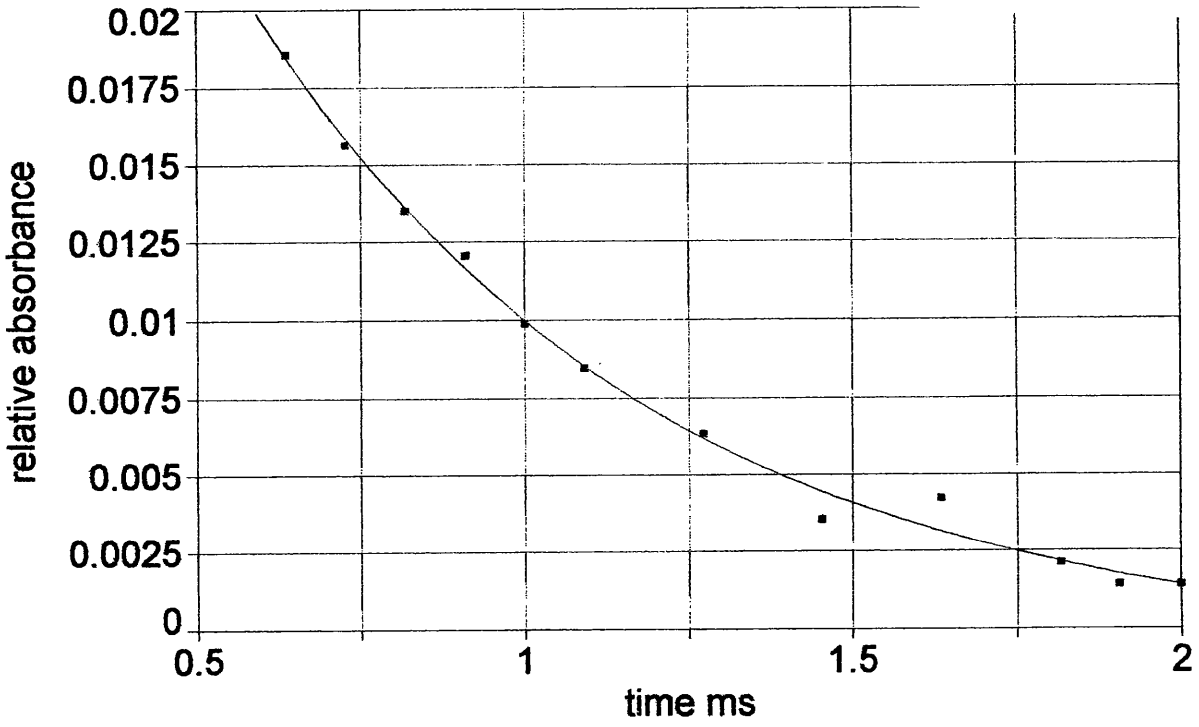

Figure 2.8.b) Flash photolysis analysis 6COPh-PT dye in acetonitrile (298K: air equilibrated). Log relative absorbance against time (ms).

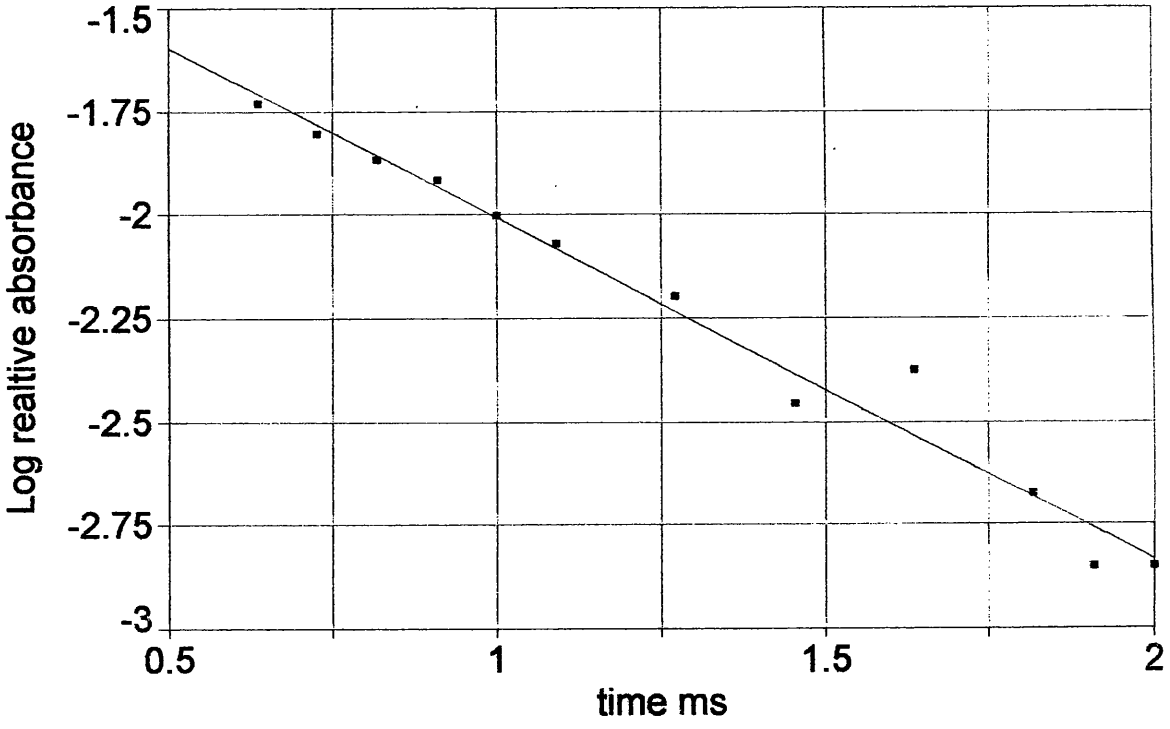

Figure 2.9.a) Flash photolysis data 6COPh-PT dye in acetonitrile (298K: purged with nitrogen). Absorbance against time (ms).

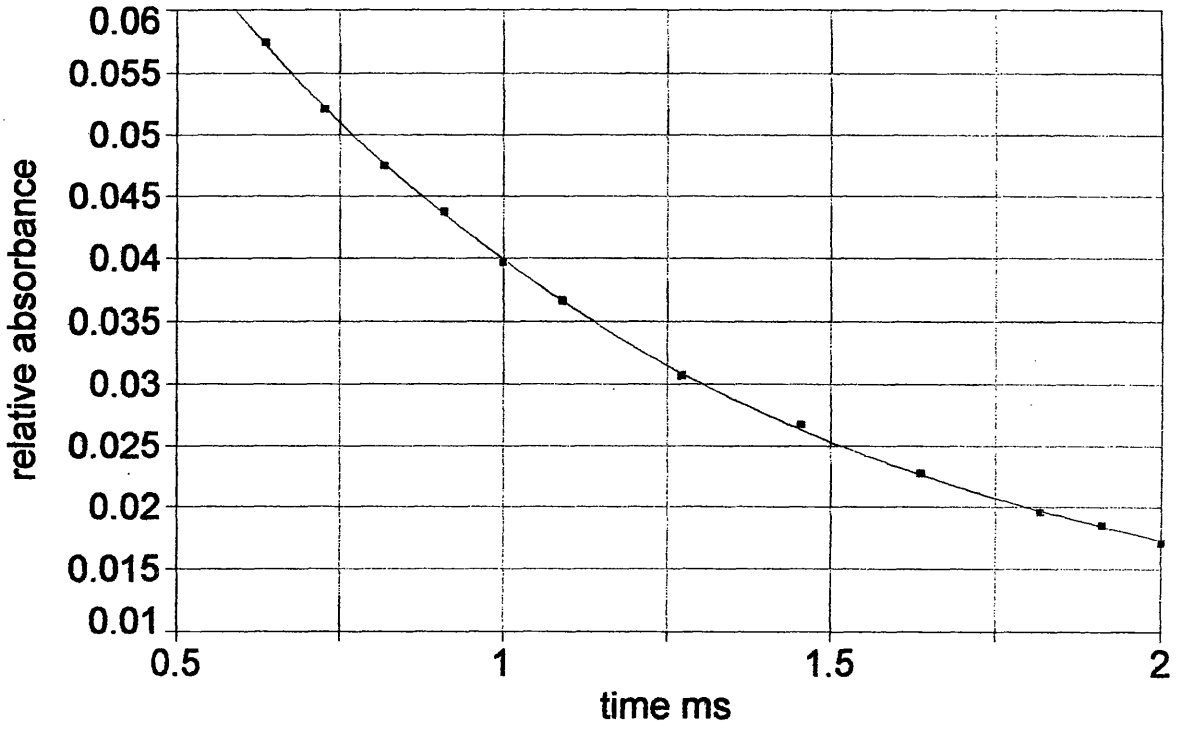

Figure 2.9.b) Flash photolysis analysis 6COPh-PT dye in acetonitrile (298K: purged with nitrogen). Log absorbance against time (ms).

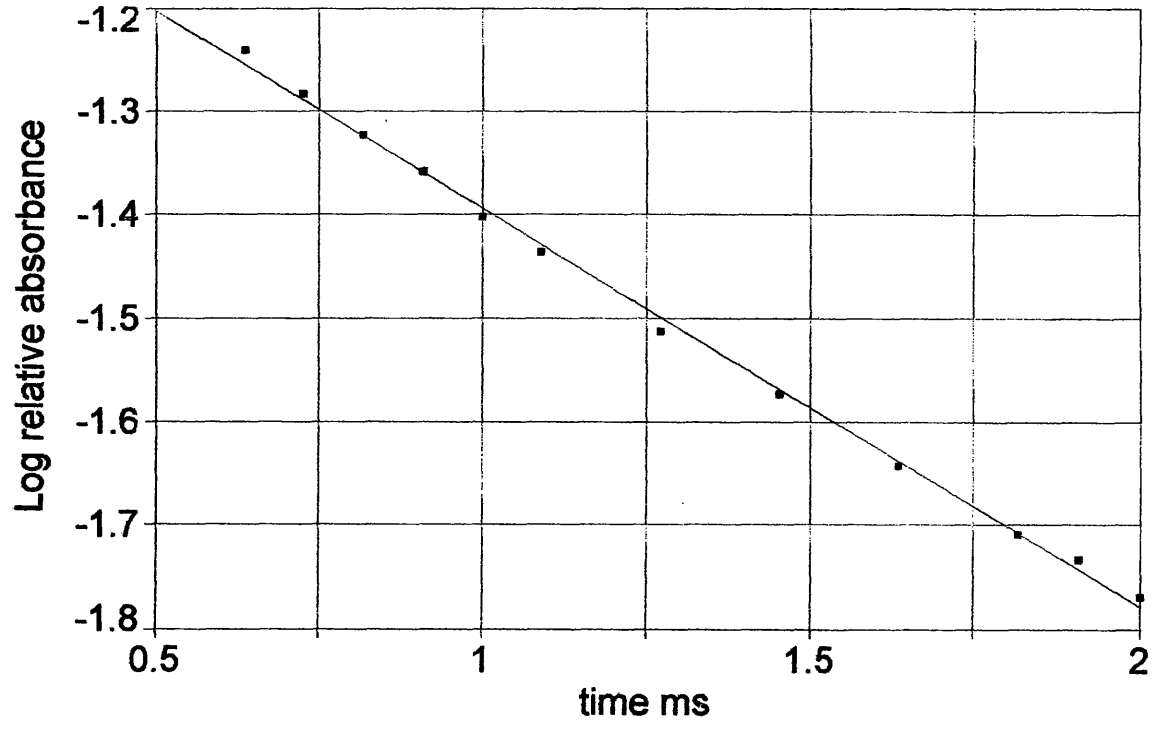

TABLE 2.3

Effects of oxygen quenching on isomer yield

DYE	SOLVENT	$\Delta A(N_2)/\Delta A(Air)$
$6CO_2Et$-PT	n-hexane	3.80 (+/- 0.35)
6H-PT	n-hexane	0.98 (+/- 0.05)
$6CO_2Et$-PT	acetonitrile	2.90 (+/- 0.3)
6H-PT	acetonitrile	1.00 (+/- 0.05)
$6CF_3$-PT	n-hexane	1.00 (+/- 0.05)
6COPh-PT	n-hexane	2.5 (+/- 0.3)

As can be seen both the 6H-PT and $6CF_3$-PT dyes give identical isomer yield under nitrogen and air whilst both the $6CO_2Et$-PT and 6COPh-PT dyes give an enhanced isomer yield under nitrogen as compared to air.

Similar studies were carried out with $6CO_2Et$-PT in methanol and ethanol. However uv-excitation in these solvents resulted in a bleaching of the dye which did not recover on standing, suggesting u.v. photolysis. The 6COPh-PT dye was also examined in ethanol and methanol, but again the result of irradiation following oxygen purging was irreversible bleaching of the dye.

As table 2.3 shows for $6CO_2Et$-PT the ratio of isomer yield under nitrogen and air is solvent dependent. It was thought that their behaviour might be due to the different absorption characteristics of the solvents used and for this reason filters were introduced into the flash-photolysis experiments to study the effects of excitation wavelength on isomer yield. The filters used have cut-off wavelengths in the 300-400 nm region. Both the 6H-PT and the $6CO_2Et$-PT dyes were examined. The results are collected in a table 2.4. From this it can be seen that the 6H-PT dye shows no oxygen quenching of isomer yield under

any isomer conditions. However, the degree of oxygen quenching of isomer yield for the $6CO_2Et$-PT decreases as the excitation wavelength increases, such that upon excitation with light of wavelength much greater than or equal to 400nm, no oxygen quenching is observed. Figure 2.10 shows the effect of cut-off filter wavelength on $A(N_2)/A(O_2)$ response for the $6CO_2Et$-PT dye in hexane.

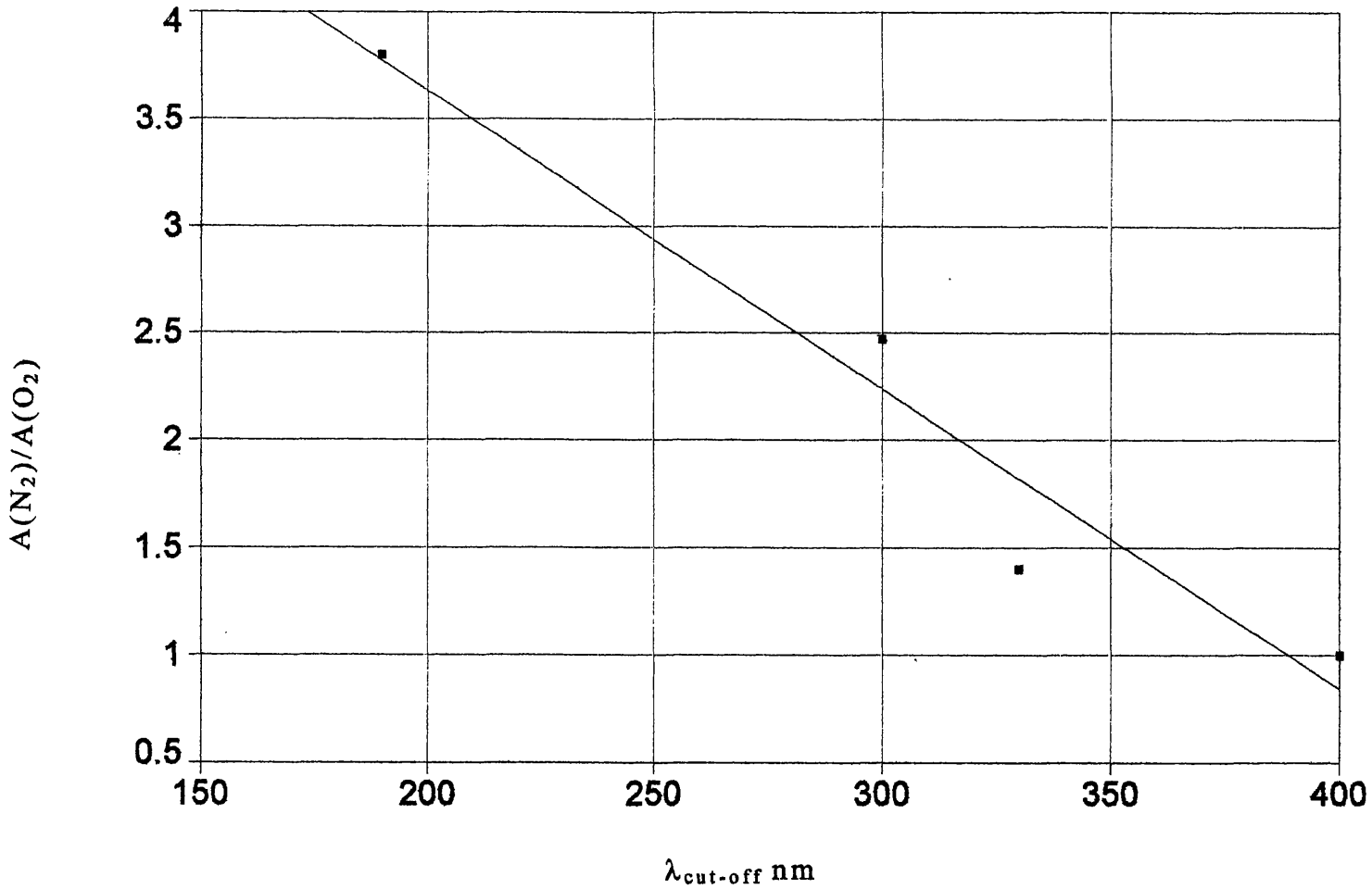

Figure 2.10. Ratio nitrogen purged absorbance: air equilibrated absorbance against filter wavelength cut-off (nm).

TABLE 2.4

Effect of filters on transient absorption.

DYE	FILTER	$A(N_2)/A(O_2)$
$6CO_2Et$-PT in hexane	Sodium Nitrite **(cut-off=400nm)**	1.00 (+/- 0.05)
6H-PT in hexane	Sodium Nitrite **(cut-off=400nm)**	1.00 (+/- 0.05)
$6CO_2Et$-PT in hexane	Acetone **(cut-off=330nm)**	1.40 (+/- 0.06)
6H-PT in hexane	Acetone **(cut-off=330nm)**	1.00 (+/- 0.05)
$6CO_2Et$-PT in hexane	Toluene **(cut-off=300nm)**	2.47 (+/- 0.3)
6H-PT in hexane	Toluene **(cut-off=300nm)**	1.00 (+/- 0.05)
$6CO_2Et$-PT in hexane	no filter	3.80 (+/- 0.3)

2.5 Heavy atom effects

The effect of the heavy atom solvent ethyl iodide was also examined but no change in isomer yield was detected upon purging air-saturated solutions with nitrogen.

2.6 Discussion

It can be suggested from the flash photolysis data obtained, that pyrazolotriazole azomethine dyes containing a carbonyl group are excited with UV radiation. There is excitation to a high level singlet state, S_n, with predominately carbonyl character. Excited carbonyl group chromophores are known to exhibit rapid intersystem crossing to the close-lying carbonyl triplet state[40], and it is suggested that this carbonyl triplet undergoes intra-molecular energy transfer to populate the lowest triplet state of

azomethine dye, from which it is known isomerisation can occur with significant efficiency[37]. Further, it is thought that visible light isomerisation of azomethine dyes occurs predominantly via a singlet process[14]. The data presented here suggest that, for carbonyl-substituted pyrazolotriazole dyes, ultraviolet excitation may result in isomerisation from the triplet state which is populated by an intra-molecular energy transfer from a higher triplet state of carbonyl character. Without the carbonyl substituent the excited-states available via UV excitation do not show high intersystem crossing efficiencies and both visible and UV excitation results in low yield isomerisation via the single manifold.

If this explanation is correct, then it could have important consequences for dye light stability because it would be expected that the UV light stability of carbonyl substituted dyes would be significantly less than their visible light stability and poorer that that of pyrazolotriazole dyes which do not carry such a substituent (see figure 1.7).

2.7 Conclusion

Microsecond flash photolysis has been used to investigate the effects of solvent, excitation wavelength, and oxygen on the yields of photo-induced isomerisation for a range of pyrazolotriazole azomethine dyes. The rates of thermal relaxation show no obvious dependence on the solvent solvatochromic parameters examined; this suggests that solvent factors such as dielectric properties and basicity are not uniquely significant in determining the relaxation times of the dye isomers. UV flash photolysis of CO_2Et-PT and 6-COPh-PT dyes in ethanol and methanol resulted in irreversible bleaching of the dye, possibly due to destruction of the chromophore by photoinduced solvolysis, whilst photolysis in the non polar

solvents n-hexane and acetonitrile did not destroy the chromophore.

The isomer yields for both $6CO_2Et$-PT and 6COPh-PT show an unexpected dependency on excitation wavelength and on the presence or absence of oxygen. The degree of oxygen quenching of isomer yield decreasing as excitation wavelength increased. The 6H-PT dye shows no such oxygen dependance. It is tentatively suggested that this is a consequence of the availability of substituent-localised carbonyl excited states for these dyes. It is suggested that these states are populated by UV excitation to give a localised carbonyl triplet state which can energy transfer into the pyrazolotriazole azomethine triplet state leading to relatively efficient isomerisation via the triplet manifold.

There was no change observed in isomer yield when using ethyl-iodide in a nitrogen-saturated solution with either $6CO_2Et$-PT or 6COPh-PT dyes indicating no effective external heavy atom effect from this solvent.

3. HYDROLYSIS OF PYRAZOLOTRIAZOLE AZOMETHINE DYES

3.1 Introduction

The acid hydrolysis of pyrazolotriazole azomethine dyes has not been extensively studied. Couture [43] has examined the hydrolysis of the 6H-PT dye and observed that the imine group of the dye could be protonated and that in non-hydroxylic solvents the monocationic form of the dye was relatively stable, while in ethanol/water mixtures hydrolysis occurred with first-order kinetics[43]. He also observed further protonation steps involving the aromatic amino group of the developer.

In this work those studies have been extended to include work with dyes carrying electron-withdrawing and electron-donating groups at the 6-position.

3.2 Effect of acid on the absorption spectra of $6CO_2Et$-PT and $6CF_3$-PT

Although protonation in hydroxylic media is followed by relatively rapid hydrolysis, the protonated dyes are reasonably stable in a chloroform/trifluoroacetic acid mixture.

Figures 3.1 and 3.2 show the effect of increasing acid concentration on the absorption spectra of $6CO_2Et$-PT and $6CF_3$-PT. For $6CO_2Et$-PT at least two pK_a positions are evident. One occurs between 0 and 0.01M acid and is associated with a slight bathochromic shift of λ_{max} from 606nm to 613nm, a narrowing of the absorption band and an increase in ε_{max}. The second occurs between 0.01 and >1.0M acid and is associated with a major bathochromic shift of λ_{max} from 613nm to 655nm and an isosbestic point at *ca.* 632nm. For $6CF_3$-PT

the spectral shifts are less pronounced but again two pK_a transitions can be postulated: one between 0 and 0.05M acid again associated with a very slight bathochromic shift of λ_{max} from 607nm to 608nm and an increase in ε_{max} and narrowing of the absorption band. The second occurs between 0.05M and 0.75M and in marked contrast to the behaviour of the $6CO_2Et$-PT, this transition is associated with a decrease in ε_{max} and a slight hypsochromic shift in λ_{max} from 608nm to 604nm.

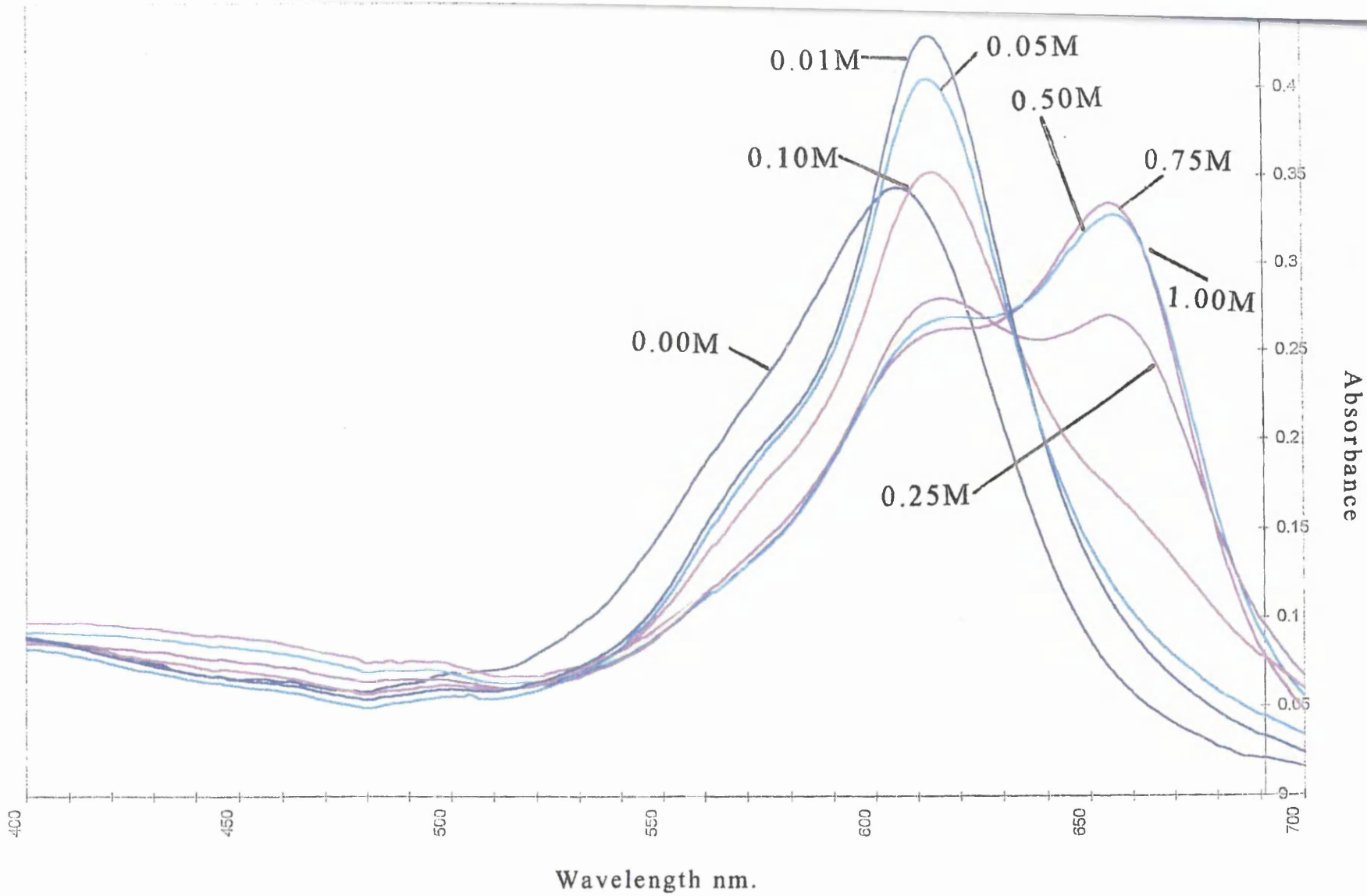

Figure 3.1 Absorption spectra $6CO_2Et$-PT dye in 0.01M to 1M TFA / chloroform (298K). Dye concentration = 5.2×10^{-6} mol dm^{-3}

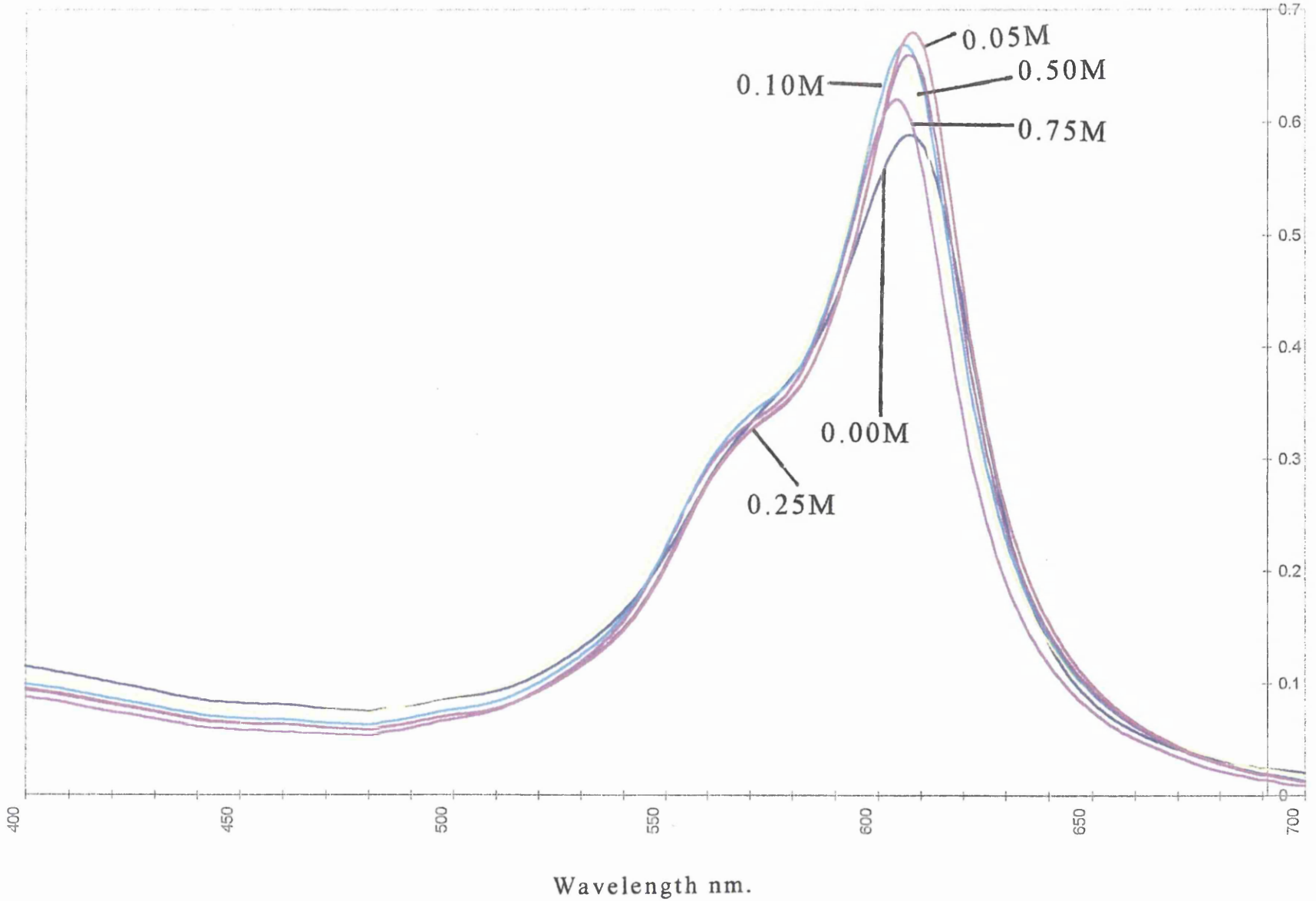

Figure 3.2 Absorption spectra $6CF_3$–PT dye in 0.01M to 1M TFA / chloroform (298K). Dye concentration = 1.2×10^{-5} mol dm^{-3}

TABLE 3.1

Spectroscopic effects of acid/base on PT dye spectra

PT-dye	$\lambda_{max\ neutral}$	$\lambda_{max\ in\ acid/base}$	Media (298K)
$6CO_2Et$ **fig 3.3**	608 nm	655 nm/ acid	TFA(0.5M)/ chloroform
$6CF_3$ **fig 3.4**	605 nm	609 nm/ acid	TFA(0.5M)/ chloroform
$6CO_2Et$ **fig 3.5**	608 nm	609 nm/ base	NaOH(0.1M)/ EtOH/water
$6CF_3$ **fig 3.6**	612 nm	613 nm/ base	NaOH(0.1M)/ EtOH/water
6H **fig 3.7**	579 nm	579 nm/ base	NaOH(0.1M)/ EtOH/water

Assuming an acid/base equilibrium exists between the dye and the protons introduced, then:

$$DYE\ H_n^{n+} \rightleftharpoons DYE + nH^+ \qquad 3.1$$

Therefore

$$K = [DYE]\ [H^+]^n / [DYE\ H_n^{n+}] \qquad 3.2$$

and so the nominal pK_a may be found as

$$pK_a = n(pH) + \log ([DYE\ H_n^{n+}]/[DYE]) \qquad 3.3$$

Now, if considerations are made of the relationship between absorbances at fixed wavelength and the relative concentrations of the protonated dye species at that wavelength, then since $A_\lambda = e.[dye].l$ (Beer-Lambert), it is possible to modify the above relationship to give:

$$pK_a = n(pH) + \log ([A_{max} - A]/ [A - A_{min}])^{(44)} \qquad 3.4$$

A_{max} is the maximum absorbance value i.e. at high acid concentration. A_{min} the minimum value, i.e. in the absence of acid, at the same wavelength. The term nominal pK_a is used because in the non-aqueous solvents used there is not the simple relationship between the activity and concentration of ionic species, such as H^+, as is found in dilute aqueous solution where the term pK_a, as represented by equation 3.3 is valid. With a large excess of strong acid

$$pH = -\log[acid] \qquad 3.5$$

Plots of log ($[A_{max} - A]/ [A - A_{min}]$) against -log[acid] will give straight lines, the intercept on -log[acid] giving the nominal pK_a value, and the slope giving the number of protons involved in the acid equilibrium.

Figure 3.3: $6CO_2Et$-PT dye / TFA (0.5M) / chloroform. Dye concentration = 5.0×10^{-6} mol dm^{-3}

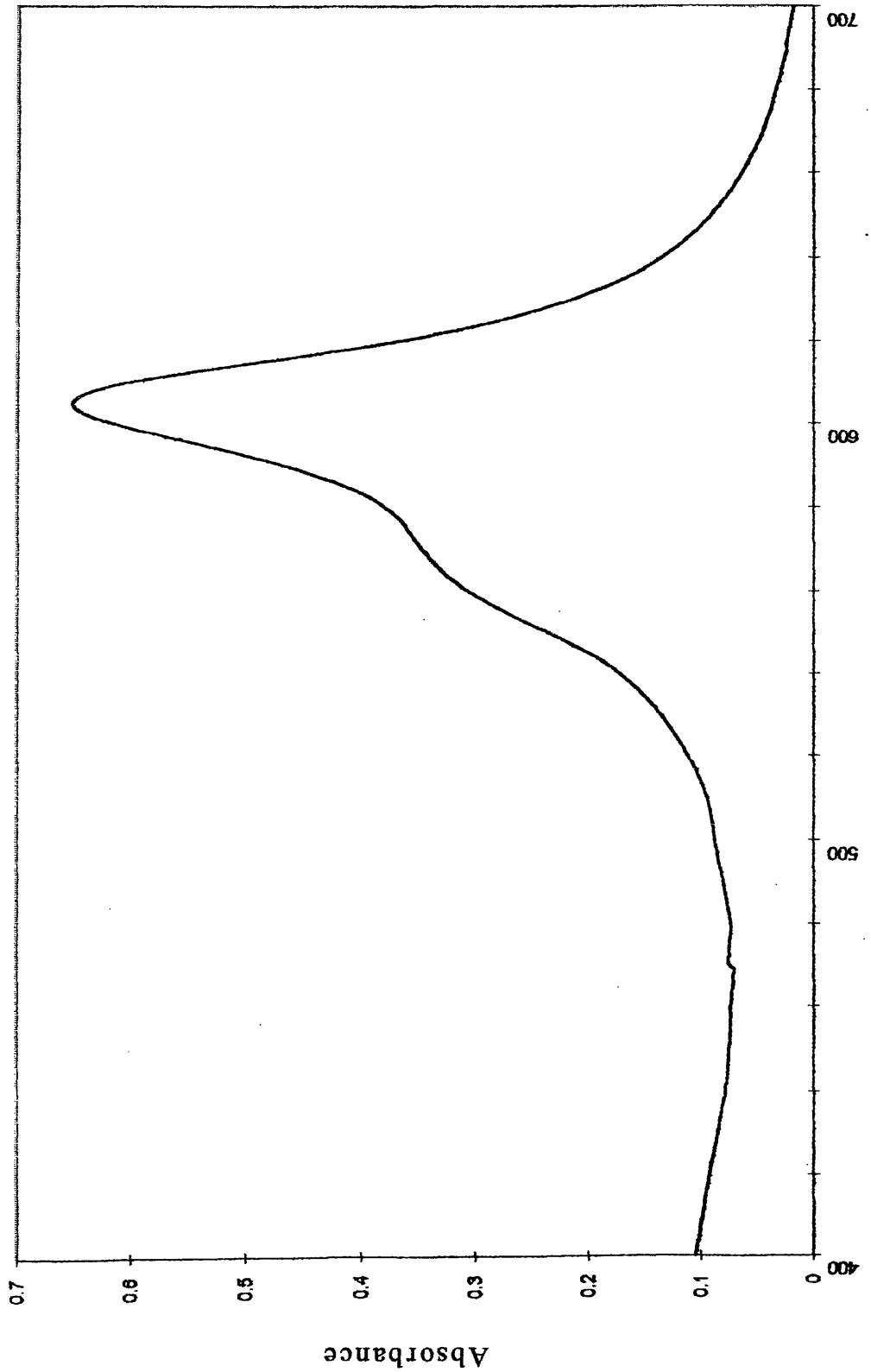

Figure 3.4: $6CF_3$-PT dye / TFA (0.5M) / chloroform. Dye concentration = 1 x 10^{-5} mol dm^{-3}

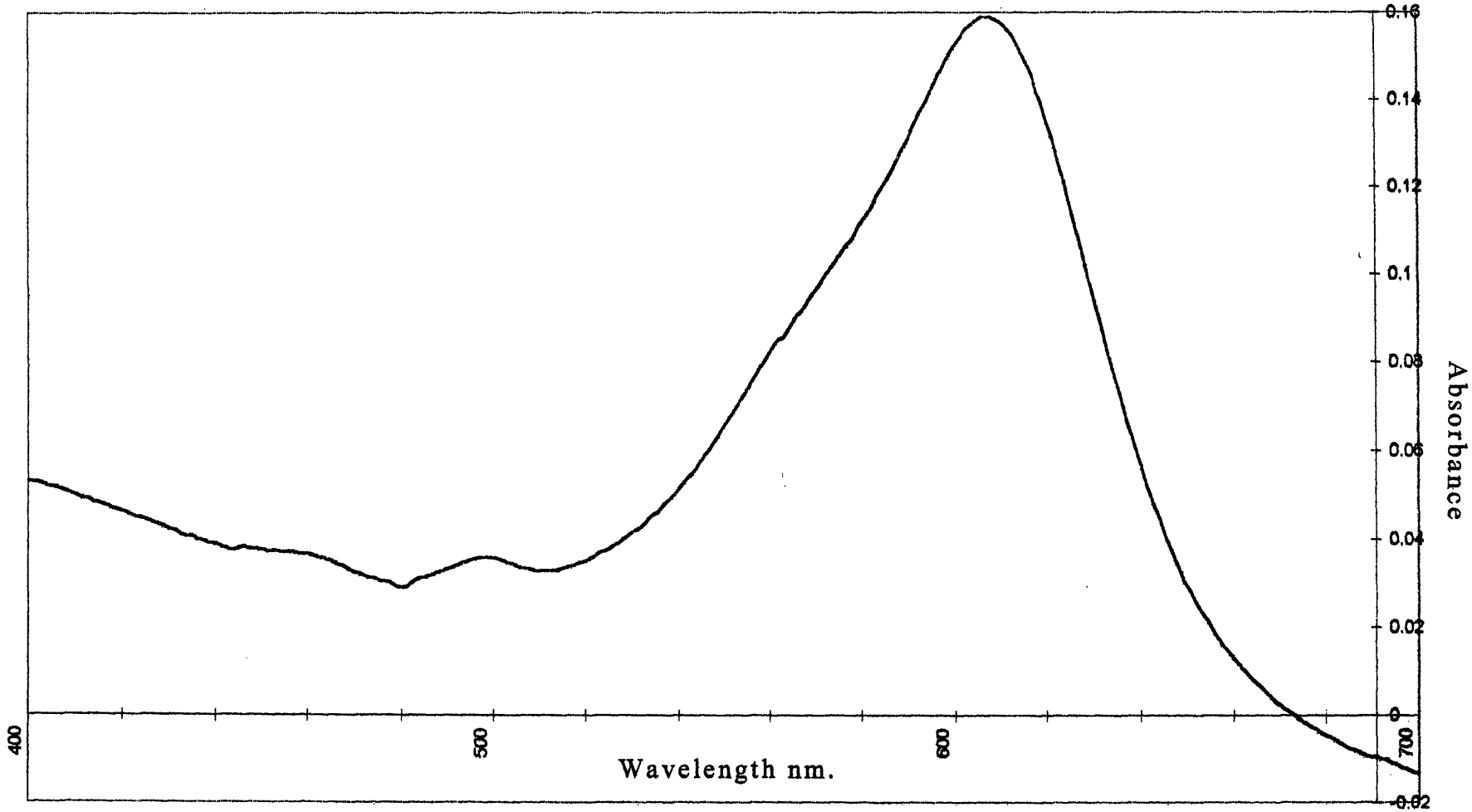

Figure 3.5: $6CO_2Et$-PT dye / NaOH (0.1M) / EtOH. Dye concentration = 2.4×10^{-6} mol dm^{-3}

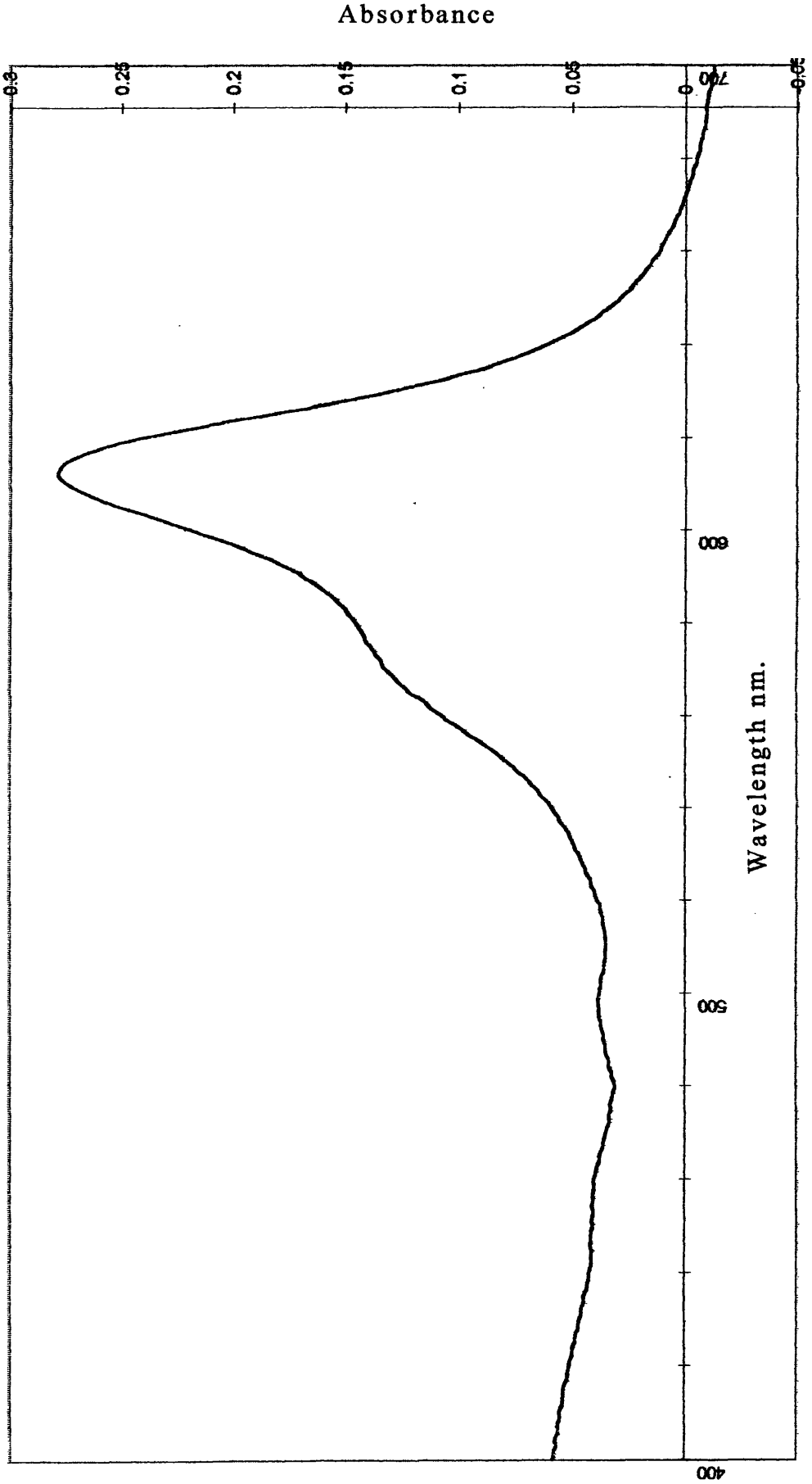

Figure 3.6: $6CF_3$-PT dye / NaOH (0.1M) / EtOH. Dye concentration $= 5.5 \times 10^{-6}$ mol dm^{-3}

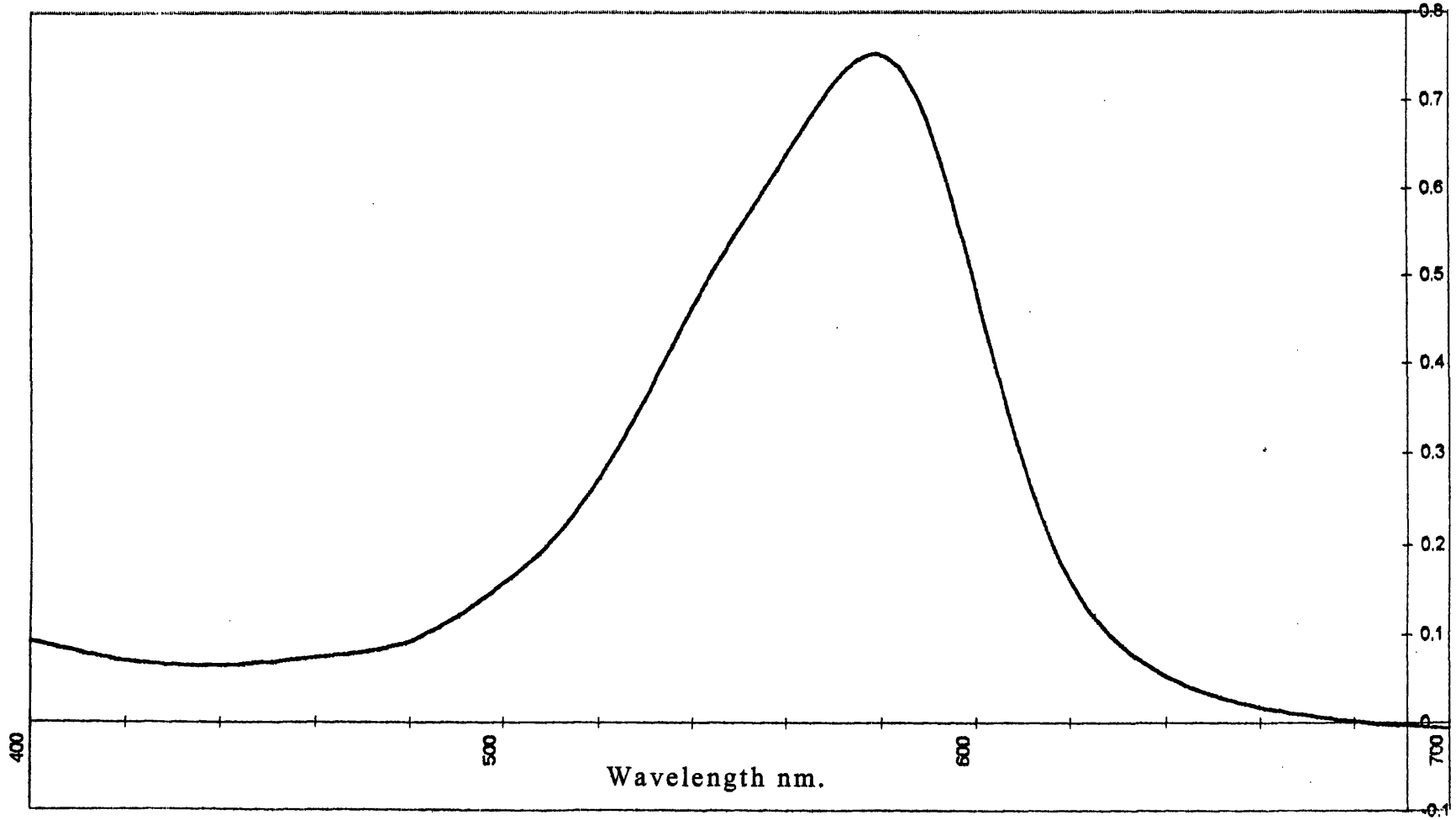

Figure 3.7: 6H-PT dye / NaOH (0.1M) / EtOH. Dye concentration = 1.5×10^{-5} mol dm^{-3}

3.3 Results

Absorption spectra for the $6CO_2Et$-PT and $6CF_3$-PT dyes in acid media (TFA/chloroform) are given in figures 3.1 and 3.2. There is a marked bathochromic shift with concomitant hyperchromic effect (increase in ε_{max}) for the $6CO_2Et$-PT dye, with acid concentrations below 0.1 M. acid concentrations greater than 0.1 M result in a hyperchromic effect at 655nm. The effect of addition of acid upon the $6CF_3$-PT dye is a small hyperchromic effect with a small hypsochromic shift, that itself is red-shifted with increasing proton concentration.

Results of the acid equilibria measurements are given for the $6CO_2Et$-PT and $6CF_3$-PT dyes in table 3.2.

TABLE 3.2

Acid equilibria measurements for $6CO_2Et$-PT and $6CF_3$-PT dyes

PT-dye	pK_a (in TFA/ chloroform)	number of protons in equilibrium
$6CF_3$	**0.71**	**1.2**
$6CO_2Et$	**0.76**	**2.1**

Plots of these data are given overleaf in figures 3.8 and 3.9.

Together with figures 3.1 and 3.2, these data show that the two dyes' behaviours in acid media are different. For the $6CF_3$-PT dye there is a single protonation step, pK_a=0.71, however with the $6CO_2Et$-PT dye the situation is more complex, with the first protonation step resulting in a bathochromic shift from 606nm to 613nm: with the $pK_a < 2$. There then follows a further protonation. This second protonation appears to have two protons associated

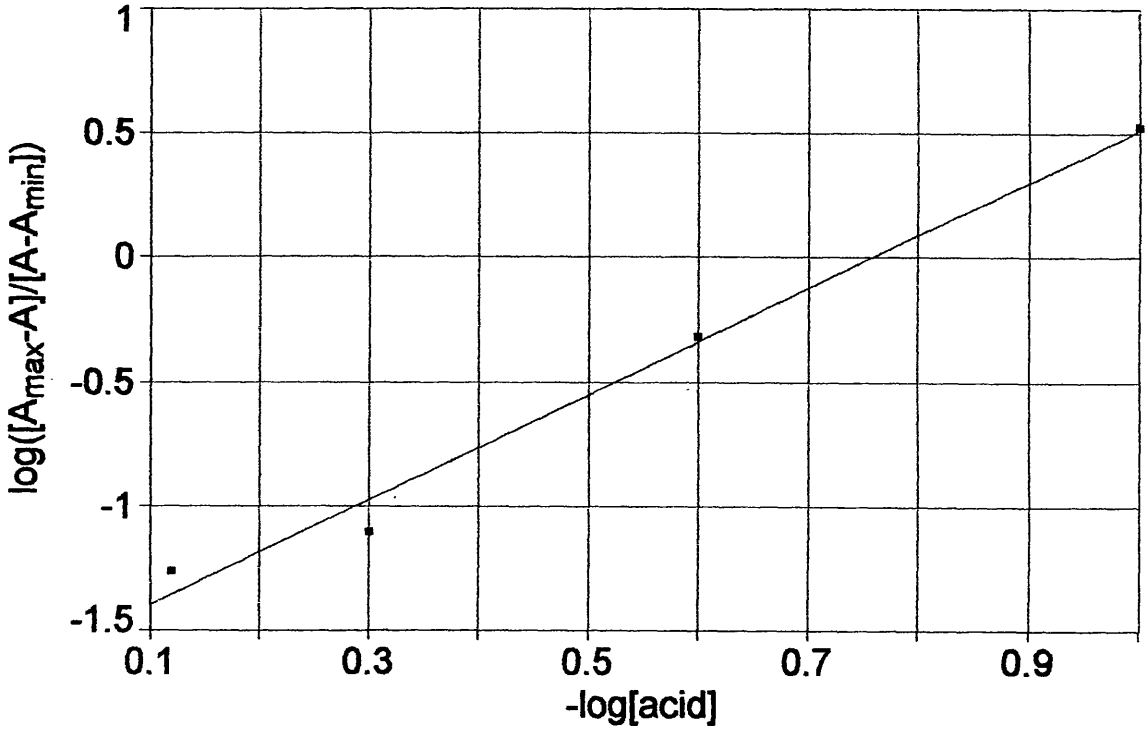

Figure 3.8: $6CO_2Et$-Pt dye in TFA/Chloroform (298K,655nm).

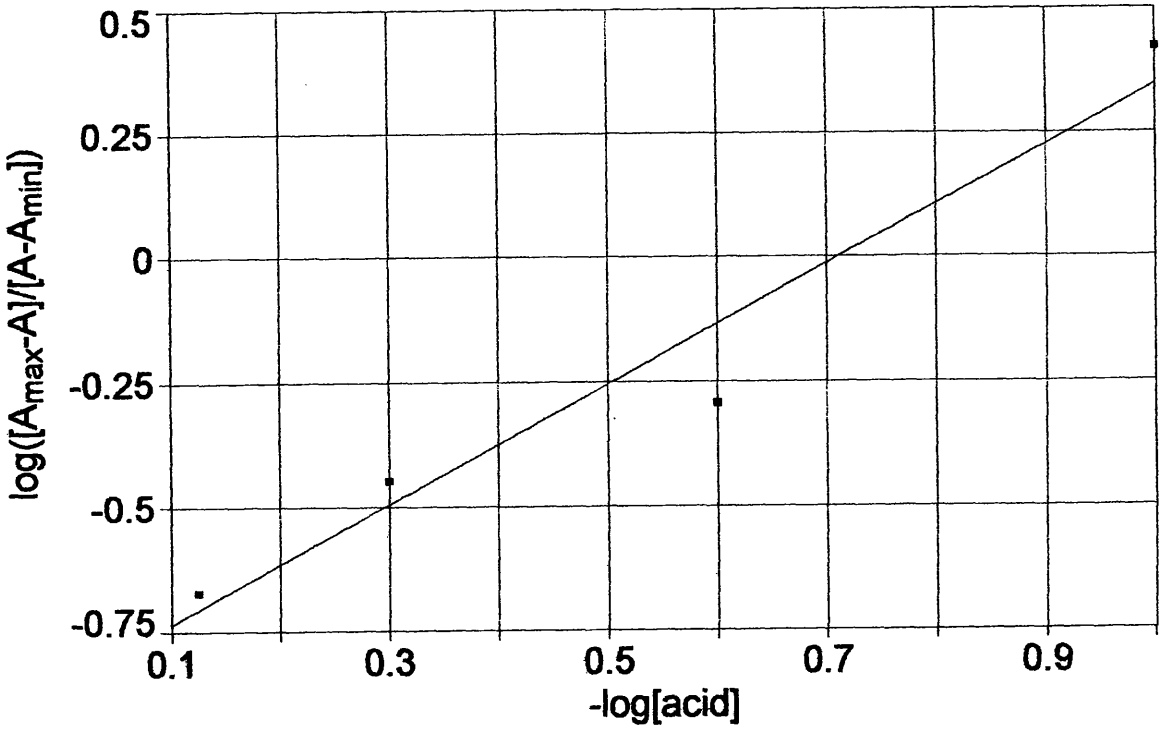

Figure 3.9: $6CF_3$-Pt dye in TFA/Chloroform (298K,607nm).

with it from the graph (figure 3.8): the slope gives a value of approximately 2. Similar results were reported by C. Couture[43].

3.4 Acid hydrolyses of PT dyes

3.4.1 Acid hydrolyses in ethanol/water

In the presence of acid in hydroxylic solvents, PT dyes undergo hydrolysis and this can be conveniently studied by following the loss of absorption at λ_{max} as a function of time. Plots of dye loss as a function of time at different proton concentrations and appropriate linear first order plots for a number of different dyes are given in figures 3.10 – 3.16.

In each case the hydrolyses proved to be first order with respect to dye concentration: plots of Ln A/A_0 against time are linear. The rate constants for these hydrolyses varied quite markedly from 2.4×10^{-6} s^{-1} (0.0086 $hour^{-1}$) for 6Me-PT to 21.7×10^{-6} s^{-1} (0.078 $hour^{-1}$) for $6CF_3$-PT (see table 3.3).

TABLE 3.3

Acid hydrolysis rate constants for PT dyes at 298K (0.3M HCl/EtOH/water(95:5))

PT dye	**Rate(10^{-6} s^{-1})**
$6CO_2Et$-PT	13.9
6Me-PT	2.4
$6SO_2Me$-PT	5.0
$6CF_3$-PT	21.7

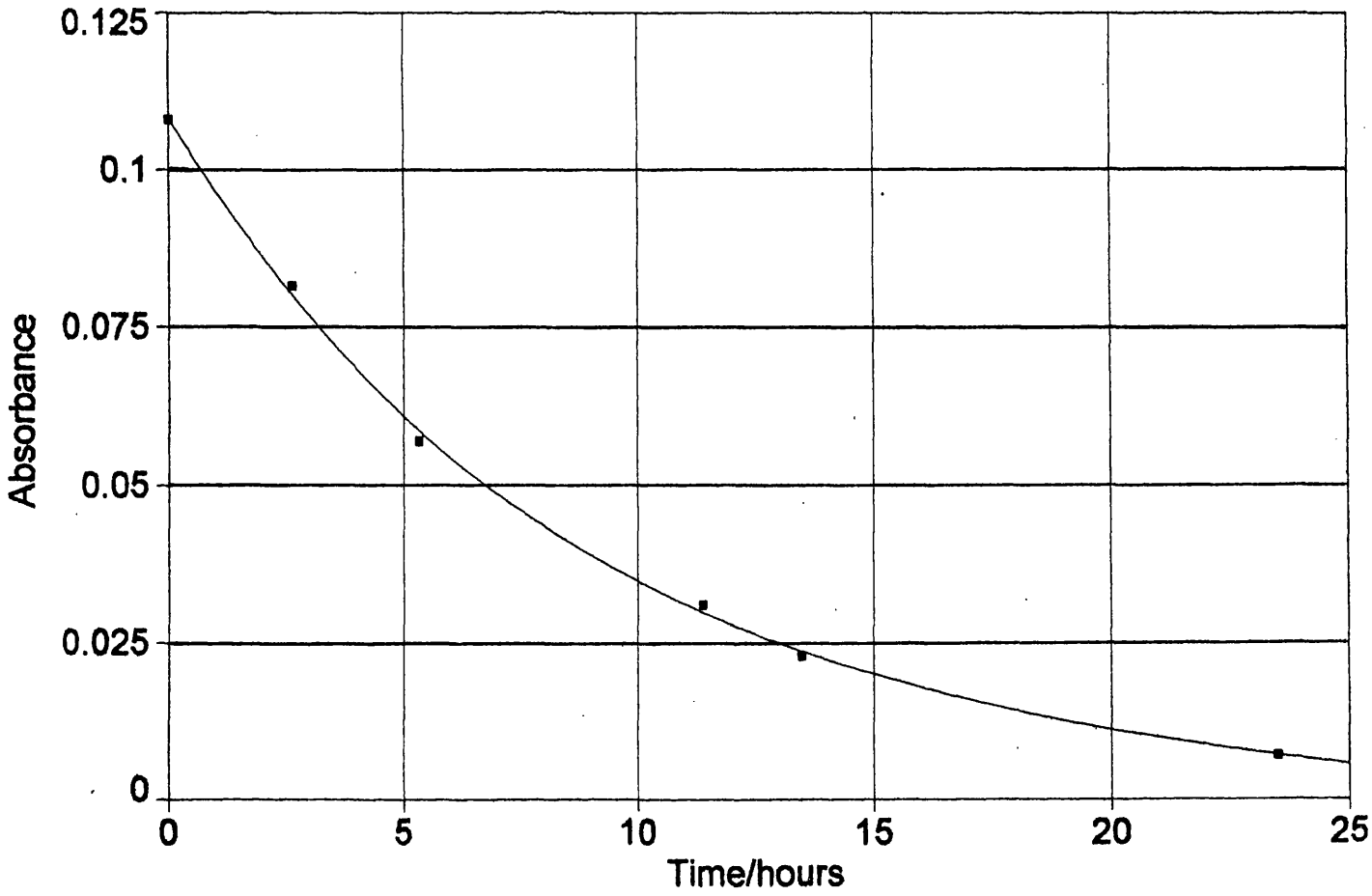

Figure 3.10: Acid hydrolysis $6CO_2Et$-PT dye (EtOH/water/HCl:0.3M). 608nm. 298K. Dye concentration = 1.7 x 10^{-6} mol dm^{-3}

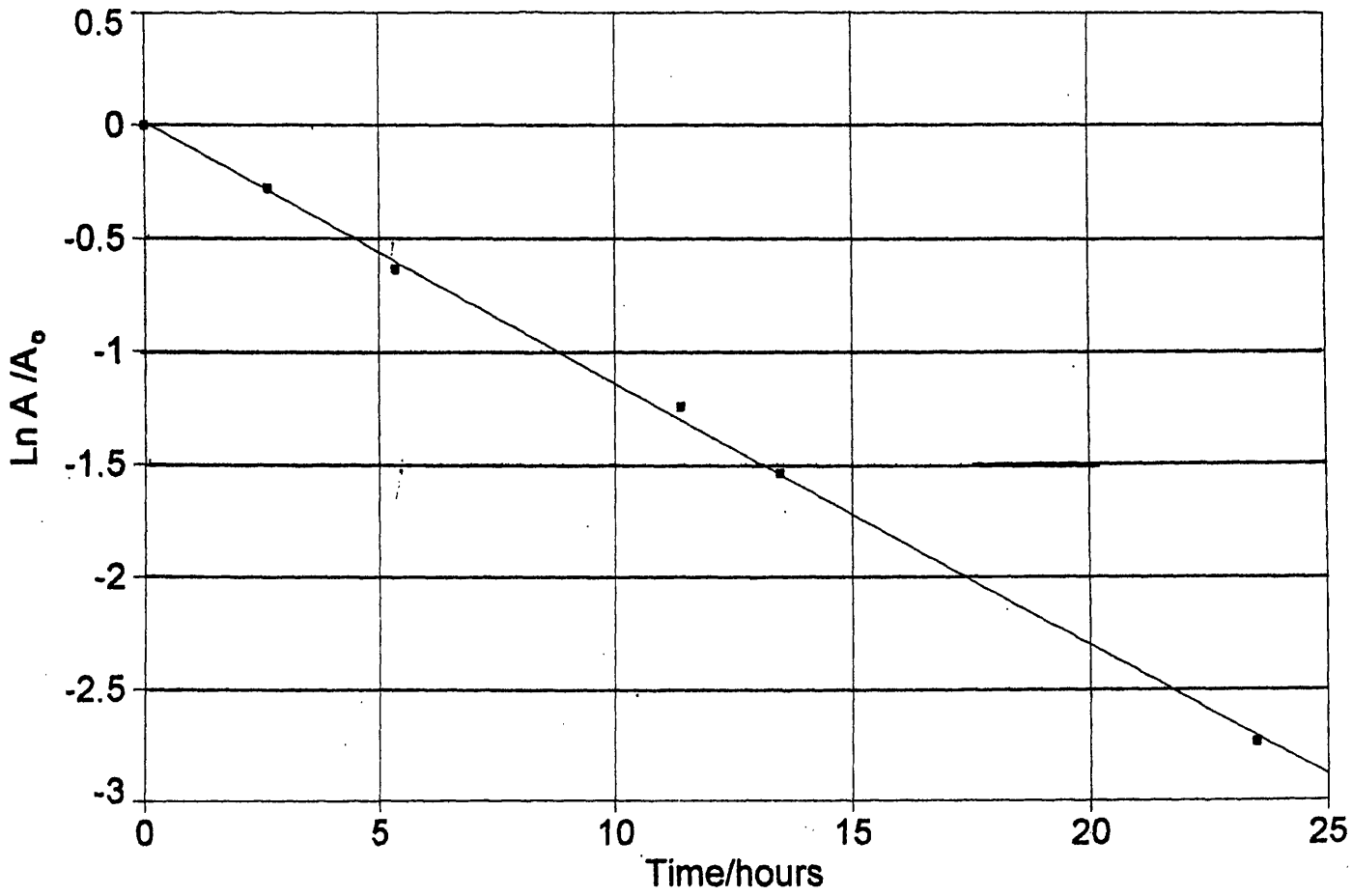

Figure 3.11: Acid hydrolysis $6CO_2Et$-PT dye (EtOH/water/HCl:0.3M). 608nm. 298K. Ln(A/A_0) vs Time(hours).

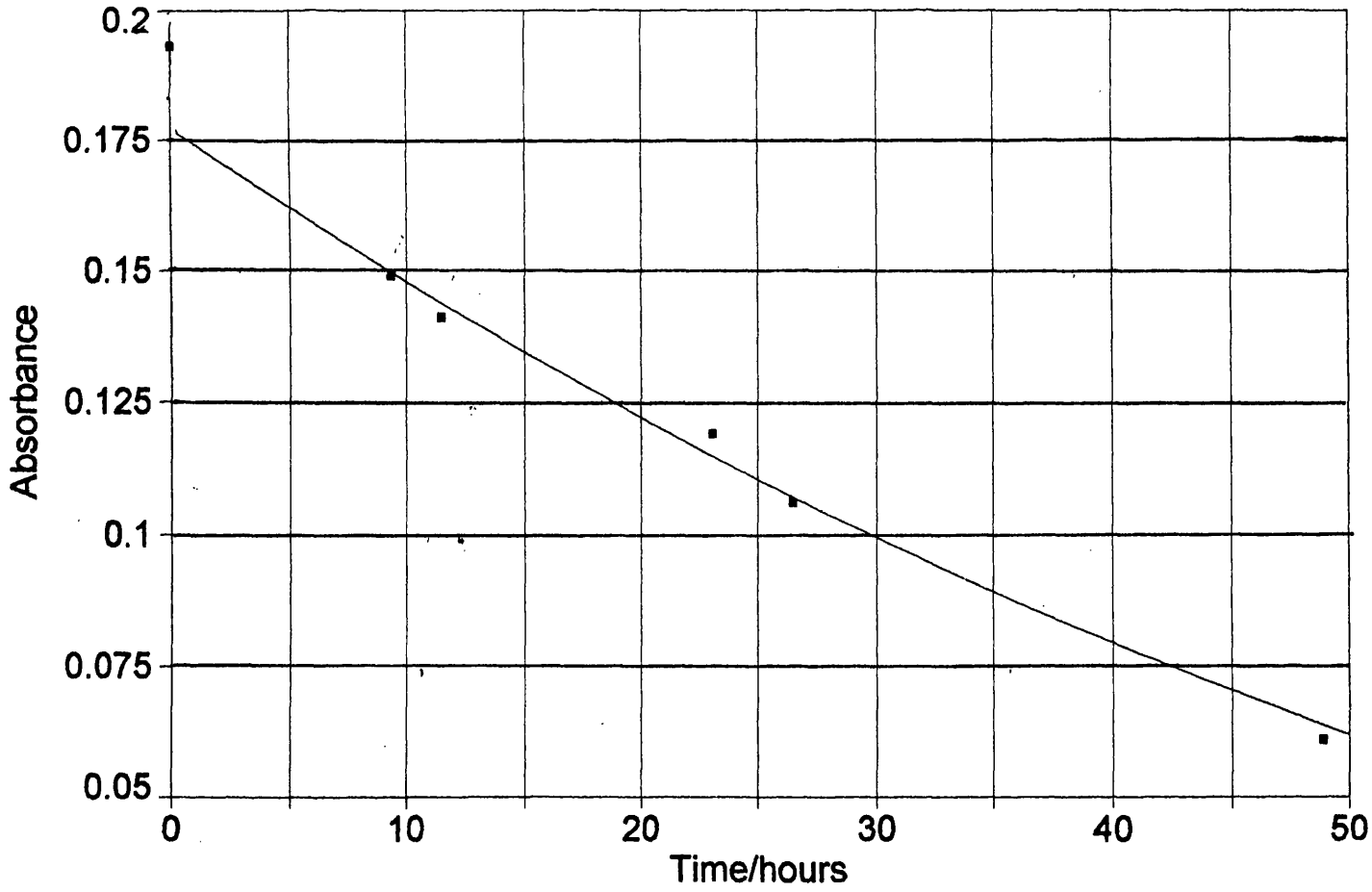

Figure 3.12: Acid hydrolysis 6Me-PT dye (EtOH/water/HCl:0.3M). 608nm. 298K. Dye concentration = 3.8 x 10^{-6} mol dm^{-3}

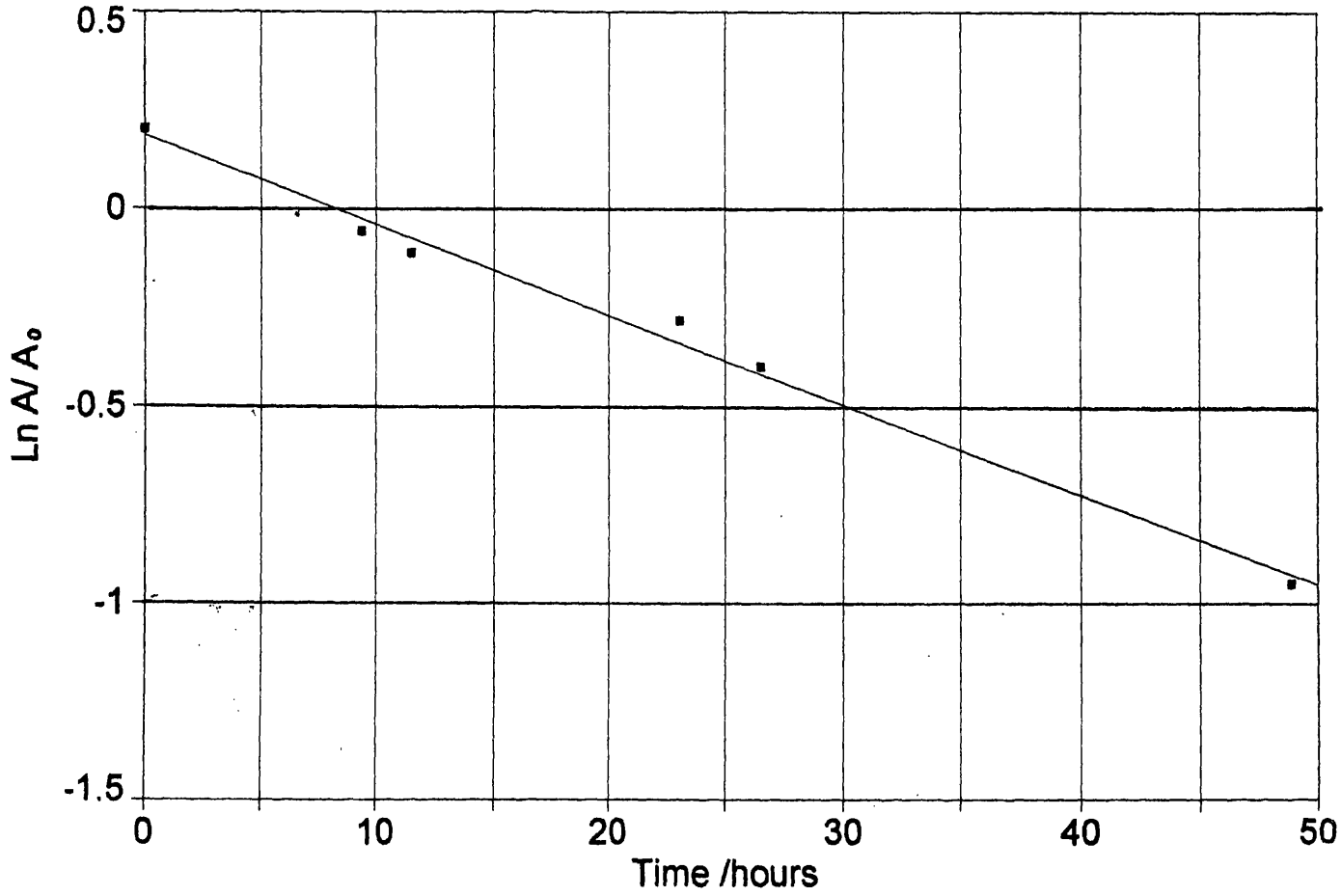

Figure 3.13: Acid hydrolysis 6Me-PT dye (EtOH/water/HCl:0.3M). 608nm. 298K. Ln(A/A_0) vs Time(hours).

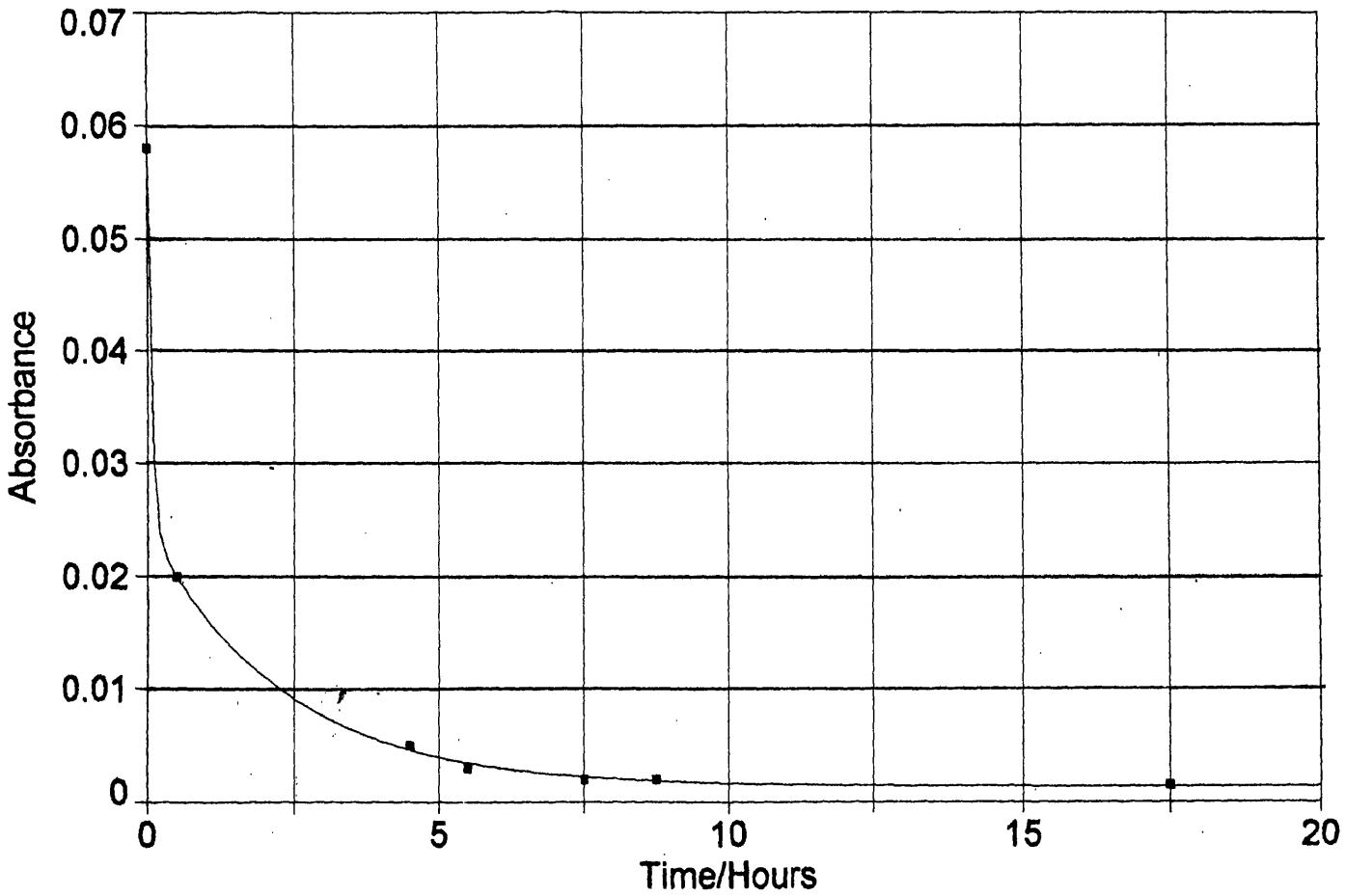

Figure 3.14: Acid hydrolysis 6H-PT dye (EtOH/water/HCl:0.3M). 608nm. 298K. Dye concentration = 1.2×10^{-6} mol dm^{-3}

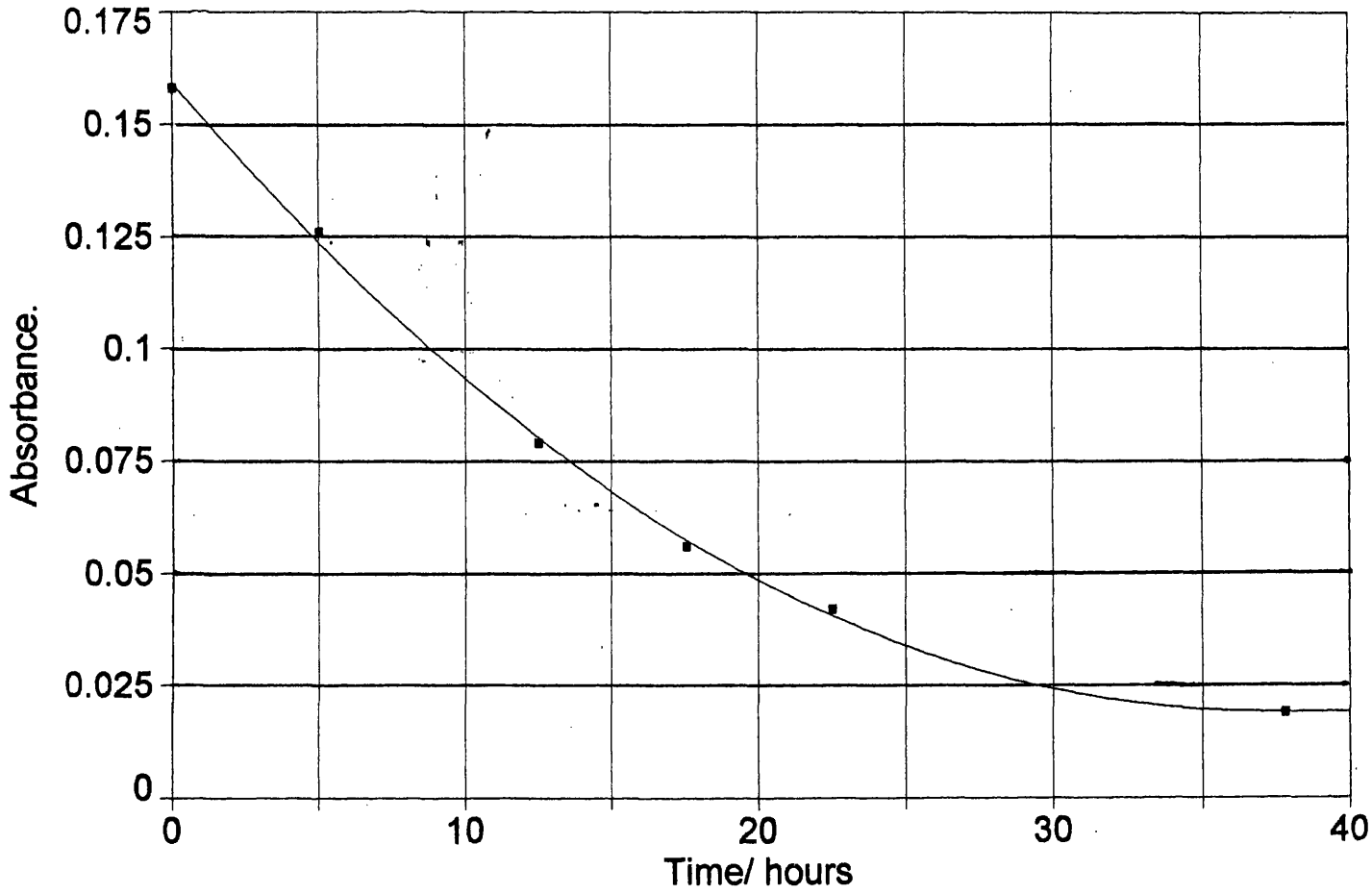

Figure 3.15: Acid hydrolysis $6SO_2Me$-PT dye (EtOH/water/HCl:0.3M). 608nm. 298K. Dye concentration = 3.16 x 10^{-6} mol dm^{-3}

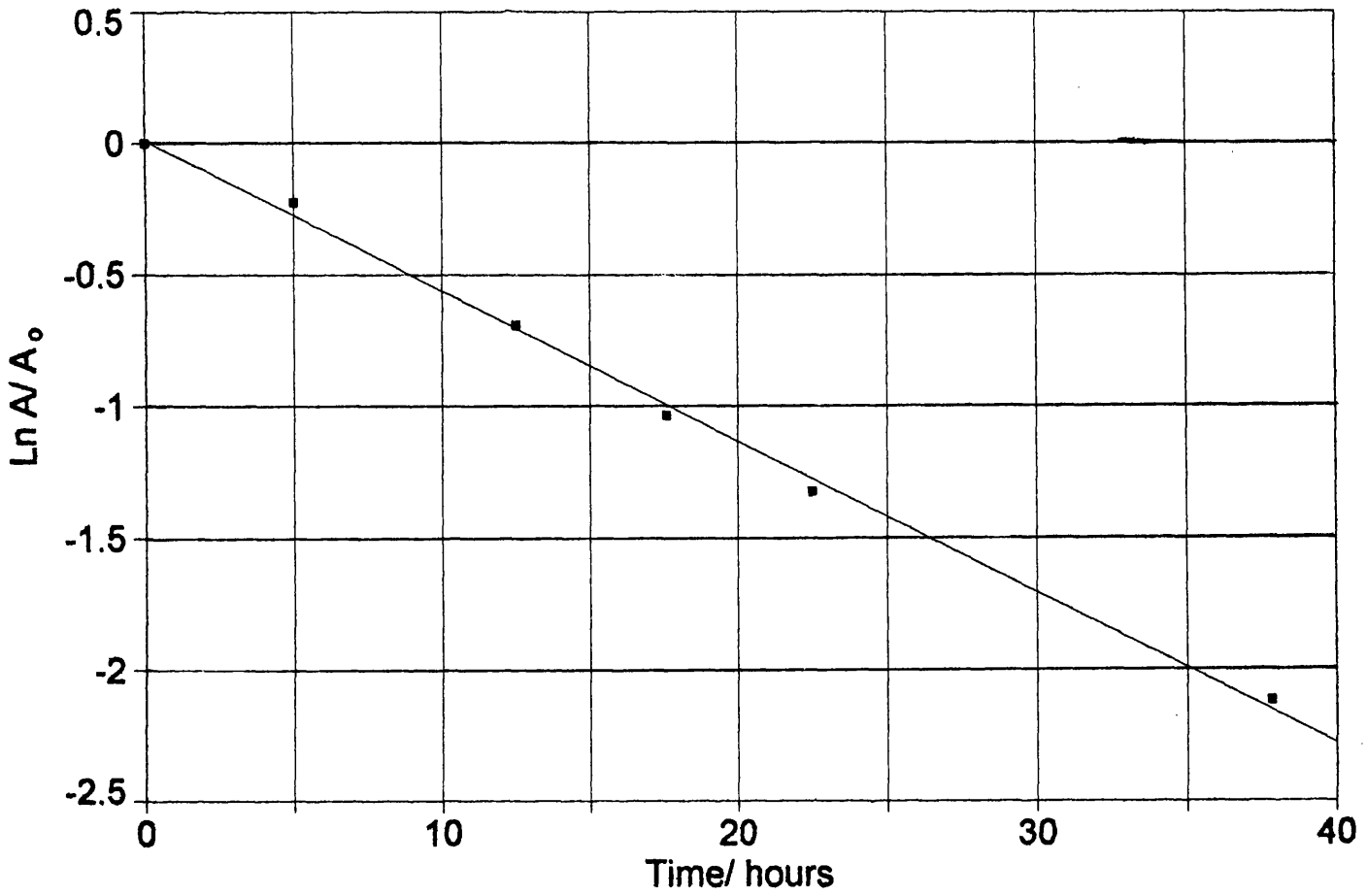

Figure 3.16: Acid hydrolysis $6SO_2Me$-PT dye (EtOH/water/HCl:0.3M). 608nm. 298K. $Ln(A/A_0)$ vs Time(hours).

3.4.2 Acid hydrolyses in dimethylsulphoxide/water

In order to evaluate the effect of solvent, a number of PT dyes were also studied in acidified dimethylsulphoxide/water. In each case the acid hydrolysis of the dye was followed at λ_{max} in a thermostated bath at 298 K (see chapter four, experimental section). Plots of dye fade with time and appropriate linear first order plots are given in figures 3.17 to 3.20.

TABLE 3.4

Acid hydrolysis rate constants for PT dyes at 298K (0.3M HCl/DMSO:water(95%:5%v/v))

Dye	**Rate(10^{-6} s^{-1})**
$6CO_2Et$-PT	1.34
$6CF_3$-PT	0.91

The two sets of data show that there is a marked decrease in rate in the DMSO/water system for all PT-dyes compared to the EtOH/water system.

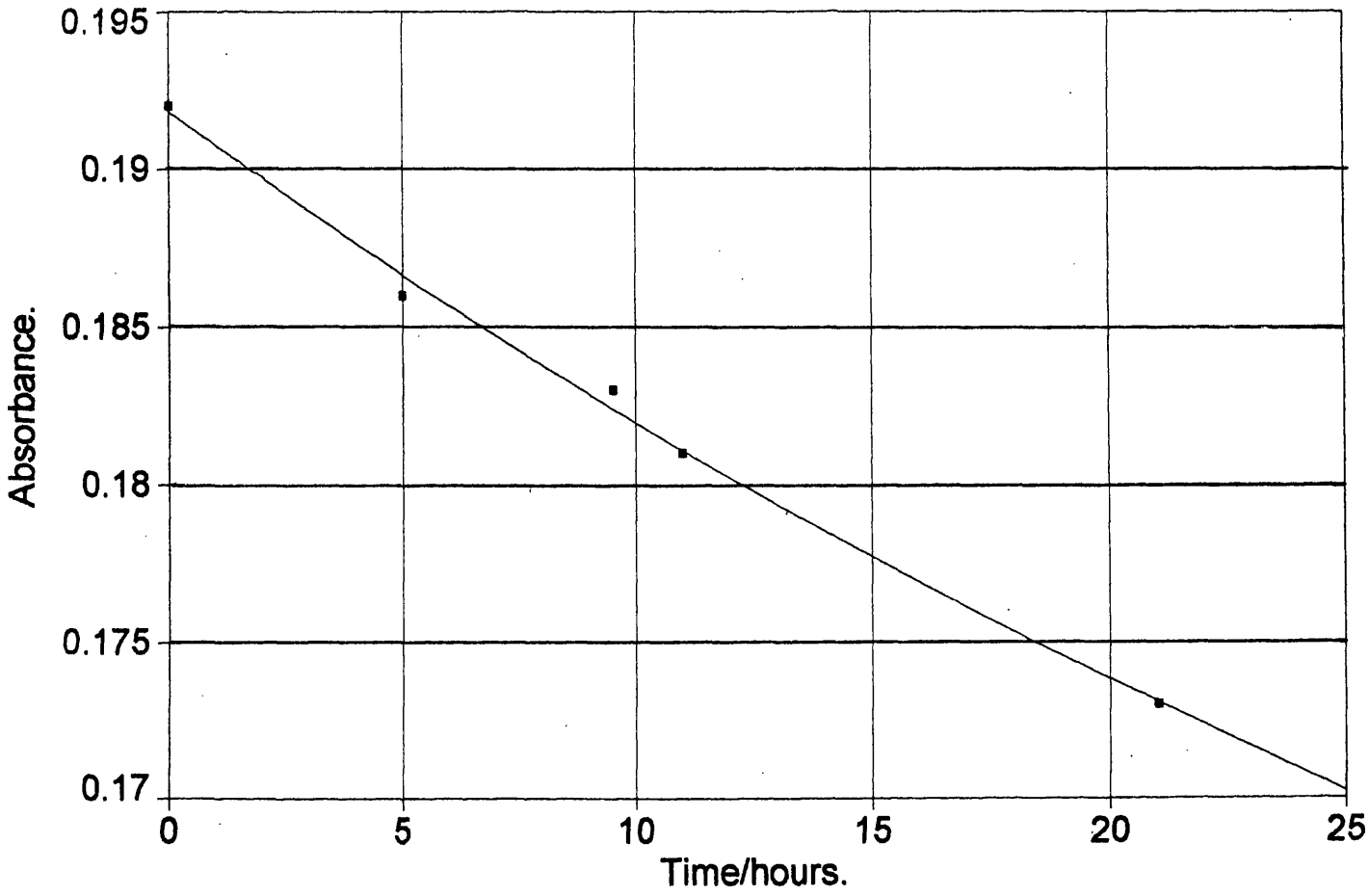

Figure 3.17: Acid hydrolysis $6CO_2Et$-PT dye (DMSO/water/HCl:0.3M). 608nm. 298K. Dye concentration = 2.9 x 10^{-6} mol dm^{-3}

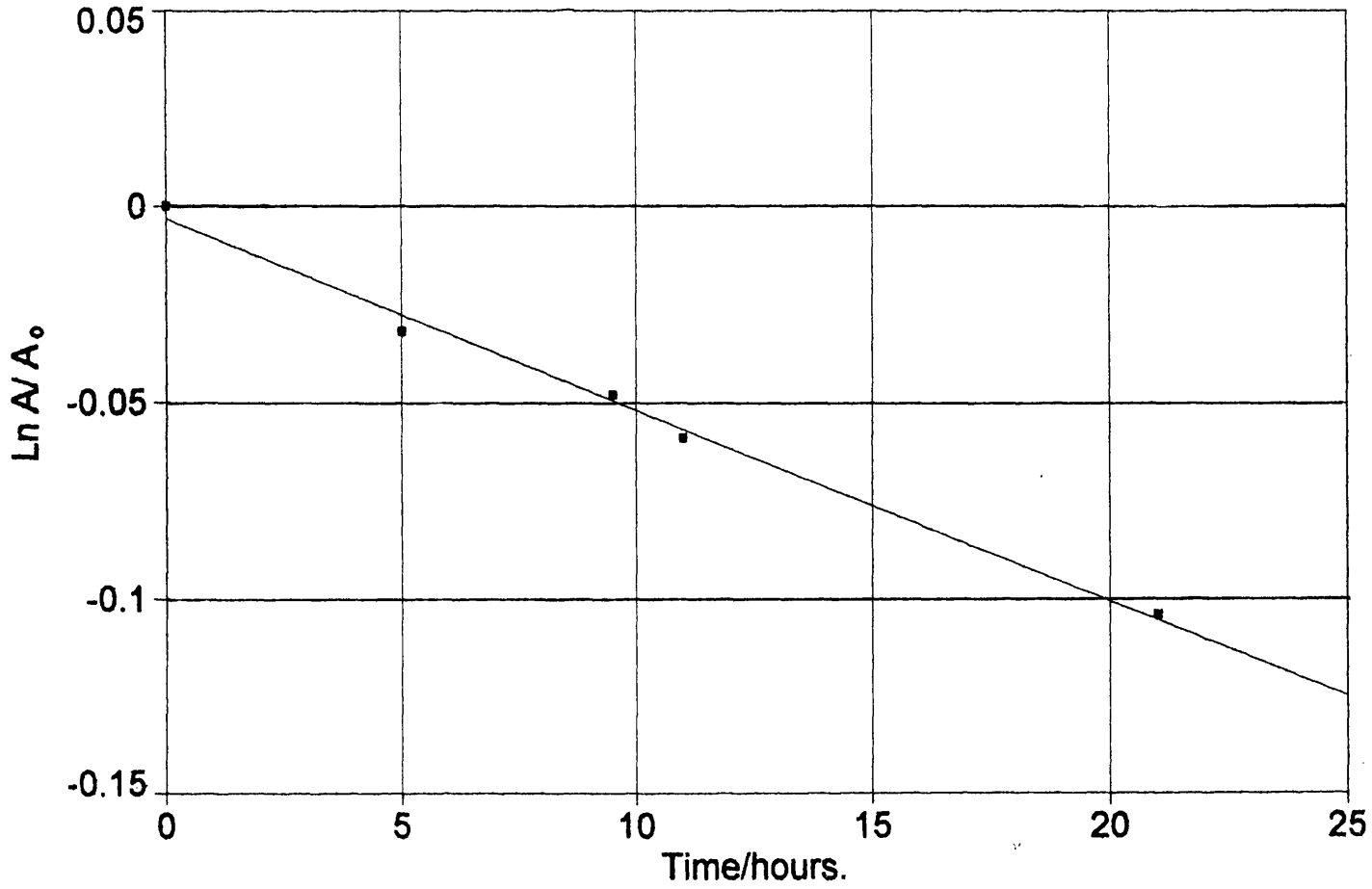

Figure 3.18: Acid hydrolysis $6CO_2Et$-PT dye (DMSO/water/HCl:0.3M). 608nm. 298K. Ln(A/A_0) vs Time(hours).

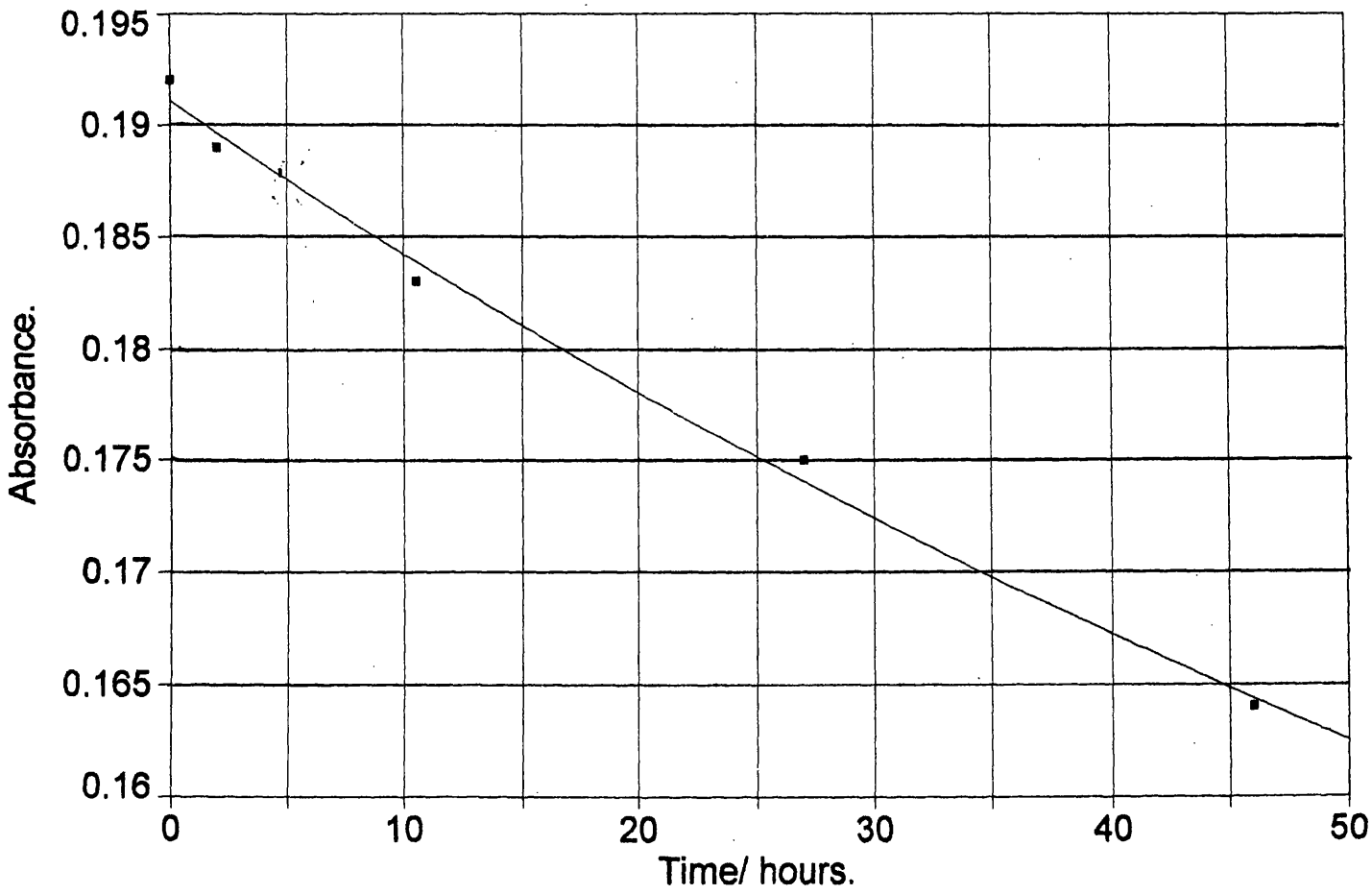

Figure 3.19: Acid hydrolysis $6CF_3$-PT dye (DMSO/water/HCl:0.3M). 608nm. 298K. Dye concentration = 3.8×10^{-6} mol dm^{-3}

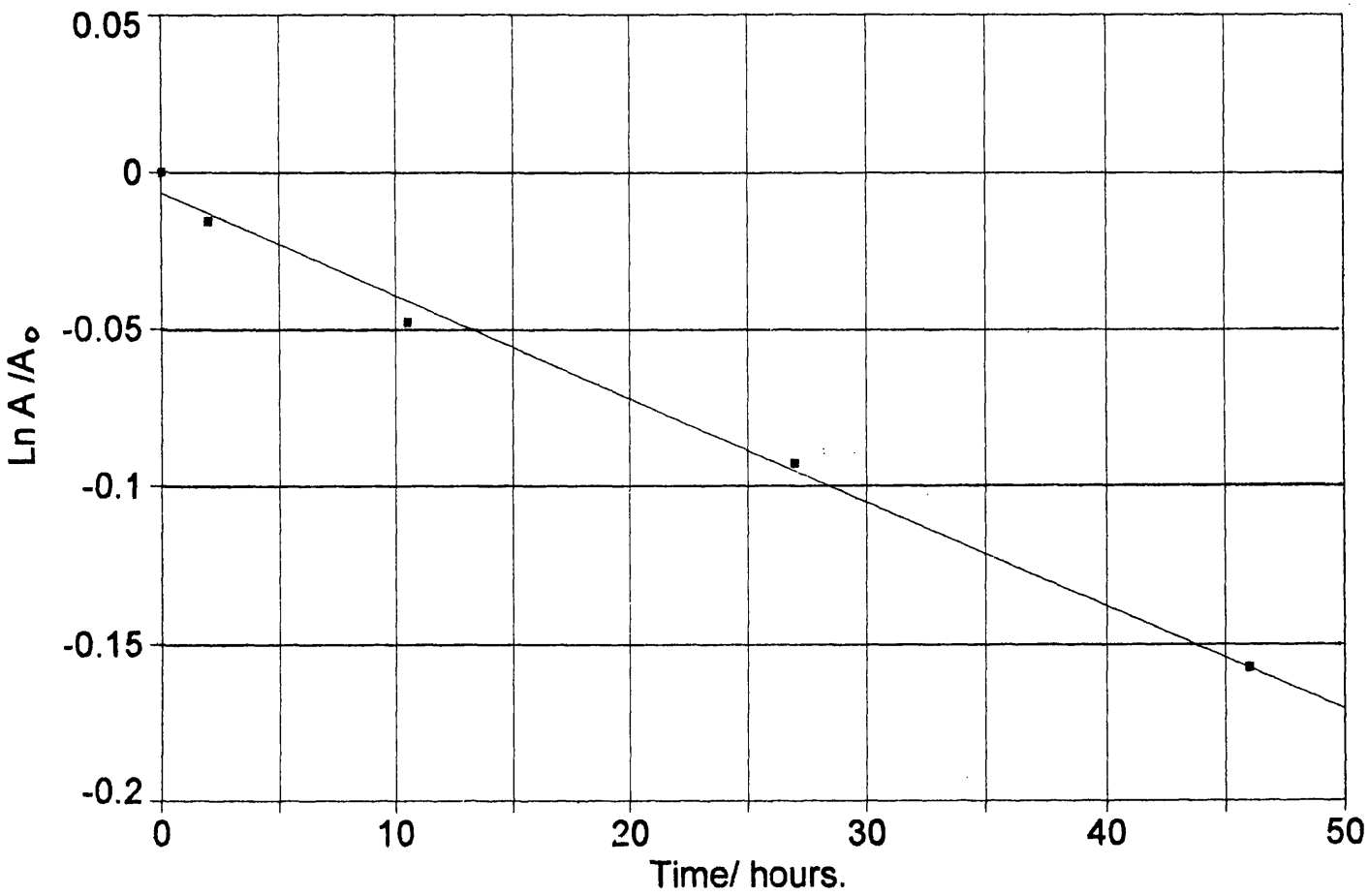

Figure 3.20: Acid hydrolysis $6CF_3$-PT dye (DMSO/water/HCl:0.3M). 608nm. 298K. Ln(A/A_0) vs Time(hours).

3.4.3 Acid concentration and its effect on rate constant

Dye solutions were examined in the ethanol/water and DMSO/water media at different acid concentrations and the rate constants determined. The tabulated results of these hydrolyses are given in tables 3.5 to 3.12.

3.4.4 Acid hydrolyses of PT-dyes in DMSO and EtOH/water

TABLE 3.5

6CO_2Et- PT acid hydrolysis HCl / DMSO:water (95%:5%v/v)

$[H^+]$ / mol dm^{-3}	k / (10^{-6} s^{-1})
0.38	1.39
0.5	2.78
0.7	6.11
0.9	13.89
1.0	19.44

TABLE 3.6

6SO_2Me- PT acid hydrolysis HCl / DMSO:water(95%:5% v/v)

$[H^+]$ / mol dm^{-3}	k / (10^{-6} s^{-1})
0.38	0.111
0.5	2.5
0.7	5.56
0.9	12.78
1.0	19.44

TABLE 3.7

$6CF_3$ - PT acid hydrolysis HCl / DMSO:water(95%:5% v/v)

$[H^+]$ / mol dm^{-3}	k / (10^{-6} s^{-1})
0.38	0.694
0.5	1.81
0.7	5.28
0.79	11.11
0.89	19.44
0.95	37.78

TABLE 3.8

$6CO_2Et$ - PT acid hydrolysis HCl/ EtOH:water (95%:5% v/v)

$[H^+]$ / mol dm^{-3}	k / (10^{-6} s^{-1})
0.24	2.22
0.5	13.89
0.7	22.22
0.94	47.22

TABLE 3.9

$6SO_2Me$ - PT acid hydrolysis HCl/ EtOH:water (95%:5% v/v)

$[H^+]$ / mol dm^{-3}	k / (10^{-6} s^{-1})
0.24	0.833
0.47	4.72
0.61	8.89
0.71	12.22
0.94	27.78

TABLE 3.10

6CF_3 - PT acid hydrolysis HCl/ EtOH:water (95%:5% v/v)

$[H^+]$ / mol dm^{-3}	k / (10^{-6} s^{-1})
0.1	0.55
0.24	1.86
0.5	21.67
0.7	36.67

TABLE 3.11

6Me - PT acid hydrolysis HCl/ EtOH:water (95%:5% v/v)

$[H^+]$ / mol dm^{-3}	k / (10^{-6} s^{-1})
0.24	0.347
0.47	2.39
0.61	4.17
0.71	5.28
0.94	9.44

TABLE 3.12

6NHPh - PT acid hydrolysis HCl/ EtOH:water (95%:5% v/v)

$[H^+]$ / mol dm^{-3}	k / (10^{-6} s^{-1})
0.47	6.11
0.61	10.28
0.71	13.89
0.94	23.61

Plots of rate constant against proton concentration for the dyes studied for both hydrochloric acid in ethanol/water and in DMSO are given in figures 3.21, and 3.22.

Figure 3.21: 6X-PT dye hydrolyses HCl/EtOH/water. 298K

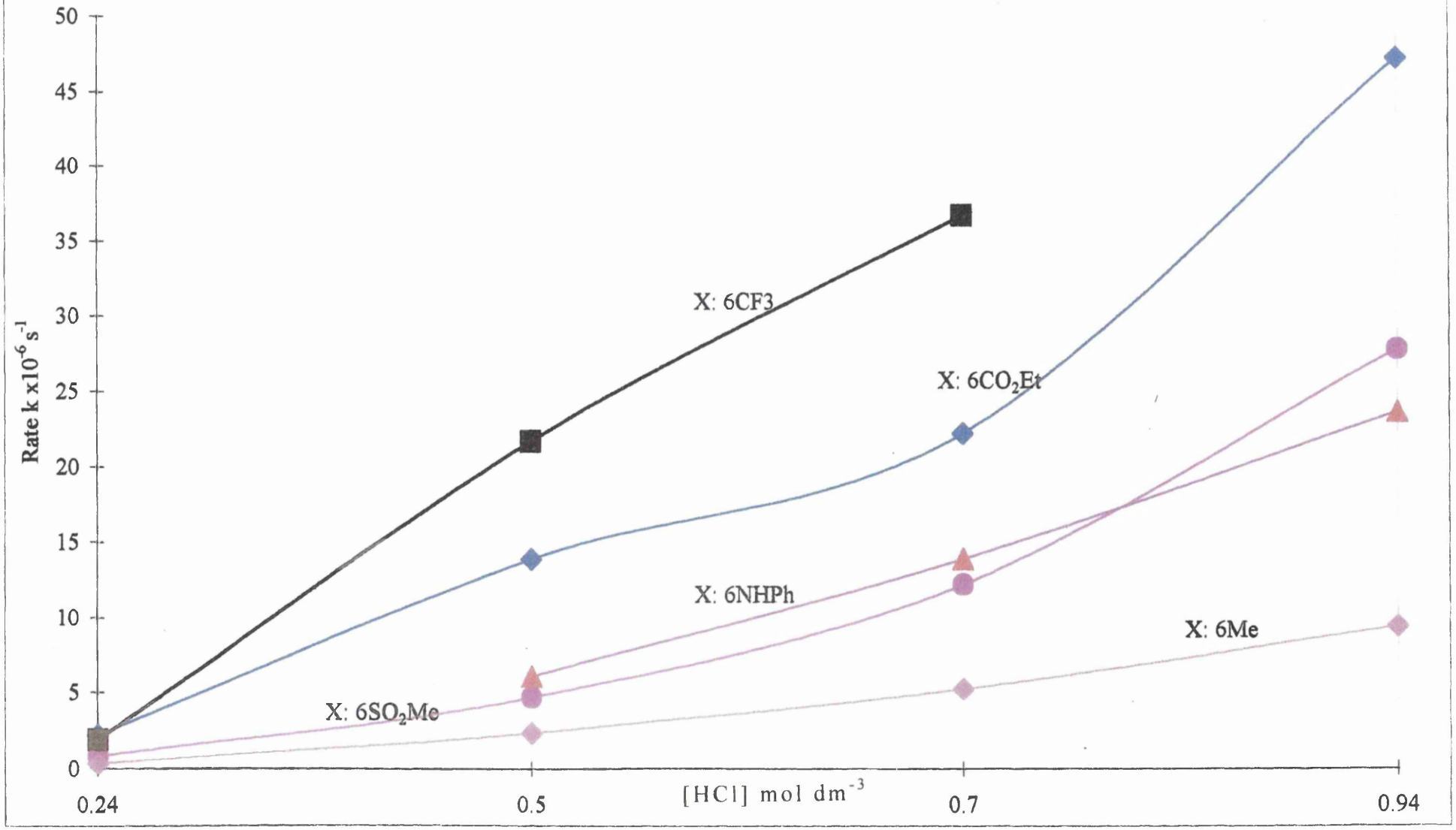

Figure 3.22: 6H-PT dye hydrolyses HCl/DMSO. 298K

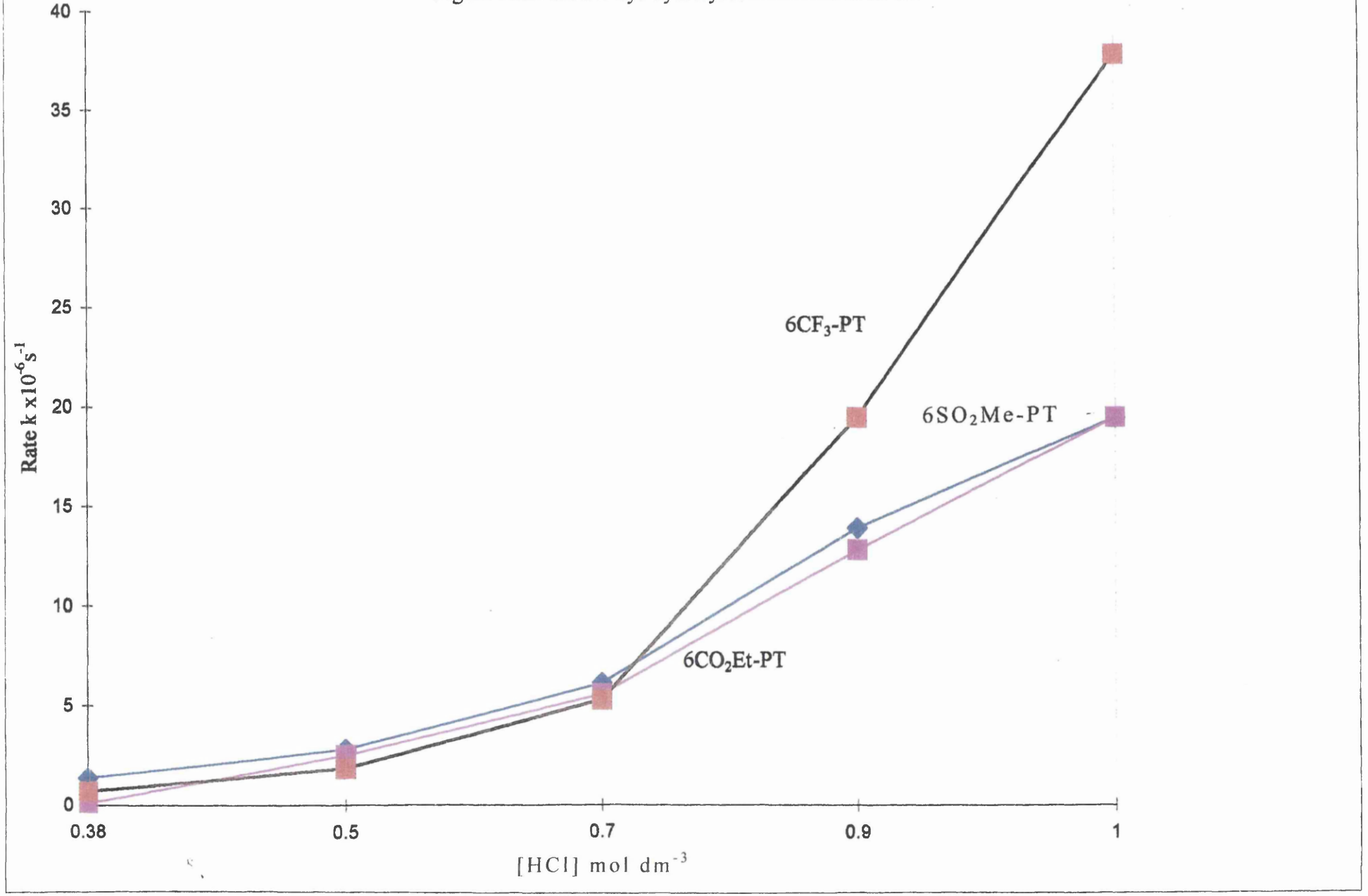

Unfortunately, the dependence of hydrolysis rate on acid concentration is difficult to rationalise and the situation is made complex by the series of protonation equilibria which occur in the acid concentration range studied.

3.5 Hammett relationships

The rate constants (k) at acid concentration 0.47M and 0.94M HCl in ethanol/water media were examined for a possible Hammett relationship via a plot of logk against σ_ρ. The result is given in figure 3.23, which demonstrates no linear correlation between Hammett σ_ρ values and hydrolysis rate constants. However some, albeit tenuous, indication of a possible change in mechanism is evident in the deviation from linearity seen. Further Hammett plots were produced using σ_ρ^-, σ_I and σ_R values; these are reproduced in figures 3.23 to 3.27.

The Hammett values[44] for each substituent are given in table 3.13.

Table 3.13

0.47M and 0.94M HCl/ EtOH:water (95%:5% v/v)

Substituent	$[H^+]M$	k/ $x10^{-6}$ s^-	logk	σ_ρ	σ_ρ^-	σ_I	σ_R
CO_2Et	0.47	13.9	-4.86	0.44	0.74	0.31	0.16
	0.94	47.2	-4.33				
SO_2Me	0.47	4.7	-5.33	0.73	1.05	0.55	0.12
	0.94	27.8	-4.56				
CF_3	0.47	21.7	-4.66	0.53	0.65	0.42	0.11
	0.94	-	-				
Me	0.47	2.4	-5.62	-0.17	-	-	-
	0.94	9.4	-5.02				
NHPh	0.47	6.1	-5.21	-0.25	-	0.12	-0.48
	0.94	23.6	-4.36				
H[43]	0.47	51.0	-4.29	0.00	0.00	0.00	0.00
	0.94	138.0	-3.86				

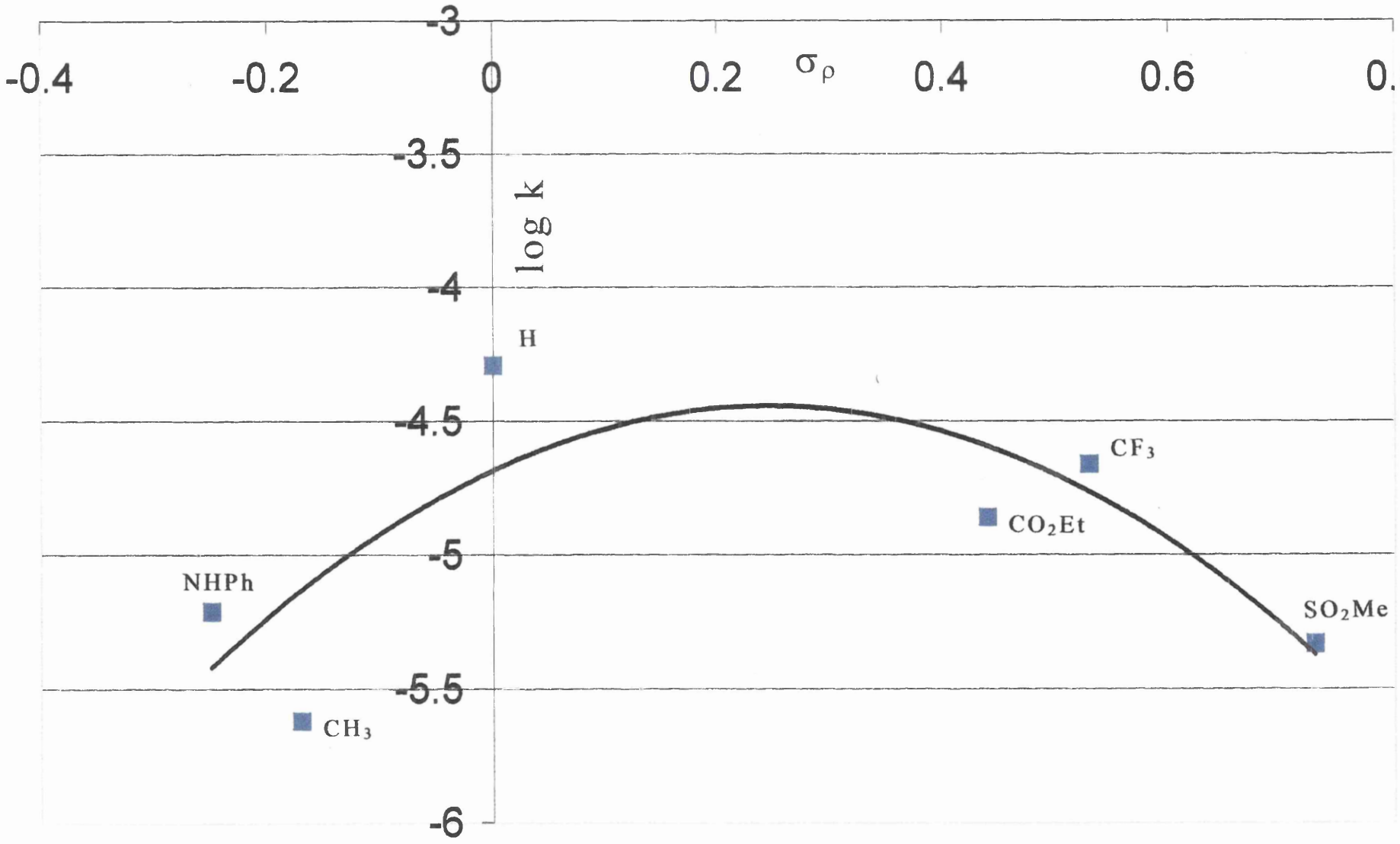

Figure 3.23: Hammett constant plot. Log k vs. σ_ρ.
EtOH/water/HCl:0.47M 298K.

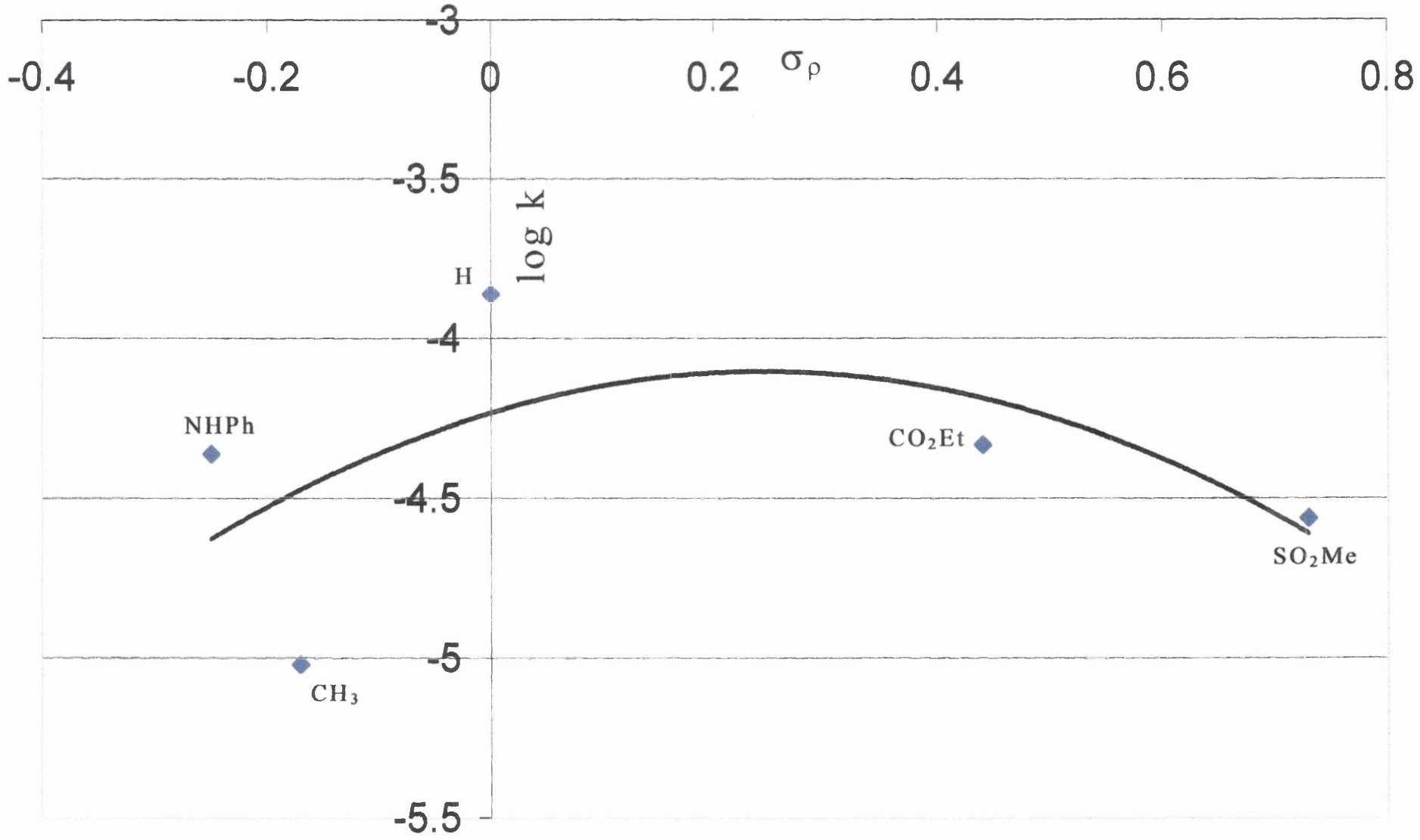

Figure 3.24: Hammett constant plot. Log k vs. σ_ρ.
EtOH/water/HCl:0.94M 298K.

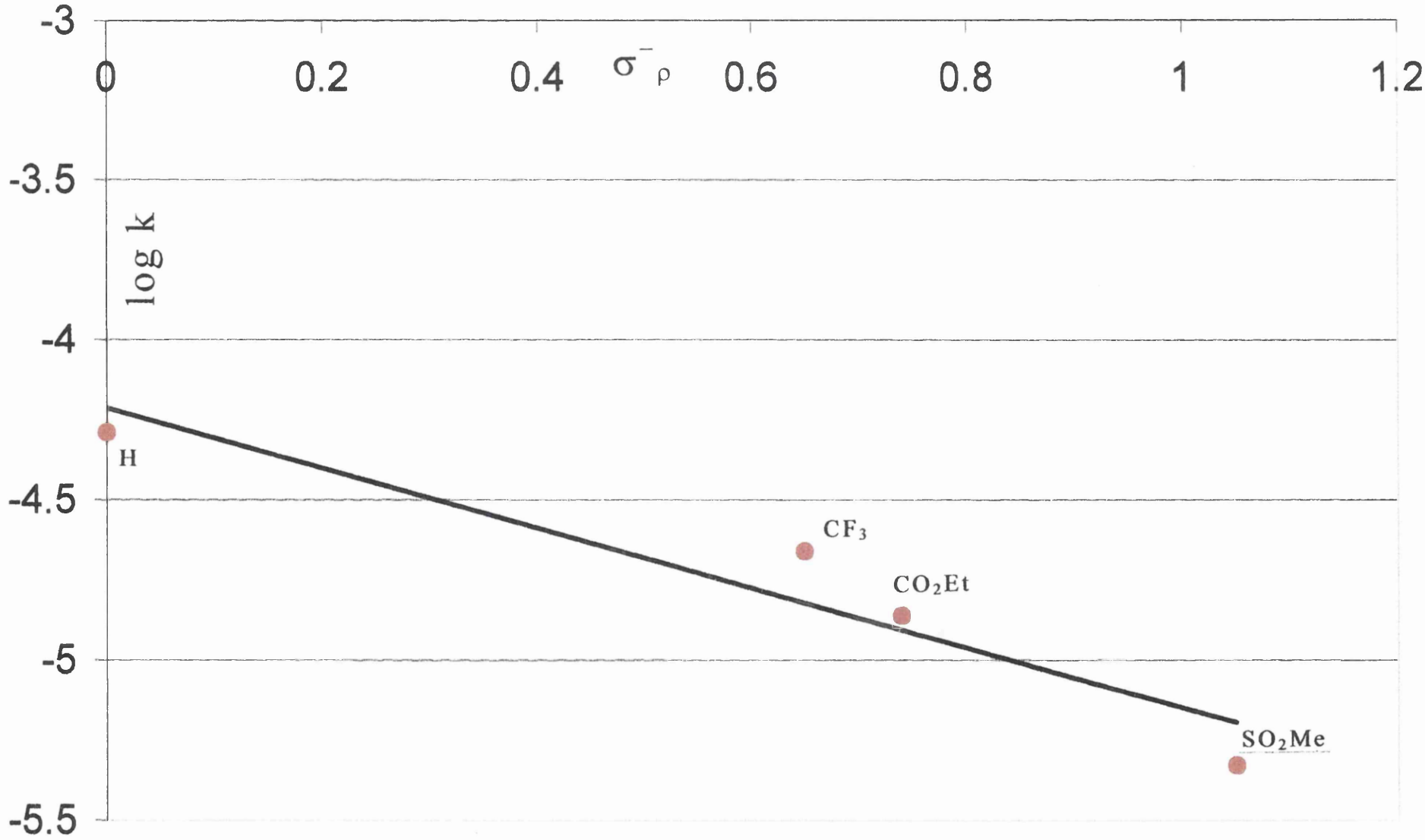

Figure 3.25: Hammett constant plot. Log k vs. σ^{-}_{ρ}.
EtOH/water/HCl:0.47M 298K.

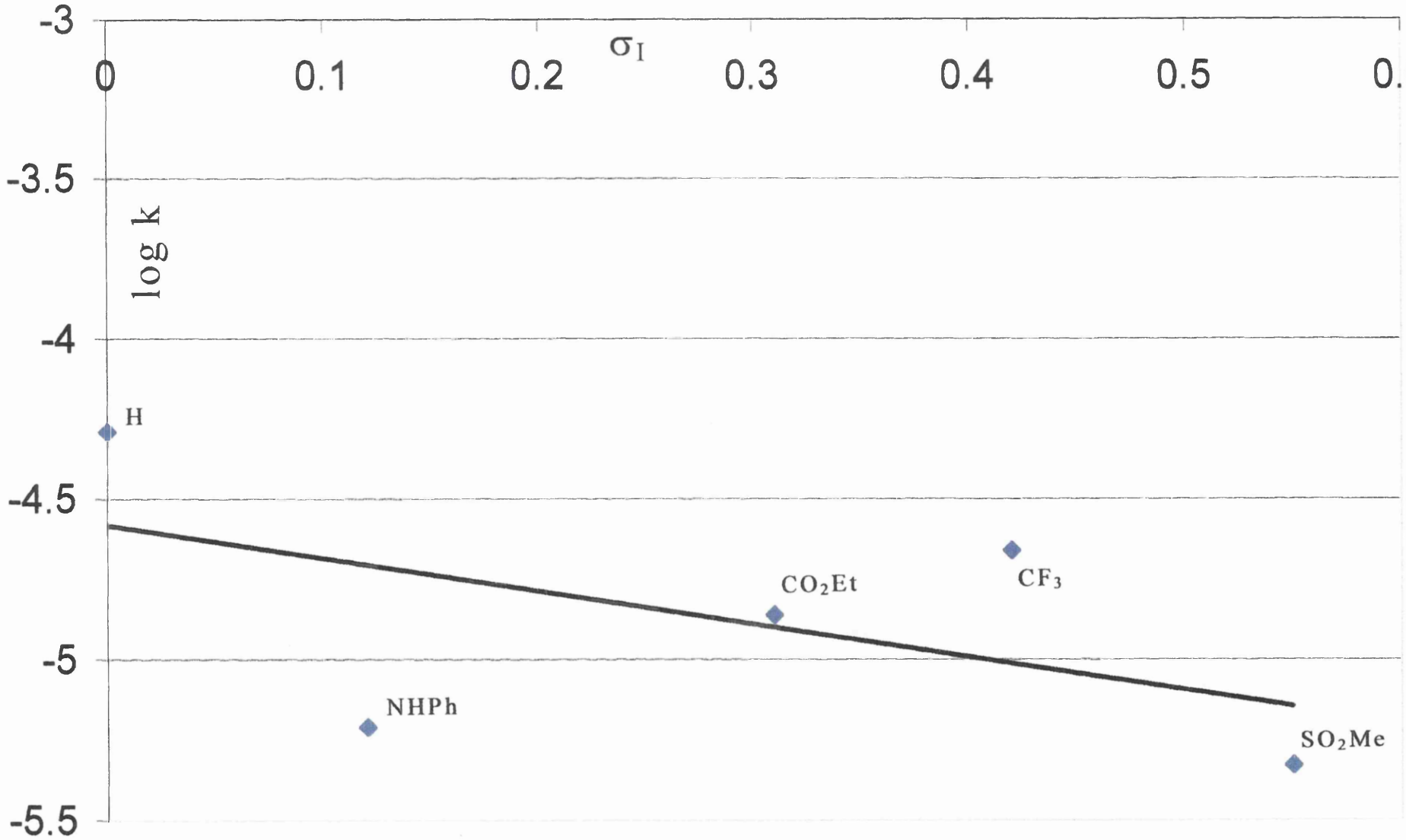

Figure 3.26: Hammett constant plot. Log k vs. σ_I.
EtOH/water/HCl:0.47M 298K.

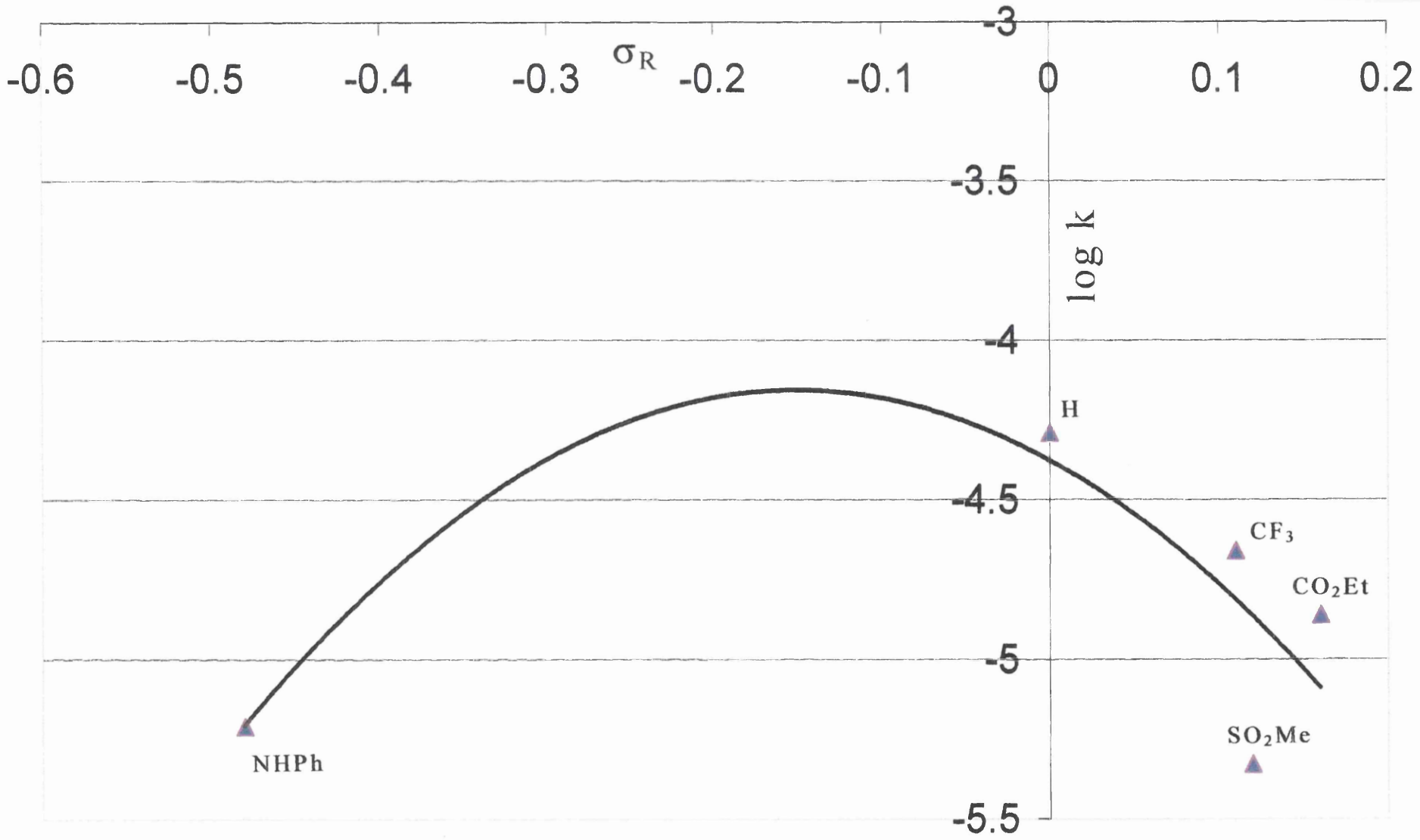

Figure 3.27: Hammett constant plot. Log k vs. σ_R.
EtOH/water/HCl:0.47M 298K.

3.6 Temperature dependence of hydrolysis rates

Table 3.14 gives the temperature dependence of hydrolysis rate constants for $6CO_2Et$-PT, $6SO_2Me$-PT and $6CF_3$-PT dyes in EtOH:water (95%:5% v/v)/HCl(0.3M).

TABLE 3.14

Arrhenius data

T(^{0}C)	T(K)	1/T (K^{-1})	k (s^{-1})	Logk
		$6CF_3$-PT		
31	304	0.00329	0.019	-1.72
25.5	298.5	0.00335	0.011	-1.98
19	292	0.00342	0.0063	-2.2
16	289	0.00346	0.0042	-2.38
		$6CO_2Et$-PT		
35	308	0.00325	0.218	-0.662
31	304	0.00329	0.153	-0.815
27	300	0.00333	0.112	-0.95
18	291	0.00344	0.056	-1.25
15	288	0.00347	0.042	-1.38
		$6SO_2Me$-PT		
31	304	0.00329	2.056×10^{-5}	-4.687
28	301	0.00332	1.820×10^{-5}	-4.74
25.5	298.5	0.00335	1.556×10^{-5}	-4.808
20	293	0.00341	0.962×10^{-5}	-5.017

Plots of logk against 1/T give linear plots over temperature ranges between 15°C (288K) and 35°C (308K) (figures 3.28 to 3.30), showing that over this temperature range the Arrhenius relationship is valid[45, 46] i.e.

$$\log k = \log A - (\Delta E/2.303R)/T$$

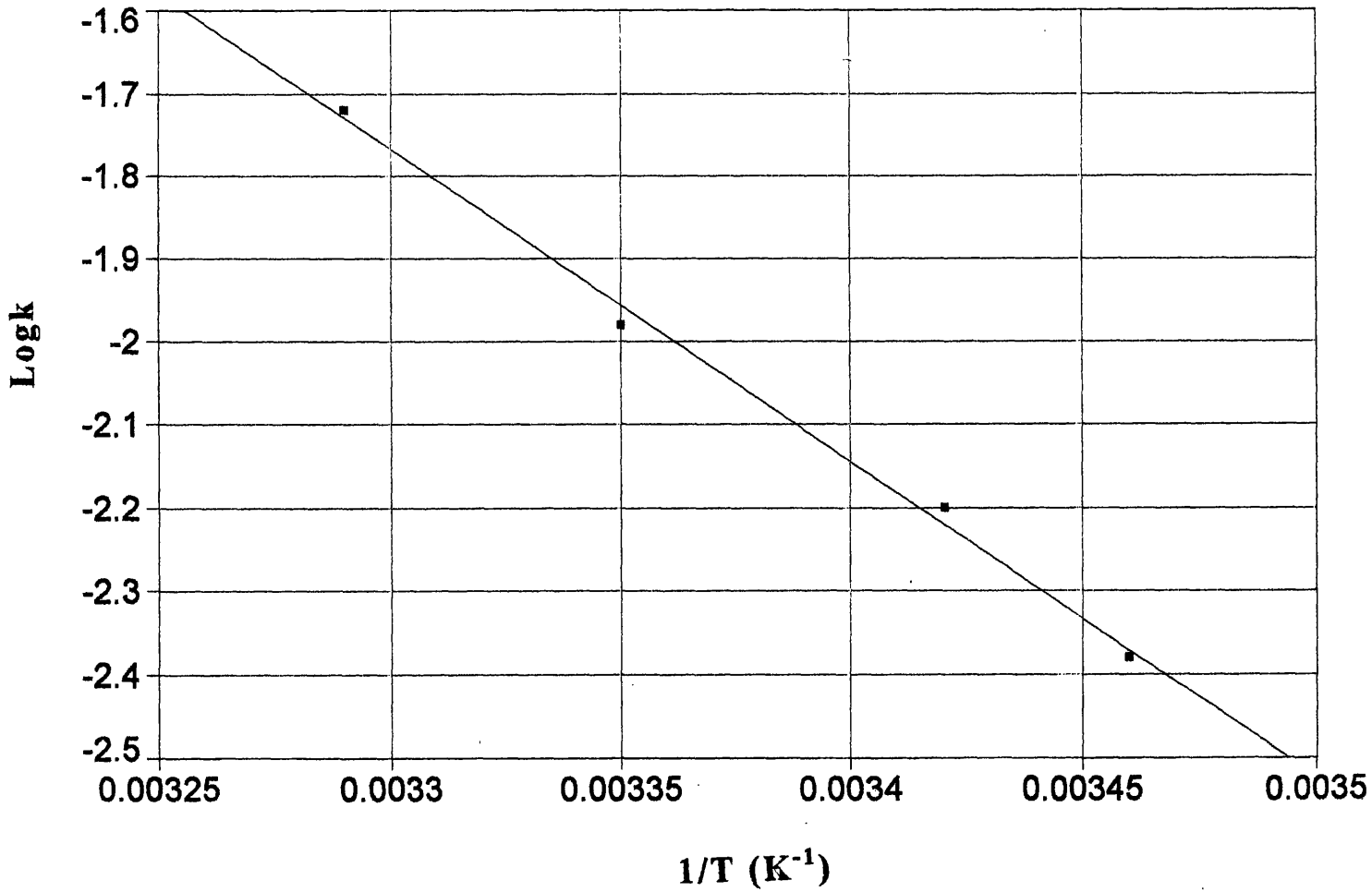

Figure 3.28: Arrhenius plot. Log k vs. 1/T for $6CF_3$-PT in EtOH/water/HCl (0.3 M).

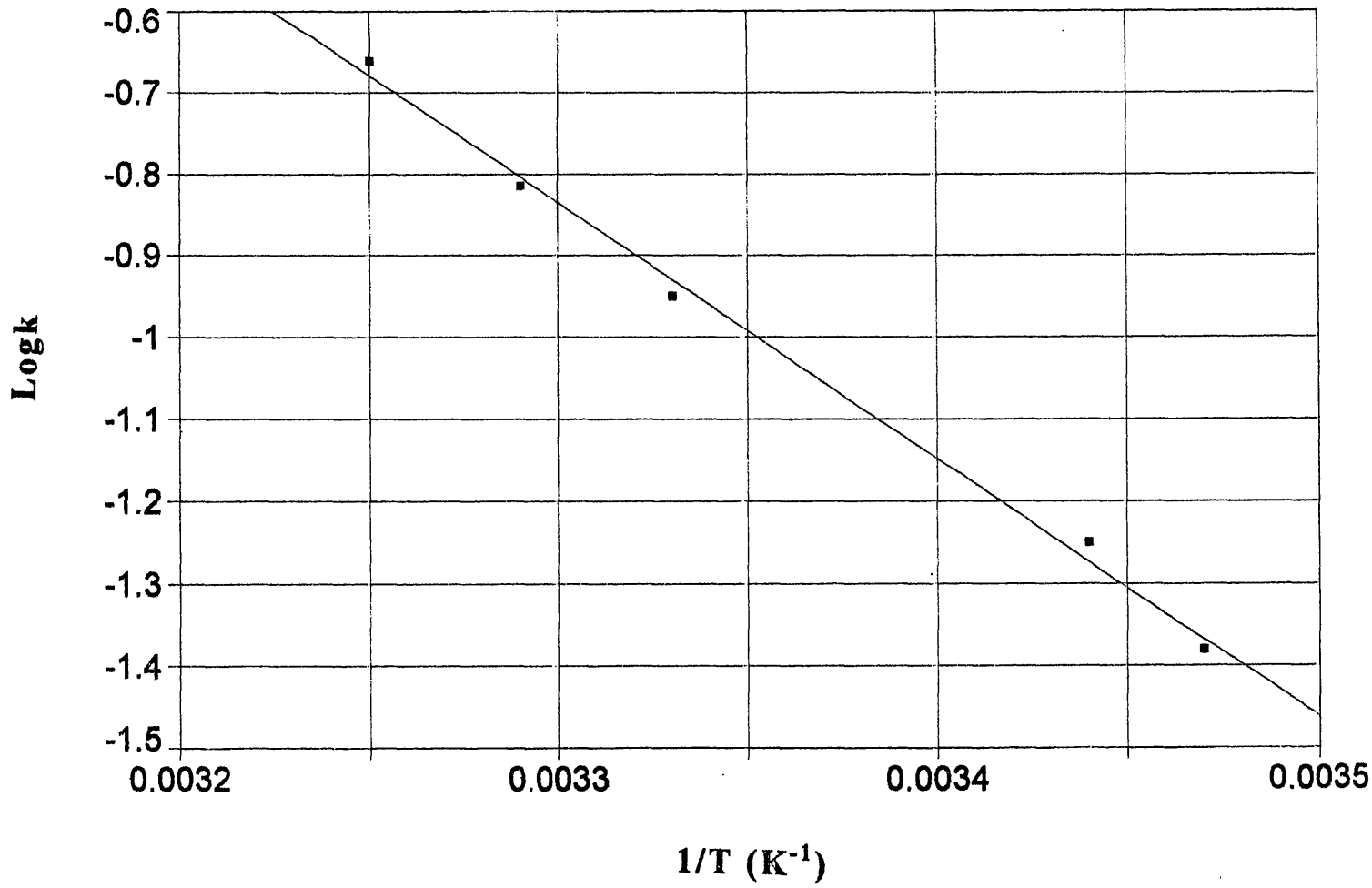

Figure 3.29: Arrhenius plot. Log k vs. 1/T for $6CO_2Et$-PT in EtOH/water/HCl (0.3 M).

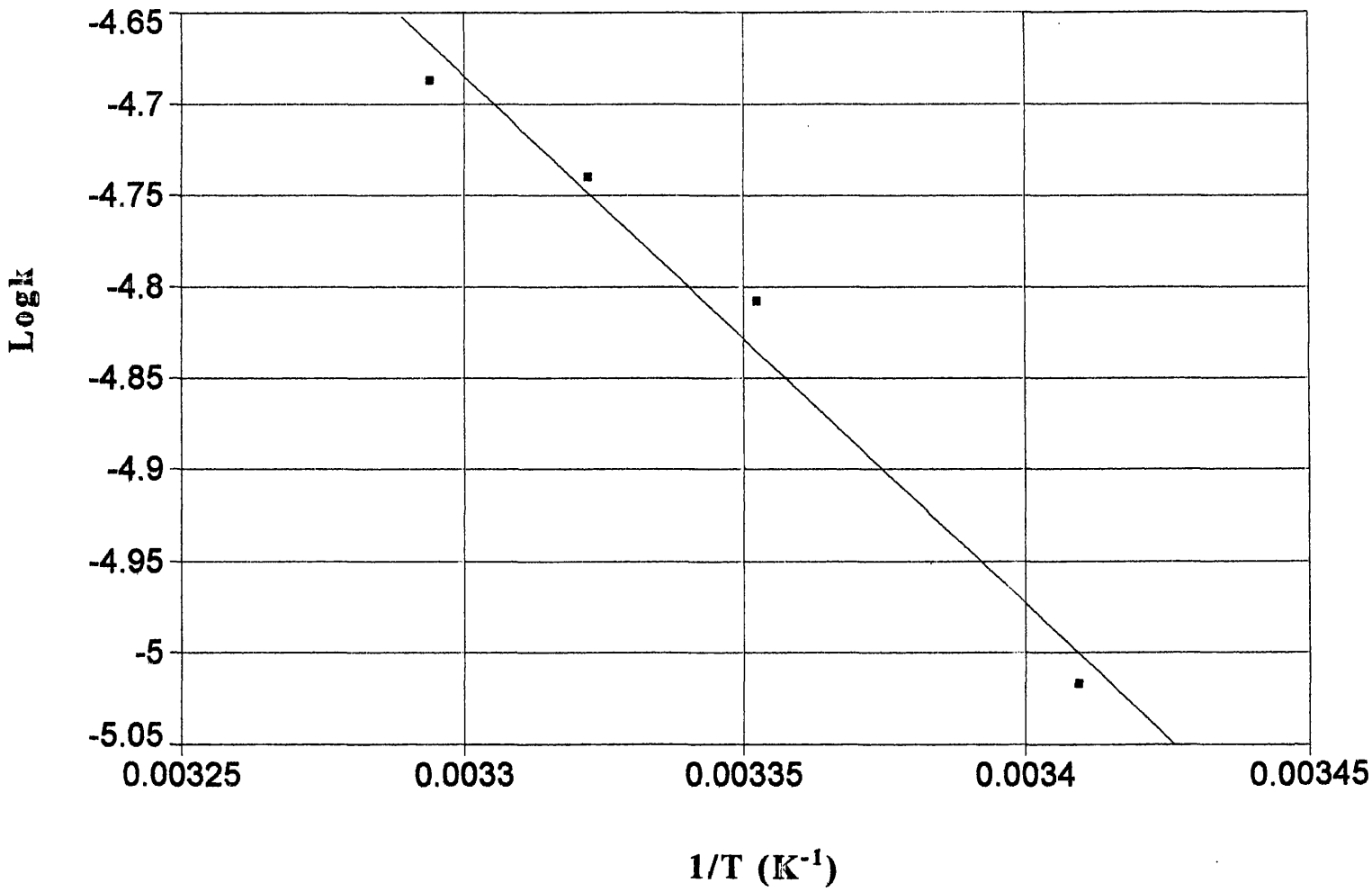

Figure 3.30: Arrhenius plot. Log k vs. 1/T for $6SO_2Me$-PT in EtOH/water/HCl (0.3 M).

Arrhenius constants and pre-exponential factors are given in table 3.15.

TABLE 3.15

Arrhenius data[47]: PT dyes in ethanol/water 0.3M HCl

PT-DYE	(E_{act})/kJ mol^{-1}	A/10^3 s^{-1}
$6CF_3$	71.9 +/- 5	12 x 10^3
$6CO_2Et$	57.9 +/- 5	380
$6SO_2Me$	55.3 +/- 6	67

Values of $\Delta H^{\#}$, $\Delta S^{\#}$ and $\Delta G^{\#}$ were determined, using the following relationships[46]:

$$A = ekT/h(e^{\Delta S\#/R})$$

$$E_{act} = \Delta H^{\#} + RT$$

$$\Delta G^{\#} = \Delta H^{\#} - T\Delta S^{\#}$$

The results are given below in table 3.16.

TABLE 3.16

Entropy, enthalpy and free energy data: PT-dyes in ethanol/water 0.3M HCl.

PT-DYE	ΔS^* JK^{-1}mol^{-1}	$\Delta H^{\#}$/kJ mol^{-1}	$\Delta G^{\#}$/kJ mol^{-1}
$6CF_3$	-137	69 ± 5	110.2
$6CO_2Et$	-146	55 ± 5	99.0
$6SO_2Me$	-161	53 ± 5	100.7

It is interesting to note that the large increase in E_{act} and $\Delta H^{\#}$, for the $6CF_3$-PT dye as compared to $6CO_2Et$-PT and $6SO_2Me$-PT, is offset by a large increase in the pre-exponential factor (A) and a

more modest increase in $\Delta S^{\#}$ such that $\Delta G^{\#}$ is similar for all three compounds. Such compensation effects are relatively common. [29]

3.7 Base hydrolyses

It is observed that, as with acid, PT-dyes undergo hydrolysis in the presence of alkali and this can be conveniently studied in the same manner i.e. by following the loss of absorption at λ_{max} as a function of time.

Plots of dye concentration as a function of time are given in figures 3.31 to 3.32. From the data of these hydrolyses it is apparent that the kinetics are not first order with respect to [dye]. Plots of $\ln A/A_0$ against time are non-linear.

When base hydrolysis data for the CO_2Et-Pt and CF_3-Pt dyes were assessed for second order kinetics with respect to [dye], a plot of $1/A_o$ against $t_{1/2}$ gave approximately linear responses (figures 3.33 and 3.34). This suggests a second order contribution with respect to [dye] for hydrolysis in basic media[45].

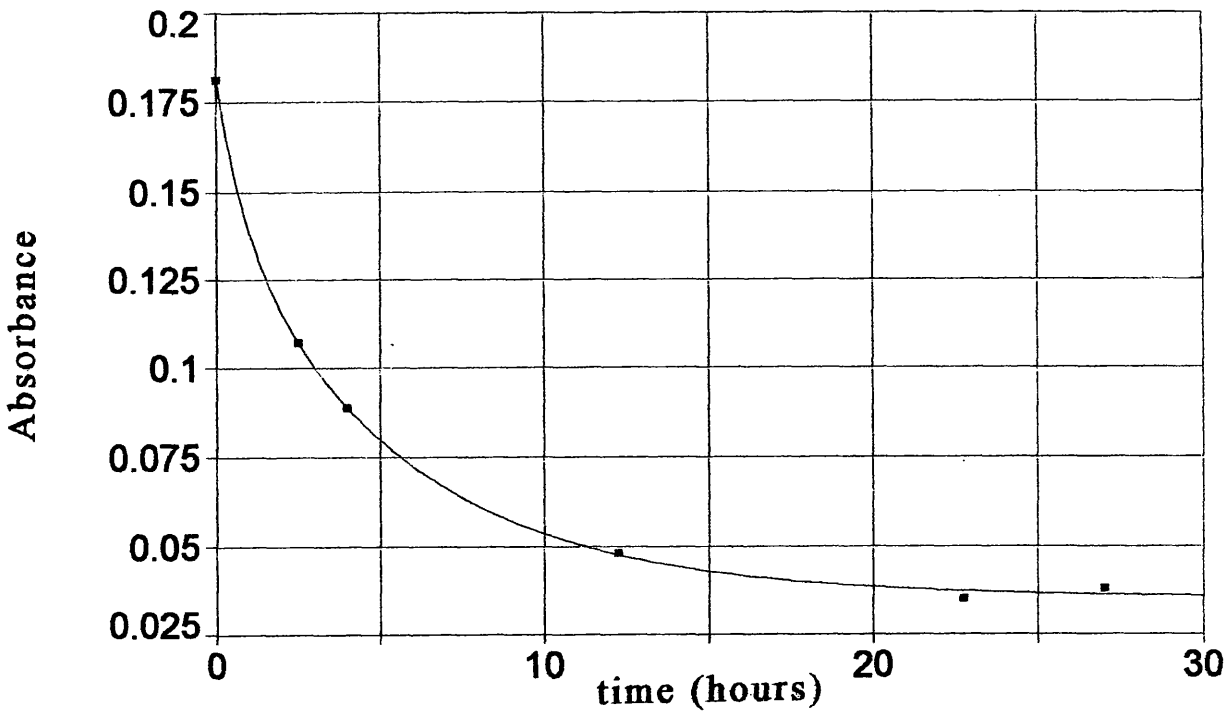

Figure 3.31 Base hydrolysis $6CO_2Et$-PT in EtOH/water/NaOH (0.3 M). 608nm. 298K. Dye concentration = 2.7×10^{-6} mol dm^{-3}

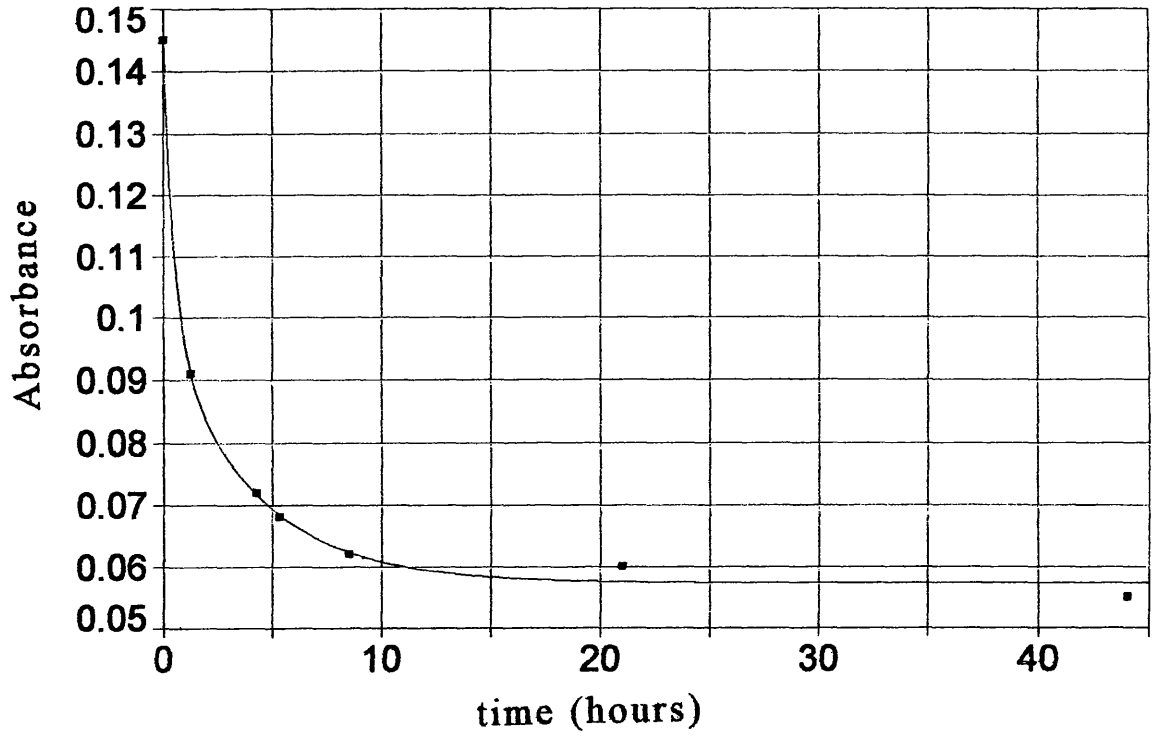

Figure 3.32 Base hydrolysis $6CF_3$.PT in EtOH/water/NaOH (0.3 M). 608nm. 298K. Dye concentration = 2.9×10^{-6} mol dm^{-3}

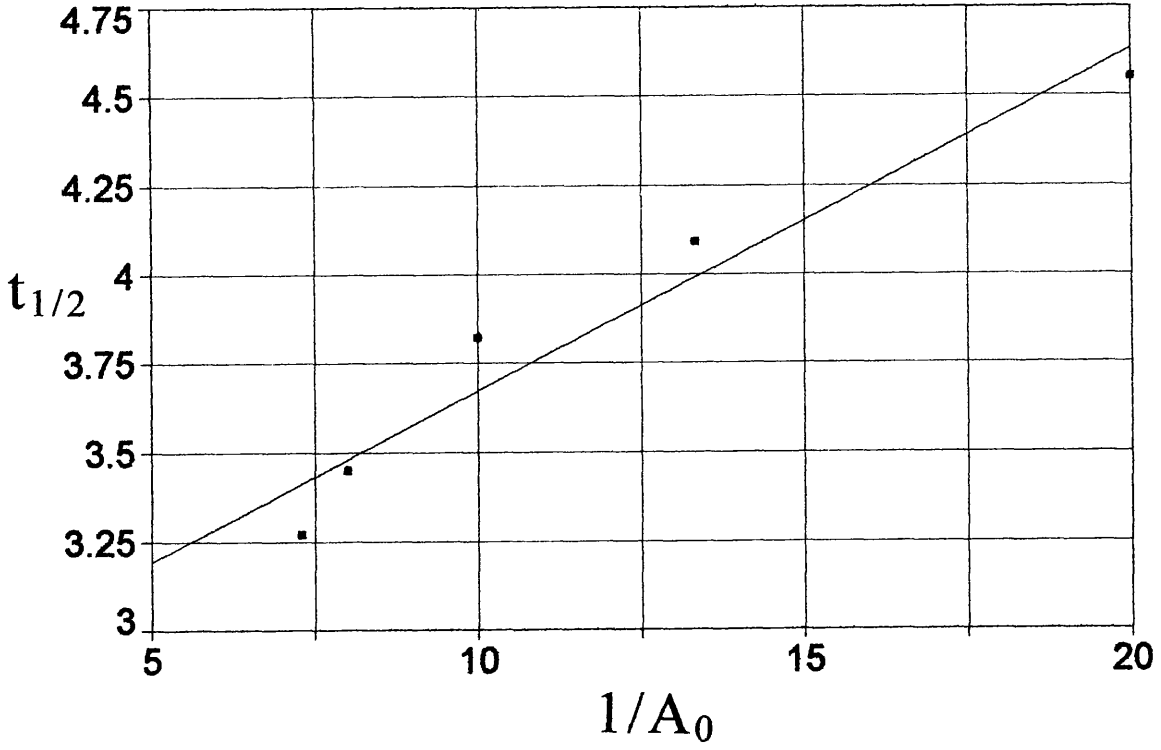

Figure 3.33: Plot $1/A_0$ vs. $t_{1/2}$. Base hydrolysis $6CO_2Et$-PT in EtOH/water/NaOH (0.3 M). 608nm. 298K.

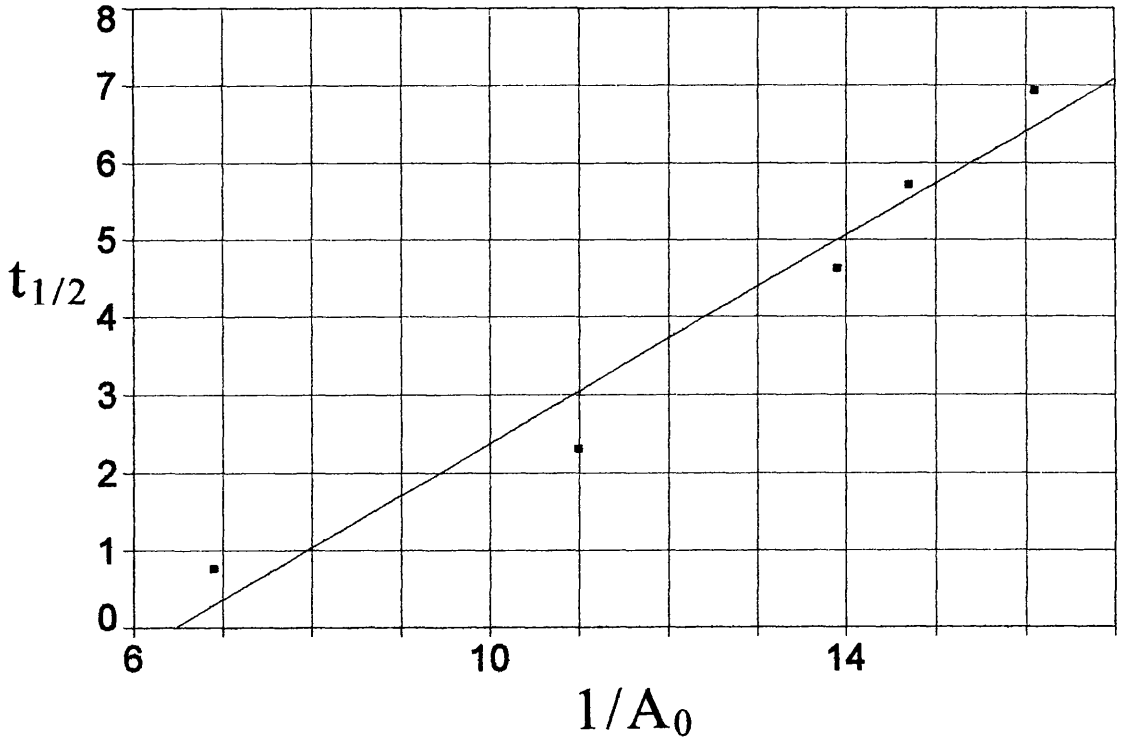

Figure 3.34: Plot $1/A_0$ vs. $t_{1/2}$. Base hydrolysis $6CF_3$-PT in EtOH/water/NaOH (0.3 M). 608nm. 298K.

3.8 Stopped Flow Analysis

3.8.1 Introduction

As has already been mentioned, it was noticed that when the various PT dyes were subjected to acid hydrolysis or reacted with a base, a distinct change in colour was noticeable on mixing. This was perceived to be very rapid, taking less than a second in time, and appeared to be accompanied by a concomitant change in absorbance. See figures 3.35, 3.36 and 3.37 for the dyes $6CO_2Et$-PT and $6CF_3$-PT

The rate at which this prompt reaction took place was about 1,000 times faster than the rates of hydrolyses documented in this chapter. Consequently it was decided to employ milli-second stopped-flow techniques to study the behaviour of the PT dyes when introduced into acid and base media and over the first few seconds of hydrolysis. Time constraints meant that this investigation was of a very preliminary nature. Furthermore the complexity of the behaviour observed meant that few definitive results could be obtained. However this was, to my knowledge, the first time such rapid kinetic techniques were applied to a study of PT dye hydrolysis. For this reason alone, these very preliminary results are included in this thesis in the hope they may be of value to future workers in the field who might consider the use of stopped-flow for such studies.

3.8.2 Results

A typical example of a stopped flow hydrolysis is given in figure 3.38 - the kinetics appear quite complex. The trace can be separated into two or three distinct regions, an initial decay (I), a formation step (II) and then a further decay sequence (III). The results seem to be consistent with a series of two (or even three) consecutive (or successive) reactions.

3.8.3 Successive reactions

In a sequence of successive reactions:

$$A \xrightarrow[kI]{} B \xrightarrow[kII]{} C$$

at time=0, [B] and [C]=0. But as the reaction proceeds [A] decreases to 0. As B is formed its concentration increases to a maximum value as seen in figure 3.38; this occurs at time, t_m. [B] will then fall to zero as C is formed. Now, the faster the rate of formation of B relative to its decomposition to C the larger will be the ratio k_I / k_{II} and consequently the larger will be the value of y_m[47]. If we assume that each intermediate is involved in first order kinetics, then:

$$d[C]/dt = k_{II}[B] \qquad 3.5$$

which yields the following differential equation:

$$d[C]/dt + k_{II}[C] = k_{II} a_t \left(1 - e^{-k_I t} \right) \qquad 3.6$$

Where $a_t = [A]/[A]_t$. Solving this gives:

$$[C]_t = a_t \left(1 + [k_{II} e^{-k_I t} - k_I e^{-k_{II} t}] / k_I - k_{II} \right) \qquad 3.7$$

and

$$[B]_t = [A]_t - [C]_t = [a_t k_I / k_I - k_{II}] \left(e^{-k_{II} t} - k_I e^{-k_I t} \right) \qquad 3.8$$

Differentiating equations 3.7 and 3.8 gives the maximum absorbance (y_m) and the value t_m, the time to the maximal value:

$$t_m = (\ln k_I / k_{II}) / k_I - k_{II} \qquad 3.9$$

$$y_m = a_t (k_{II} / k_I)^{k_{II} / k_I - k_{II}} \qquad 3.10^{(47)}$$

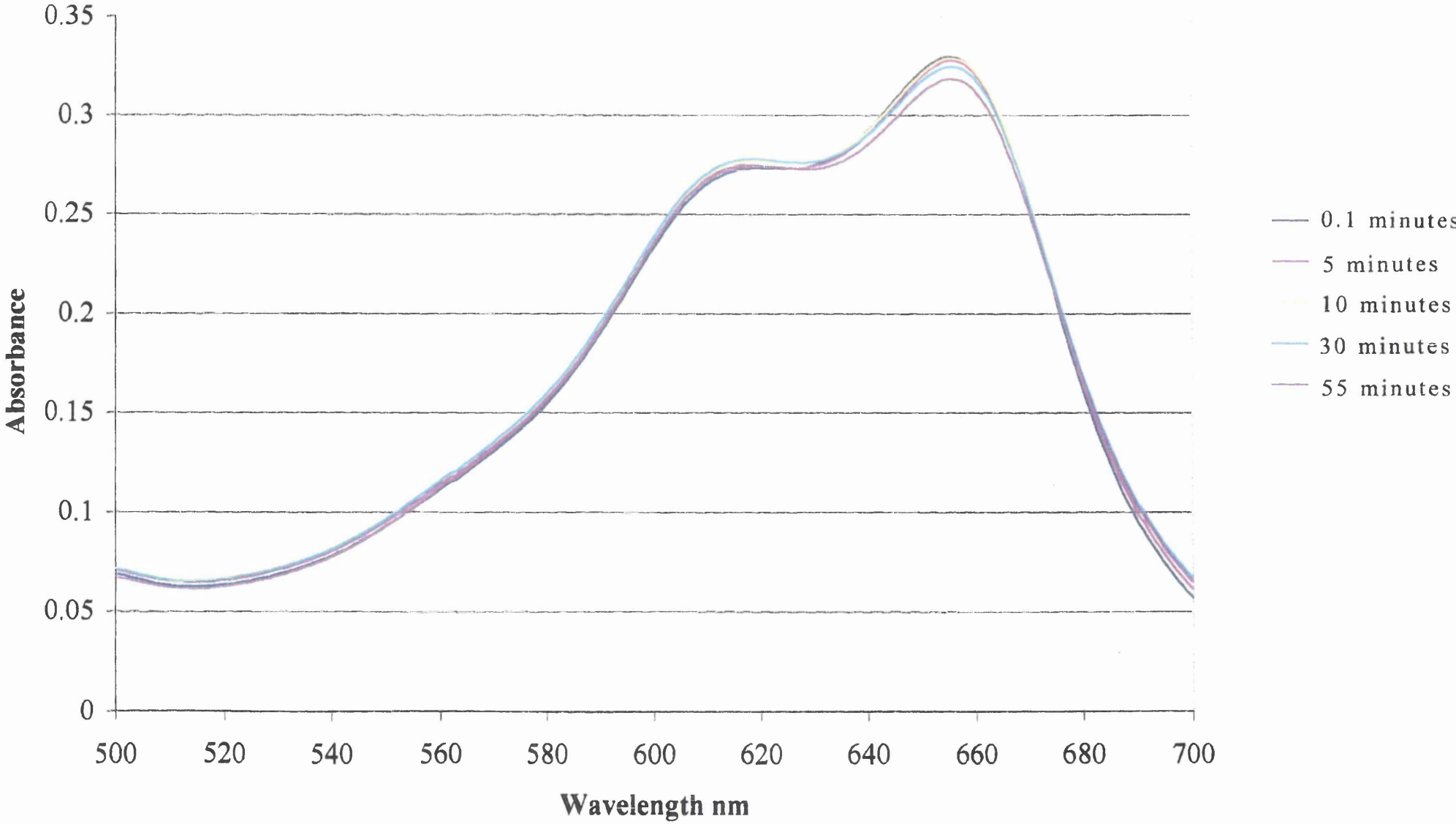

Figure 3.35 $6CO_2Et$-PT dye in 0.5M TFA/chloroform. Spectra taken at time intervals 0.1 to 55 minutes. 298K. Dye concentration = 5.2×10^{-6} mol dm^{-3}

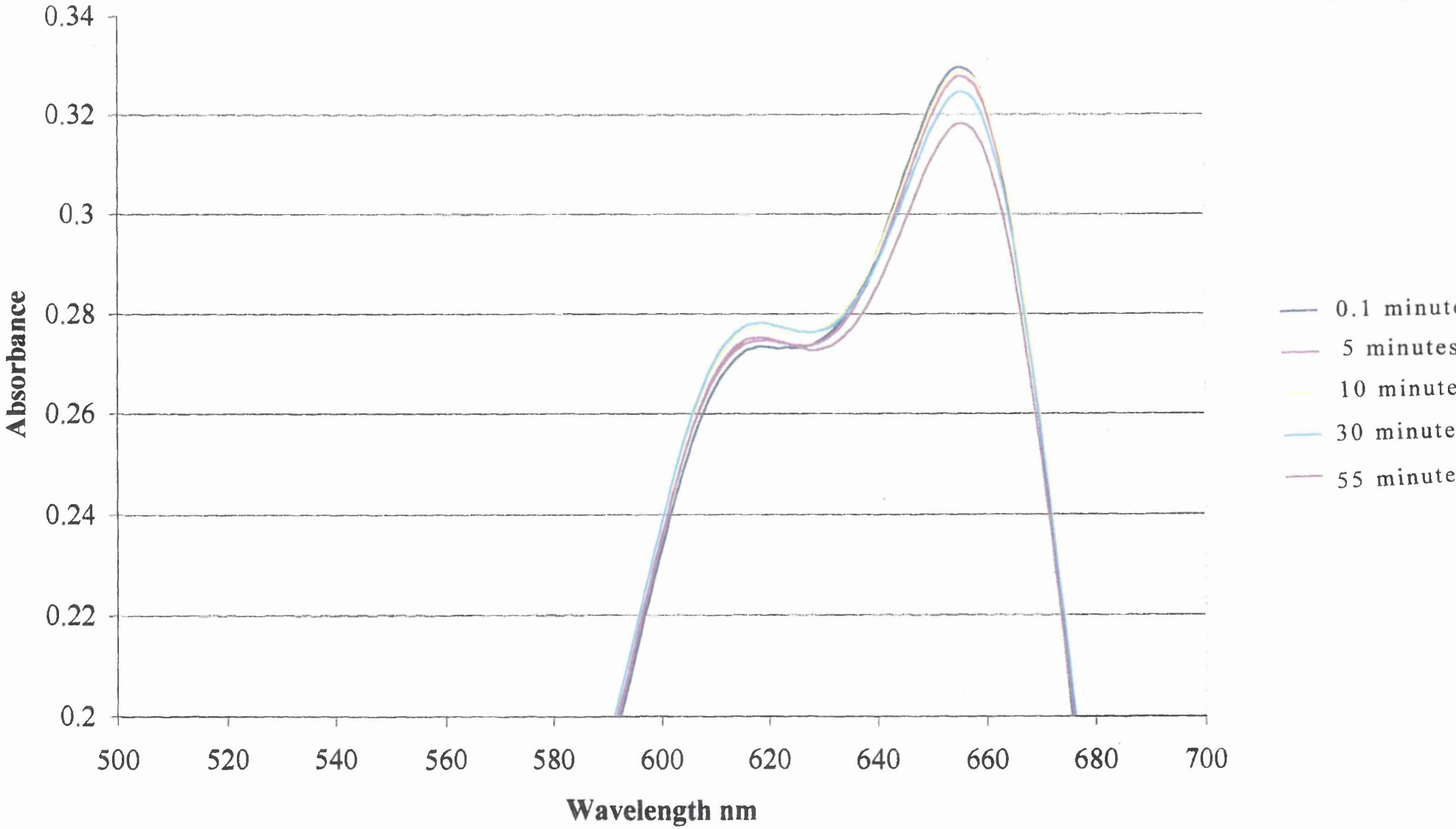

Figure 3.36 Detail from $6CO_2Et$-PT dye in 0.5M TFA/chloroform. Spectra taken at time intervals 0.1 to 55 minutes. 298K. Dye concentration = 5×10^{-6} mol dm^{-3}

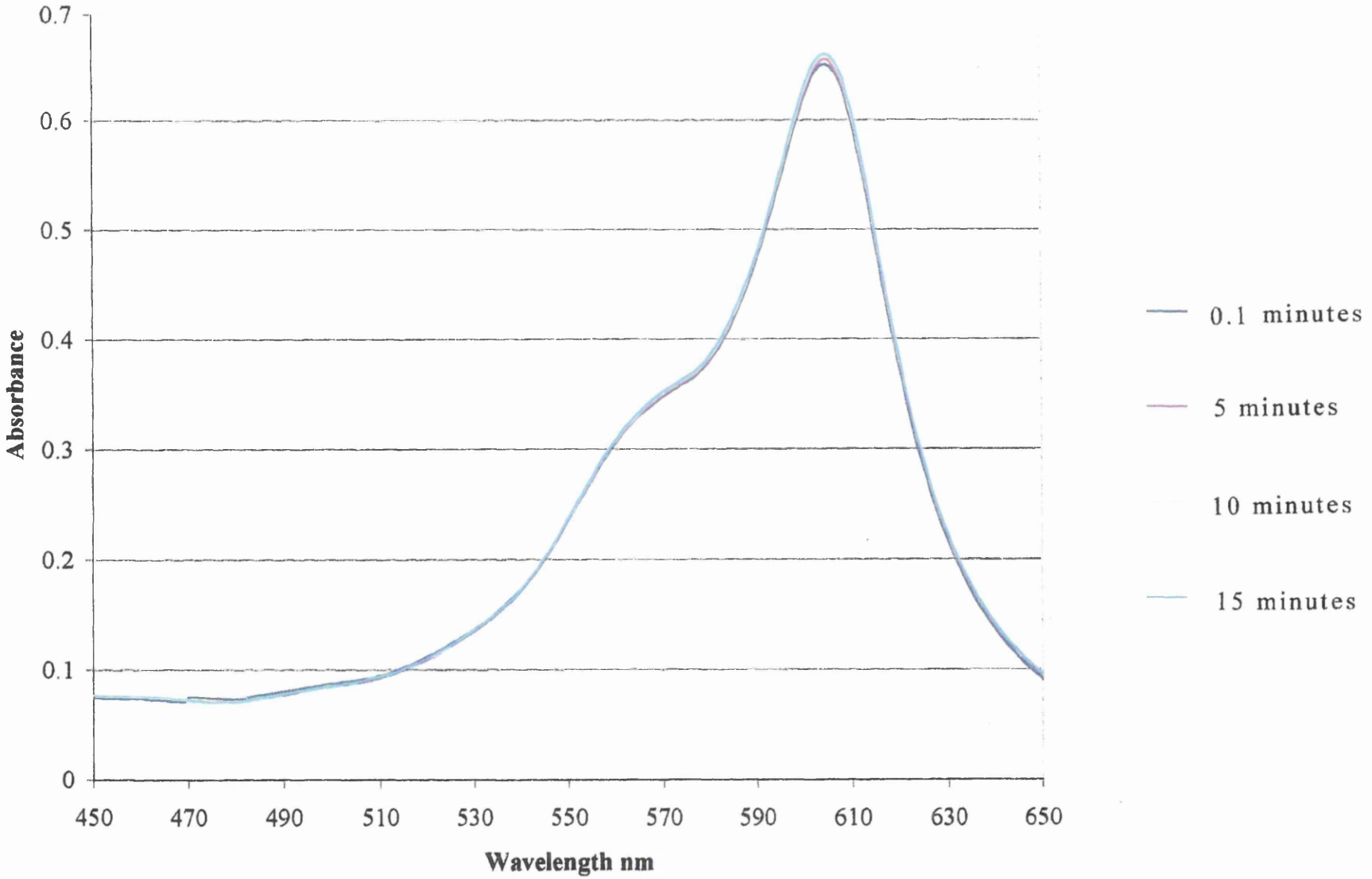

Figure 3.37 $6CF_3$-PT dye in 0.5M TFA/chloroform. Spectra taken at time intervals 0.1 to 15 minutes. Dye concentration = 1.3×10^{-5} mol dm^{-3}

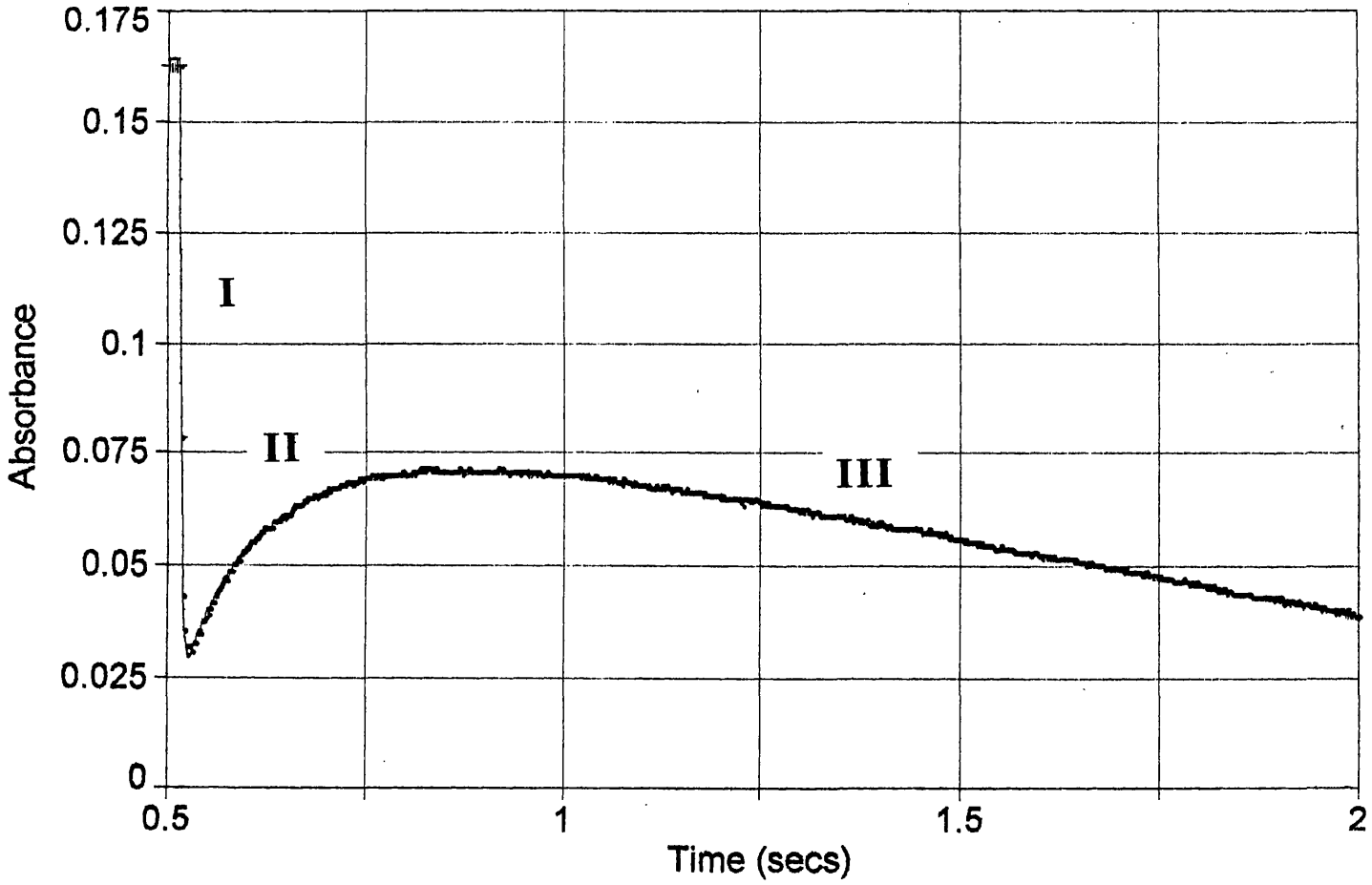

Figure 3.38. Stopped Flow $6CO_2Et$-PT dye in Chloroform/TFA (0.5M / 298K).

3.8.4 Evidence

A number of these stopped flow traces were analysed using a mathematics modeling program (i.e. 'Tablecurve v. II'. Jandell). A number of these are reproduced in figures 3.39 to 3.42 - the solid line being the best fit to an equation of the form of y=a+bc (exp(-cx)-exp (-dx))/(d-c) where c>d. Whilst these analyses need to be treated with some caution, it does appear that a sequence of consecutive reactions are in evidence possibly with the formation of a protonated intermediate. This would be consistent with the pK_a analyses completed previously.

It was possible to analyse the stopped flow acid hydrolysis of the $6CO_2Et$ dye concentrating on the final phase of the reaction i.e. region III. Treating this region in isolation and as a first order reaction, rate constants were determined for the dye in varying acid concentrations (0.5 to 5 M). A significant increase in rate is observed with increase in acid concentration; this is illustrated in figure 3.43.

Using a similar approach of isolating the kinetic regions of the curves, it was possible to determine the rate constants for regions II and III at constant acid concentration these are given in table 3.15:

TABLE 3.17

Rate constants for $6CO_2Et$-PT dye. Acid hydrolysis (H_2SO_4).

[Acid] M	k_{II} [s^{-1}]	k_{III} [s^{-1}]
4	14.03 +/- 0.3	1.42 +/- 0.2
0.5	0.62 +/- 0.05	0.21 +/- 0.05

From these data it is apparent that the second and third phase rate constants differ by about a factor of 3 - 10.

Obtaining the values of k_I proved to be more problematic, the timescales for the first phase being less than 0.1 second.

The results from this preliminary study must be viewed with some caution. However, the study did show a surprising complexity in nature of these reactions. Further work involving a detailed spectral study, and a "global" curve analysis will be necessary to help unravel this complex series of reactions.

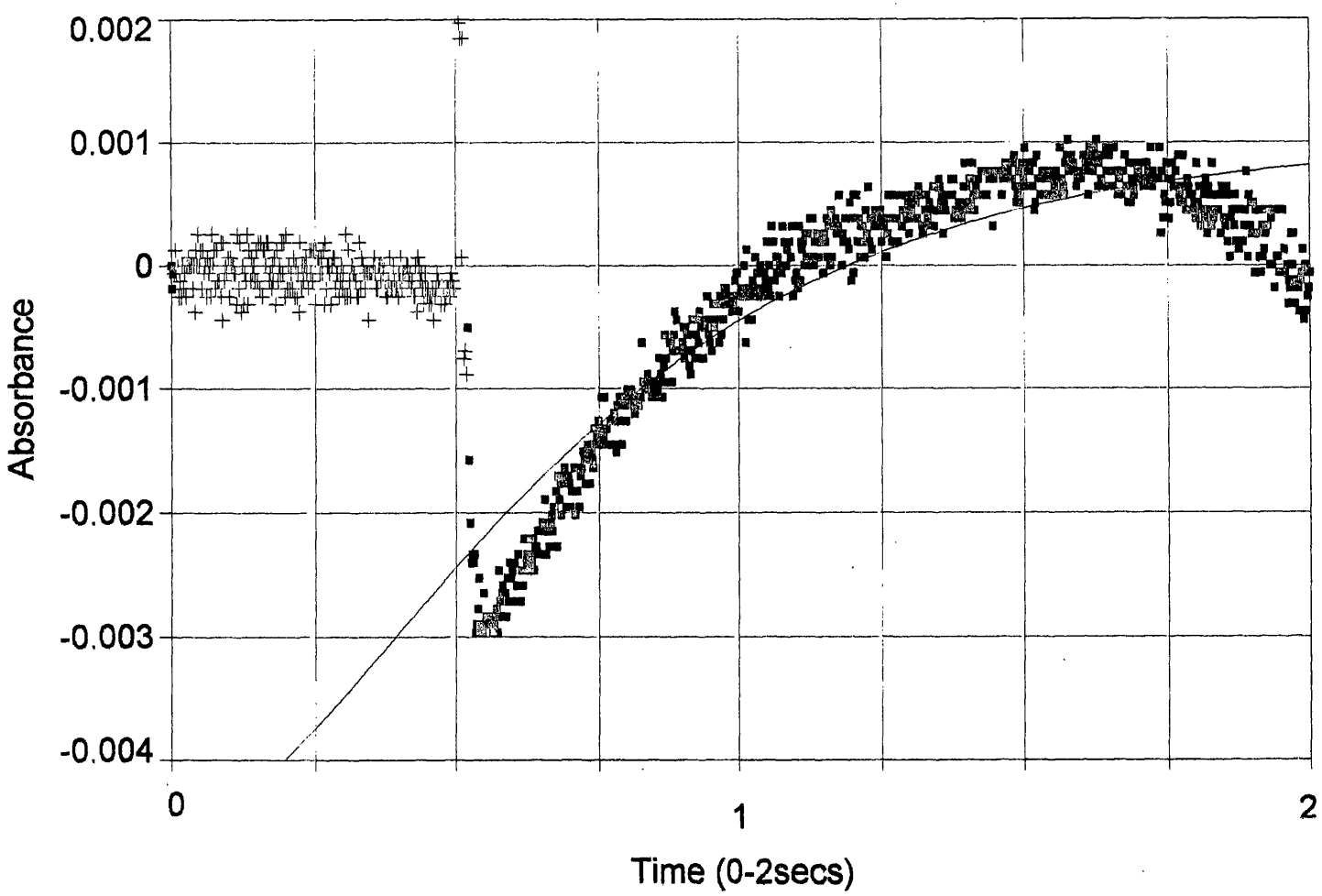

Figure 3.39. Stopped Flow $6CO_2Et$-PT dye in Ethanol/water (50:50%) Sulphuric acid (0.5M / 298K).

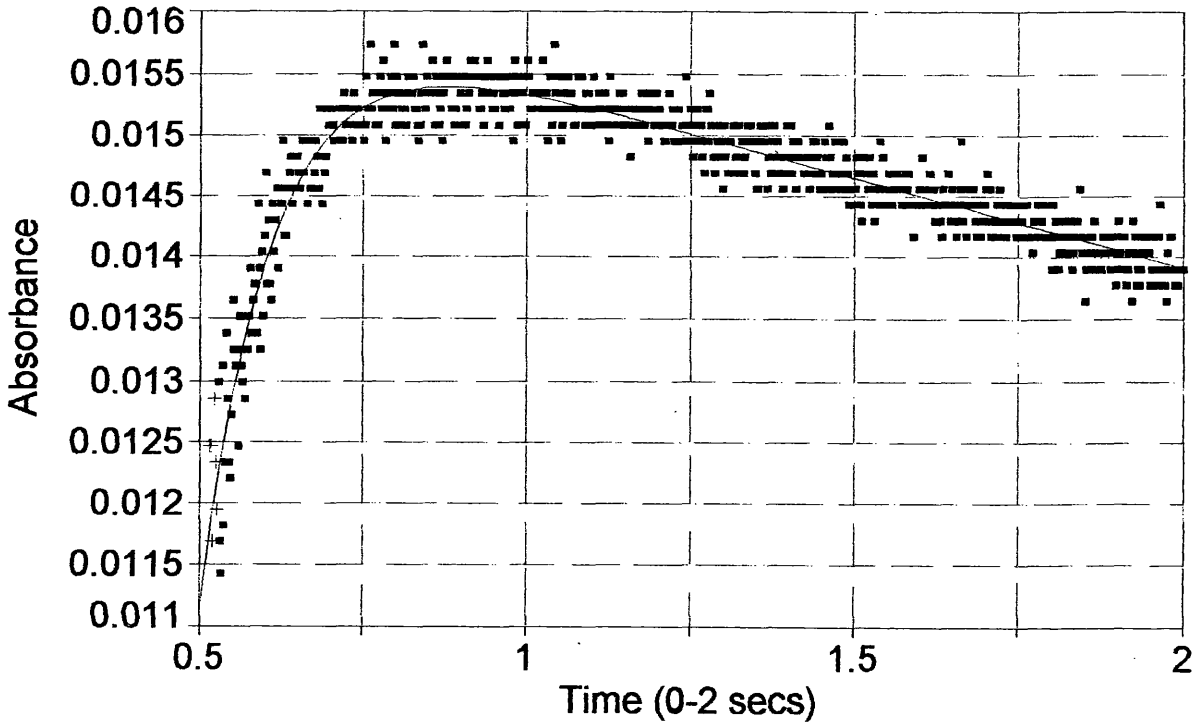

Figure 3.40. Stopped Flow $6CO_2Et$-PT dye in Ethanol/water (50:50%) Sulphuric acid (1.0M / 298K).

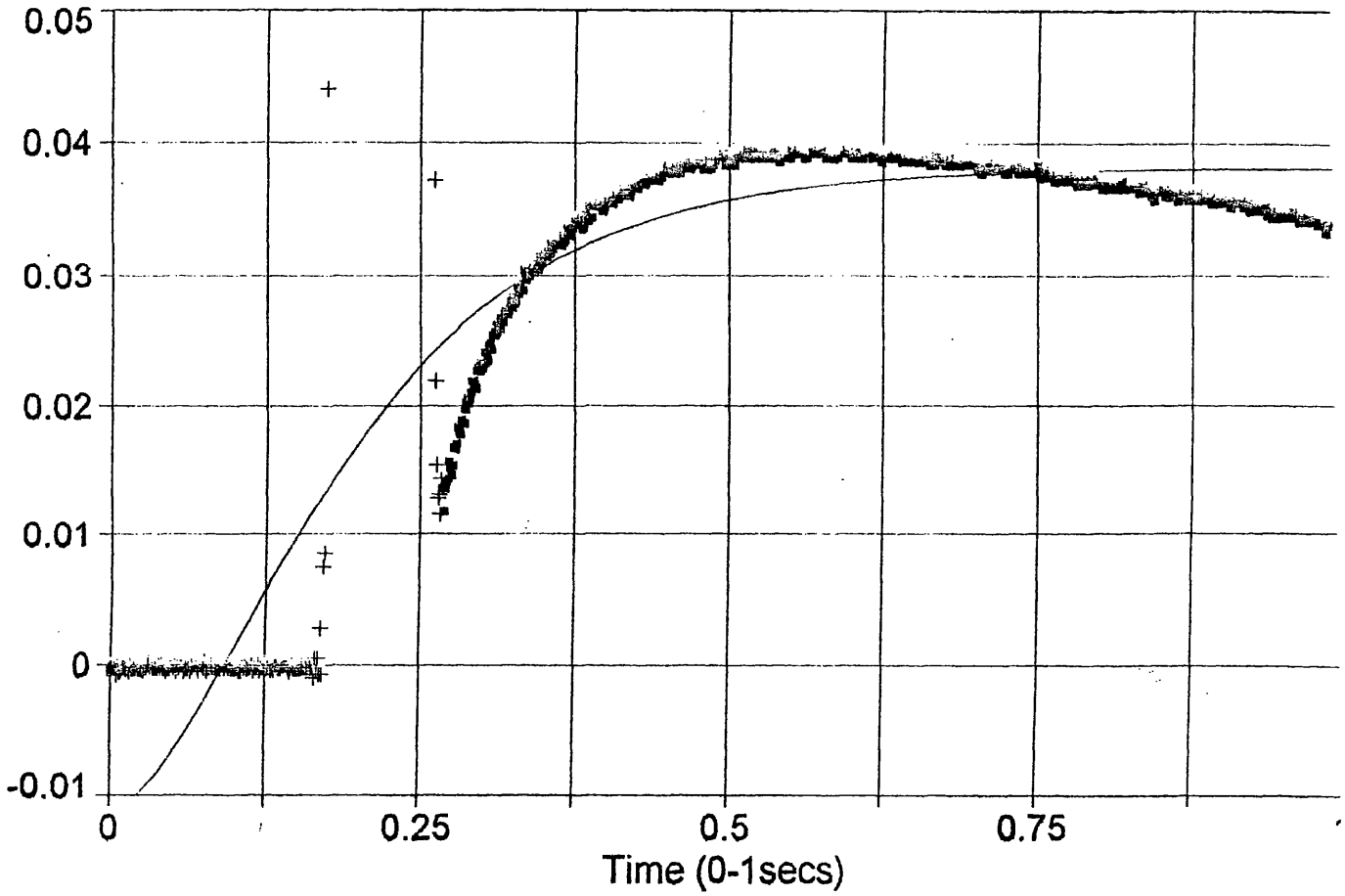

Figure 3.41. Stopped Flow $6CO_2Et$-PT dye in Ethanol/water (50:50%) Sulphuric acid (4.0M / 298K).

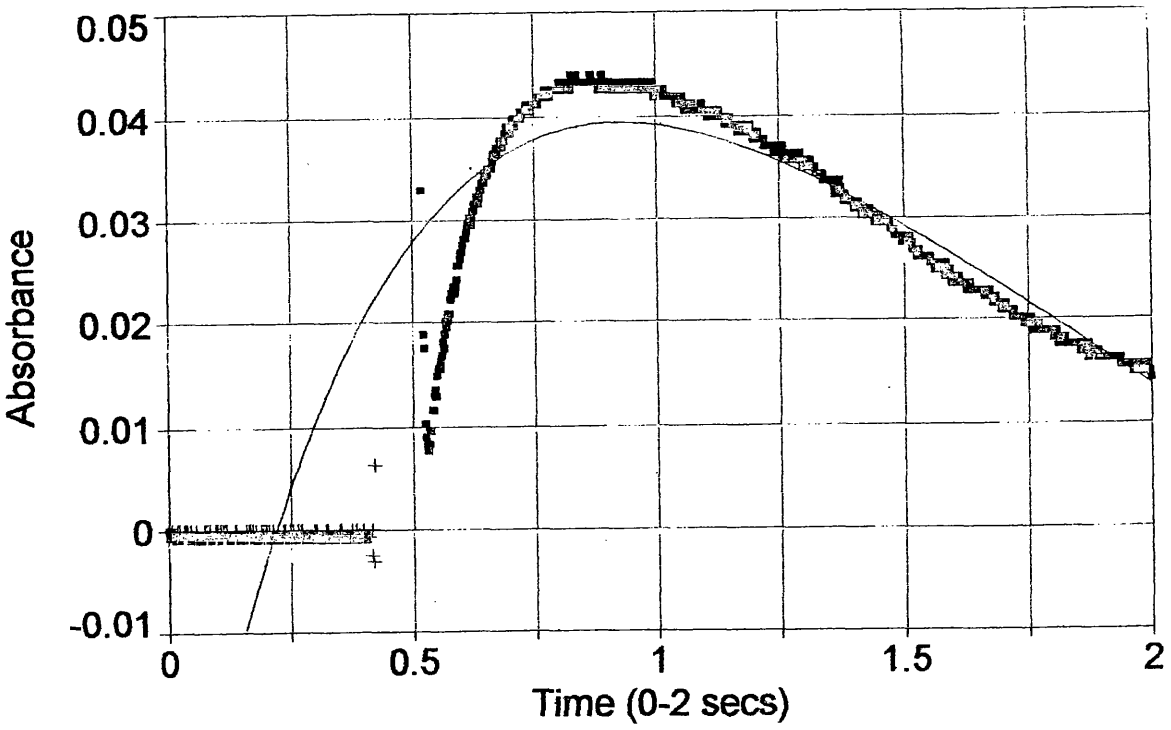

Figure 3.42. Stopped Flow $6CO_2Et$-PT dye in Ethanol/water (50:50%) Sulphuric acid (5.0M / 298K).

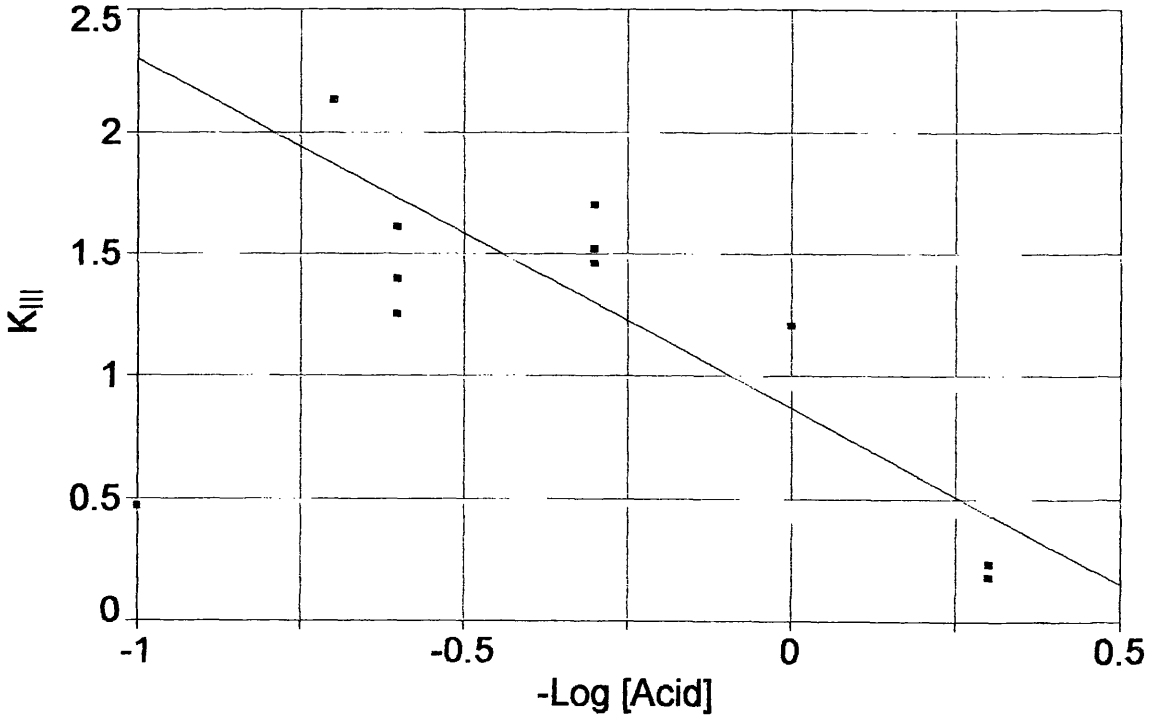

Figure 3.43. Rate Constant K_{III} vs. –Log[Acid]. Stopped Flow $6CO_2Et$-PT dye in Ethanol/water (50:50%) Sulphuric acid 298K).

3.9 Conclusion

Protonation of the $6CO_2Et$-PT dye in chloroform results in an increase in emax and a narrowing of the absorption band together with a bathochromic shift. At least two pKa transitions are apparent. The $6CF_3$–PT dye displays similar characteristics, but the second pKa transition accompanies a slight hypsochromic shift in λmax. This is consistent with studies of the 6H-PT dye conducted by C. Couture[43]. Studies of the $6CO_2Et$-PT dye suggest that a complex mechanism with two protonation steps. It is suggested that the second protonation step has two protons in equilibrium. Again, this is consistent with previous studies[43].

In acidic hydroxylic media the pyrazolotriazole azomethine dyes all fade following first order kinetics. Rate constants range from 2 x 10^{-6} s^{-1} (6Me-PT dye) to 22 x 10^{-6} s^{-1} ($6CF_3$-PT dye). However, the rate constants were greatly reduced by a factor of 200 for the $6CF_3$-PT, and a factor of 10 for $6CO_2Et$-PT dye.

Base hydrolyses of $6CO_2Et$-PT and CF_3-PT dyes were found to be second order with respect to dye concentration.

Indications of a possible change in mechanism for the hydrolysis of dyes in ethanol: water (95%:5% v/v) is suggested by plots of log k against Hammett sr and sR values. There appears to be a marked "L-shaped" correlation between sr values and log k suggesting a change in mechanism for inductive groups (e.g. CH^3) with negative sr values and electron withdrawing groups (e.g. CF_3 and $6CO_2Et$ groups) with positive sr values. With sR values a similarly pronounced "L-shaped" correlation is seen.

Arrhenius constants and pre-exponential constants were calculated. Average Eact values of 61KJ mol^{-1} were observed for the three dyes. ΔG# values were similar for the three dyes studied: average

value being 103 KJ mol^{-1}. The CF_3–PT dye demonstrated a large pre-exponential factor (120 x $10^3 s^{-1}$) compared to the $6CO_2Et$-PT and the $6SO_2Me$-PT dyes. This suggests a compensation effect[29] for the large rise in Eact and ΔH# values seen for the CF_3–PT dye.

Preliminary investigations of millisecond stopped flow hydrolyses were carried out in aqueous and non-aqueous media. The results are complex: there is evidence to suggest three successive reactions, the second and third phase of which differ in rate by a factor of between 3-10.

4. EXPERIMENTAL

4.1 Chemicals

The following chemicals were supplied by BDH (Poole, Dorset, UK): n-hexane, chloroform, acetonitrile, methanol, ethanol, 95% (w/v) hydrochloric acid, 38% (w/v) sulphuric acid, sodium hydroxide (AnalaR). Trifluoroacetic acid and dimethylsulphoxide (AnalaR) were obtained from Fluka chemicals and nitrogen from BOC gases. Kodak Limited supplied all dyes. The structures of the dyes are given in figure 1.7.

4.2 Solutions

Solutions of PT-dyes

The solutions of dyes were prepared by adding a small quantity of dye (typically < 20mg) to 100ml of solvent. This was then sonicated for one hour at room temperature. Uv-visible spectra were carried out on all solutions to ascertain the concentration of dye solution using a value of $\varepsilon_{max} = 10^4 mol^{-1} dm^3 cm^{-1}$ [29].

Solutions of hydrochloric acid

Aqueous solutions of hydrochloric acid were prepared by dilution of 12M (density=1.18 g/ml) hydrochloric acid. In non-aqueous media (e.g. ethanol/water [95%:5% v/v]) solutions of different concentrations were prepared by adding the appropriate mass of concentrated acid to the solvent/water mixture.

Mixed media

Solutions of organic/aqueous media were prepared using AnalaR or spectroscopic grade ethanol, methanol and DMSO with doubly distilled deionised water. Typically, media consisting of solvent

to water in the proportions 95:5 v/v were used. Where possible all dye solutions and acid and alkali reagents were prepared from the same stock aqueous solution.

Non-aqueous media

Solutions of non -aqueous media were prepared using AnalaR or spectroscopic grade chloroform, acetonitrile, n-hexane.

4.3 Methods

4.3.1 Uv/visible spectrophotometry

Uv/visible spectrophotometry was carried out using one of three instruments. Following preparation of solutions of the dyes, spectra were run on a single beam scanning spectrophotometer PU 8720 UV/VIS using a 1cm quartz cell. From the absorbance and using extinction coefficients of 5×10^4 $mol^{-1}dm^3cm^{-1}$ for $6CF_3$–PT, 6H-PT and 6COPh-PE dyes and a value of $6.61 \times 10^4 mol^{-1}dm^3cm^{-1}$ for the $6CO_2ET$ dye, concentrations could be calculated[29]. The instrument was reliable in absorbance range of 0.1 to 2.0. Dye solutions were typically prepared with absorbances of 1.2 to 1.5 at λ_{max} in a 1cm cell in order to achieve a suitable signal strength in flash photolysis.

Measurements of the acid hydrolyses of dyes in ethanol/ water and in DMSO were performed using a PYE UNICAM SP6 200 single beam instrument. Measurements of the rate of hydrolyses were performed on the reaction mixture in a 1cm quartz cell. The reaction mixture was prepared by pipetting a volume of the dye solution into the cell followed by a volume of the acid, delivered via a micropipette, which was chosen to give the required bulk concentration in the cell. Once the initial absorbance was determined (A_0) the cell was placed in a

thermostatted bath at 20^{O}C, and removed at appropriate intervals for measurements of absorbance. The uv/visible spectrophotometer was used on the 0-1 absorbance setting which gave a precision of about 0.005 absorbance units.

The determinations of the pK_a values for the dyes were carried out on a Perkin Elmer Lambda-9 dual beam spectrophotometer, using matched quartz cells. Aliquots of a stock solution of dye in chloroform were pipetted into a 1cm quartz cell and, as with the extended hydrolyses of the dyes in ethanol/water media, a micropipette was used to introduce a volume of trifluoroacetic acid to achieve the required acid concentration. The absorbance of the solution was then scanned from 400 - 700nm and the process repeated for the other acid concentrations. Base line values for the dyes were determined using a 'double blank'.

4.3.2 Flash photolysis measurements

Flash photolysis measurements for the dyes were obtained using an Applied Photophysics 200 J microsecond unit; the pulse duration was 10 μsec with a pulse energy of approximately 150 J. Each flash measurement was carried out on ≈ 30 cm^3 of dye solution in a cell with a path length of 10 cm. When required the dye solutions were degassed by passing oxygen-free nitrogen through a septum. Initially loss of solvent during degassing was solved by use of Dreschel bottles containing the solvent up stream of the cell. However this proved to be unwieldy so an aliquot of solvent was added to the cell prior to degassing and degassing stopped when the original volume of the solution was reached (a mark on the neck of the cell indicated this); typically this was achieved after 15 minutes of degassing. Temperature control was maintained using a water 'jacketed' cell linked to a thermostatted bath at 20^{O} C; the temperature of the solution was

checked using a standard mercury-in-glass thermometer with an accuracy of 0.1^0C.

The dyes were examined by microsecond flash photolysis and, initially, the detector wavelength was set to the λ_{max} of absorption plus 40nm. However, for $6CO_2Et$-PT dye the best signal response was found to be obtained at 680nm in all solvents used.

The transient data were recorded on a Gould OS 4020 digital storage oscilloscope and then transferred to a BBC microcomputer for data handling storage and analysis. Data stored on 5.25 inch disc was transferred to 3.5 inch format and as ascII files for further analysis on a Pentium PC using Excel (V) and Jandell Scientific packages i.e. TableCurve v II. In figures reported here automatic scaling on these packages is responsible for the x-axis time scales.

4.3.3 Stopped flow measurements

The stopped flow analyses were carried out on a 'HiTech' stopped flow apparatus, thermostatted to 298K. The kinetic data obtained were recorded on a Gould OS1000 storage oscilloscope linked to a BBC microcomputer for data storage; files were transferred to 3.5 inch format for analysis by Enzfitter and Jandel scientific packages. Temperature control was achieved with a thermostatted bath at 25^0C which covered the reactant reservoir and storage syringes. Measurements of rate data were carried out for the dyes using their respective λ_{max} as monitoring wavelength.

REFERENCES

1. J. M. Eder, History of Photography, Columbia University Press, New York, 1945.

2. J. S. Friedman, *Am. Photogra.*, 1939, **33**, 465.

3. J. C. Maxwell, *Brit. J. Photogr.*, 1861, **8**, 270.

4. P. Glendinning, Colour Photography, Prentice Hall, Inc., 1985, p5.

5. Ducos du Huron, *L. Photogr. News,* 1869, **13**, 319.

6. G. Haist, Modern Photographic Processing, Vol. 2; J. Wiley and Sons, New York, 1979, p425.

7. R. Fischer, German Patent 253335, 1912.

8. J. I. Forrest and F. M. Wing, *J. Soc. Motion Pict. Eng.*, 1937, **29**, 248.

9. R. D. Theys and G. Sosnovsky, Chemistry and Processes of Colour Photography, *Chem. Rev.*, 1997, **97**, p83-132.

10. S. Dahne, *J. Imaging Sci. Technol.*, 1994, **38**, 101.

11. R. W. Gurney and N. F. Mott, *Proc. R. Soc.*, 1938, **A164**, 151.

12. R. K. Hailstone and J. F. Hamilton, *J. Imaging Sci,*. 1985, **29**, 125.

13 L. K. J. Tong, Theory of the Photographic Process, 4th ed., Macmillan Pub. Co., New York, 1977, p339.

14. S. Townsend, PhD Thesis Photochemistry of Azomethine Dyes, University of Wales Swansea, May 1992.

15. W.G. Herkstroeter, *J. Am. Chem. Soc.*, 1975, **97**, 3090.

16. L. Fleckstein, Theory of the Photographic Process, 4th ed., Macmillan Pub. Co., New York, 1977, p353.

17. P. Vittum and G. Brown, *J. Am. Chem. Soc.*, 1946, **68**, 2235.

18. P. Vittum and G. Brown, *J. Am. Chem. Soc.*, 1947, **69**, 152.

19. C. Barr, G. Brown, J. Thirtle and A Weissberger, *Photogr. Sci. Eng.*, 1961, **5**, 195.

20. C. Maggiulli and R. Paine, Brit. Patent 1059994, 1967.

21. J. Jennen, Chem. Ind., 1952, **67**, 356.

22. K. H. Menzel and R. Puetter, Brit. Patent 1047612, 1966 (Chem. Abstr. 1965, 63, 4440E).

23. R. F. Romanet and T. H. Chen, Eur. Patent 285274, 1990 (Chem. Abstr. 1989, 111, 123652g).

24. A. T. Browne, R. F. Romanet and S. E. Normandin, Eur. Patent 284240, 1990 (Chem. Abstr. 1989, 110, 125256j).

25. J. Bailey, E. B. Knott and P. A. Marr, (Chem. Abstr. 1972, **77**, 76694q).

References

26. K. O Ganguin and E. J Macdonald, *Photogra. Sci.*, 1966, **14**, 260.

27. R. D. Theys, and G Sosnovsky, Chemistry and Processes of Colour Photography, *Chem. Rev.*, 1997, **97**, p96-99.

28. C.E.K. Mees and T.H. James, Ed., The Theory of the Photographic Process 3rd ed., McMillan, NewYork, 1966, Ch 17.

29. P.Douglas, Personal Communication, 1999.

30. W.F. Smith, *J.Phys.Chem.*, 1964, **68**, 7501.

31. J. Bailey, *J.Chem. Soc. Perkin Transactions*, 1977, 2047.

32. W. G. Herkstroeter, *J. Mol. Photochem.*, 1971, **3**, 181.

33. P. Douglas et al, *J. Chem. Soc. Perkin Transactions*, 1994, 1295.

34. P. Douglas, *J. Photo. Science*, 1988, **36**, 83.

35. F. Wilkinson, D. Worrall and R.S. Chittock, *Chem. Phys. Lett.*, 1990, **174**, 416.

36. F. Wilkinson, D. Worrall, D. McGarry and A. Goodwin, *J. Chem. Soc .Faraday Trans.*, 1993, **89**, 2385.

37. P. Douglas and S. Townsend, *J. Chem. Soc. Faraday Trans.*, 1991, **87**, 3479.

References

38. P. Douglas and D. Clarke, *J. Chem. Soc. Perkin Trans.*, 1991, **2**, 1363.

39. D. Heuhaus and M. Williamson, The Nuclear Overhauser Effect in Structural and Conformational Analysis, VCH, 1989.

40. S.L. Murov, I. Carmichael and G.L. Hug. Handbook of Photochemistry 2nd ed, Dekker, USA, 1993, ch. 2.

41. W. G. Herkstroeter, *J. Am. Chem. Soc.*, 1976, **98**, 6210.

42. D. R. Kearns, *Chem. Rev.*, 1971, **71**, 395.

43. C. Couture, MPhil Thesis Photochemistry of Protonated Pyrazolotriazole Azomethine Dyes, MPhil. University of Wales Swansea, 1992.

44. A.R. Goldfarb, A. Mele and N. Gutstein, *J. Am. Chem. Soc.*, 1955, **77**, 6194.

45. P.W. Atkins, Physical Chemistry, Oxford University Press, Oxford, 1978.

46. R.A. Alberty, Physical Chemistry. 7th ed., Wiley, USA, 1987.

47. G. Pannetier and P. Souchoy, Chemical Kinetics, Elsevier Publishing Co Ltd, Amsterdam.

BIBLIOGRAPHY

C.R. Metz. Physical Chemistry, Schams Outline Series, McGraw Hill, USA, 1976

N.J. Turron. Molecular Photochemistry.

C.E. Wayne and R.P. Wayne. Photochemistry, Oxford University Press, UK, 1999

C.H.J. Wells. Introduction to Molecular Photochemistry. Chapman Hall, UK, 1972